AD_____

Award Number: DAMD17-02-1-0638

TITLE: Preclinical Mouse Models of Neurofibromatosis

PRINCIPAL INVESTIGATOR: Kevin M. Shannon, M.D.

CONTRACTING ORGANIZATION: University of California, San Francisco
San Francisco, California 94143-0962

REPORT DATE: October 2004

TYPE OF REPORT: Annual

PREPARED FOR: U.S. Army Medical Research and Materiel Command
Fort Detrick, Maryland 21702-5012

DISTRIBUTION STATEMENT: Approved for Public Release;
Distribution Unlimited

# REPORT DOCUMENTATION PAGE

Form Approved
OMB No. 074-0188



| 1. AGENCY USE ONLY (Leave blank) | 2. REPORT DATE | 3. REPORT TYPE AND DATES COVERED |
|---|---|---|
| | October 2004 | Annual (1 Oct 2003 - 30 Sep 2004) |

**4. TITLE AND SUBTITLE**
Preclinical Mouse Models of Neurofibromatosis

**5. FUNDING NUMBERS**
DAMD17-02-1-0638

**6. AUTHOR(S)**
Kevin M. Shannon, M.D.

**7. PERFORMING ORGANIZATION NAME(S) AND ADDRESS(ES)**
University of California, San Francisco
San Francisco, California 94143-0962

*E-Mail:* kevins@itsa.ucsf.edu

**8. PERFORMING ORGANIZATION REPORT NUMBER**

**9. SPONSORING / MONITORING AGENCY NAME(S) AND ADDRESS(ES)**
U.S. Army Medical Research and Materiel Command
Fort Detrick, Maryland 21702-5012

**10. SPONSORING / MONITORING AGENCY REPORT NUMBER**

**11. SUPPLEMENTARY NOTES**
Original contains color plates: All DTIC reproductions will be in black and white.

**12a. DISTRIBUTION / AVAILABILITY STATEMENT**
Approved for Public Release; Distribution Unlimited

**12b. DISTRIBUTION CODE**

**13. ABSTRACT (Maximum 200 Words)**

This report describes the fourth year of research effort by a Consortium of investigators who are working to develop, characterize and utilize strains of mice that accurately model tumors that develop in persons with NF1 and NF2. This Consortium has made substantial progress toward accomplishing the goal of generating models of NF1 and NF2-associated tumors for biologic and preclinical therapeutic trials and of exploiting these mice to address biologic and preclinical questions. The Consortium published the proceedings of a successful conference on the pathologic classification of murine NF-associated neural tumors that was organized in the prior fund year. Many of the novel strains that have been developed have been shared widely with the research community. The investigators have collaborated closely and have shared expertise and reagents extensively. This NF Consortium is a member of the Moue Models of Human Cancer Consortium of the National Cancer Institute and is participating fully in the activities of the group. The current award will support these collaborative studies through 2005.

**14. SUBJECT TERMS**
Neurofibromatosis, cancer, mouse models

**15. NUMBER OF PAGES**
48

**16. PRICE CODE**

| 17. SECURITY CLASSIFICATION OF REPORT | 18. SECURITY CLASSIFICATION OF THIS PAGE | 19. SECURITY CLASSIFICATION OF ABSTRACT | 20. LIMITATION OF ABSTRACT |
|---|---|---|---|
| Unclassified | Unclassified | Unclassified | Unlimited |

## TABLE OF CONTENTS

## INTRODUCTION

Benign and malignant tumors are a major cause of morbidity and mortality in individuals afflicted with NF1 and NF2. The *NF1* and *NF2* genes function as tumor suppressors in humans and in mice. Although a great deal has been learned about the genetics, biochemistry, and cell biology of NF1 and NF2-associated tumors, it has proven difficult to translate these advances into new treatments. The development of accurate, well-characterized mouse models of NF-associated tumors NF1 and NF2 would provide an invaluable resource for bringing improved treatments to NF patients. The overall purpose of this consortium, which is now beginning its fifth year, is to develop such models so that they will serve as permanent resources for the scientific community. These efforts are timely for a number of reasons.

First, advances in gene targeting technologies have made it ~~is~~ feasible to introduce many types of alterations into the mouse germline. Indeed, the members of this research consortium developed the initial strains of *Nf1* and *Nf2* mutant mice, which provided major insights into a number of the complications seen in human NF1 and NF2 patients. Since the inception of this consortium effort, we have made dramatic progress in improving and extending these models, specifically in the area of engineering conditional mutant alleles of both *Nf1* and *Nf2*. Second, much has been learned about the genetic and biochemical basis of deregulated growth in *NF1* and *NF2*-deficient human cells and in cells from *Nf1* and *Nf2* mutant mice. Genetic analysis of human and murine tumors has provided compelling evidence that *NF1/Nf1* and *NF2/Nf2* function as tumor suppressor genes (TSGs) *in vivo*. Biochemical data have suggested target proteins and pathways for rational drug design. The improved mouse models developed by this consortium now provide an invaluable platform for rigorous preclinical trials of these innovative approaches. Third, new therapies are urgently needed for many of the tumors that arise in individuals with NF1 and NF2. The current treatments for neurofibroma, optic nerve glioma, vestibular schwannoma, and for NF1 and NF2-asociated malignancies are frequently ineffective and carry a substantial risk of long-term morbidity. This consortium is highly complementary to the ongoing efforts to undertake human clinical trials because it will facilitate testing novel agents and approaches in a controlled preclinical setting. The quantity of drug required, expense, and potential liability are all either greatly reduced or eliminated when mouse models are used for preclinical studies. This will facilitate testing a wide range of new therapies that might benefit NF patients. Finally, the Mouse Models of Human Cancer Consortium (MMHCC) of the National Cancer Institute (NCI) is providing an opportunity for interactions among ~20 research groups that are working to develop, validate, and enhance models of a variety of human cancers. NF is the only inherited cancer predisposition represented within the MMHCC as a discrete disease entity. Our group was admitted to the MMHCC in 2000 and has been participating in its activities. Drs. Jacks, Parada, and Shannon are members of the MMHCC Steering Committee, with Dr. Parada serving as the designated representative of the NF Consortium. Dr. Jacks was Co-Chair of the Steering Committee from its inception until last year, and Dr. Shannon is one of two Co-Chairs currently leading the MMHCC. Thus, this award has provided the NF research community with an exceptional level of representation within the mouse modeling community. The MMHCC is spearheading efforts in areas such as building repositories, devising pathologic classification schemes, imaging mouse tumors, and stimulating interactions with industry in the area of preclinical therapeutics that are of general importance to NF research. The laboratory researchers in this consortium are working with the National Neurofibromatosis Foundation (NNFF). This interaction facilitates research in NF1 and NF2 and links basic and clinical

researchers with patients. Our current award focuses on the technical objectives (aims) listed below. Progress in each area is summarized in the following sections.

(1) To enhance existing lines of *Nf1* and *Nf2* mutant mice and to develop new *in vivo* models of NF-associated tumors. We will fully characterize lesions that arise in these mice, focusing on how closely they reproduce the phenotypic, genetic, and biochemical alterations seen in comparable human tumors.

(2) To perform *in vitro* and *in vivo* studies to elucidate biochemical pathways underlying the proliferative advantage of *Nf1* and *Nf2*-deficient cells as a way of identifying molecular targets for therapeutic interventions.

(3) To use these models to perform preclinical trials that will test the efficacy and toxicities of rational therapies for tumors that arise in individuals with NF1 and NF2.

(4) To organize specialized working group meetings that will address: (1) Pathologic Classification of Tumors in NF Mouse Models, and (2) Preclinical Therapeutics in NF Mouse Models, and to develop a pilot program to support preclinical testing of promising treatments in mouse models of NF1 and NF2.

## BODY

### Background

Tumor Spectrum in NF1 and NF2 Patients. Persons with NF1 are predisposed to benign neurofibromas, optic nerve gliomas, and to specific malignant neoplasms. Individuals with NF1 typically develop multiple neurofibromas that can result in cosmetic, orthopedic, and neurologic disabilities. Optic nerve gliomas are another vexing clinical problem. Although histologically benign, these tumors frequently cause visual impairment or blindness because of their anatomic location. The malignant neoplasms seen in NF1 patients include astrocytoma, malignant peripheral nerve sheath tumor (MPNST), pheochromocytoma, and juvenile myelomonocytic leukemia (JMML). NF2 affects 1 in 40,000 persons worldwide. Individuals with NF2 develop schwannomas along cranial nerves (especially the eighth nerve), as well as peripheral nerves. Other NF2-related tumors include meningiomas, gliomas, and ependymomas.

Production and Characterization of *Nf1* and *Nf2* Mutant Mice. Drs. Jacks and Parada independently disrupted *Nf1* by inserting a neomycin *(neo)* cassette into exon 31 (1, 2). Homozygous *Nf1* mutant ($Nf1^{-/-}$) embryos die *in utero* with cardiac anomalies, which precludes the use of these mice to study important aspects of NF1 pathology, including the formation of many tumor types. To circumvent this problem, Dr. Parada's lab harnessed *Cre-loxP* technology to create a conditional *Nf1* allele (3). Importantly, the Parada's lab has shown that the $Nf1^{flox}$ allele functions as a wild-type allele in spite of harboring *loxP* sites and a *neo* gene within its intronic sequences. The $Nf1^{flox}$ allele is readily recombined *in vivo* to make a null allele through co-expression of *Cre* recombinase. Drs. McClatchey, Jacks, and Giovannini used gene targeting to disrupt the *Nf2* locus (4, 5). Homozygous *Nf2* mutant embryos failed without initiating

gastrulation. Although heterozygous *Nf2* mutant mice are cancer prone, these animals do not develop schwannoma or meningioma. To circumvent the early embryonic-lethal phenotype associated with homozygous inactivation of *Nf2* and to test the hypothesis that the tumor spectrum might be modulated by the rate of the loss of the normal allele in specific tissues, Dr. Giovannini and his colleagues generated a conditional mutant *Nf2* allele (6). A two-step strategy was utilized to construct a mutant $Nf2^{flox2}$ allele characterized by the presence of *loxP* sites in the intronic regions flanking exon 2. As expected, mice homozygous for the $Nf2^{flox2}$ mutant allele ($Nf2^{flox2/flox2}$) were viable and fertile suggesting that the introduction of *loxP* sites did not hamper *Nf2* expression. Induced expression of *Cre* recombinase in $Nf2^{flox2/flox2}$ mice results in biallelic inactivation of *Nf2* in specific tissues. The major research goals of this Consortium include exploiting these conditional mutant alleles of *Nf1* and *Nf2* to develop tractable models of NF-associated tumors for use in our labs and by other investigators for biologic and preclinical applications. A list of investigators who have received these mice appears in the Reportable Outcomes section.

Models of NF1 and NF2-Associated Tumors. In work published prior to 2004, the participants in this consortium have reported the phenotypic and biologic features of NF1-associated mouse tumor models of MPNST/Triton tumor, astrocytoma, JMML, plexiform neurofibroma, and chemotherapy-induced leukemia (7-12) and of NF2-associated tumors such as vestibular Schwannoma and meningioma (5, 6). These data have been published and are also described in detail in our previous annual reports.

**Progress Report**

*Technical Objective (Aim) 1: To enhance existing lines of Nf1 and Nf2 mutant mice and to develop new in vivo models of NF-associated tumors*

An Enhanced Model of JMML. JMML is a lethal myeloproliferative disorder (MPD) characterized by over-production of infiltrative myeloid cells (13). JMML has been modeled in mice by transferring *Nf1*-deficient fetal liver cells into irradiated recipients (14, 15). However, this system is cumbersome and expensive because it requires embryo dissections around E13 and injecting fetal liver cells into irradiated hosts. To circumvent these problems, Drs. Shannon and Parada collaborated to breed $Nf1^{flox}$ and *Mx1-Cre* mice with the goal of inducing somatic *Nf1* inactivation in hematopoietic cells. The results of these studies are presented in detail in the attached reprint by Le, *et al.* (16). Briefly, the Cre recombinase is expressed from the interferon-inducible *Mx1* promoter in the *Mx1-Cre* strain. Injecting *Mx1-Cre,* $Nf1^{flox/flox}$ mice with polyinosinic-polycytidylic acid (pIpC) induced endogenous interferon production and efficiently ablated *Nf1* in the hematopoietic compartment. These mice consistently developed MPD, which was associated with elevated myeloid cell counts and progressive splenomegaly.

*Mx1-Cre,* $Nf1^{flox/flox}$ bone marrow cells showed a modest increase in baseline Ras-GTP levels, but phosphorylation of the downstream effectors MEK and Akt were similar in mutant and control cells (data not shown). Exposing *Mx1-Cre,* $Nf1^{flox/flox}$ and wild-type bone marrow to granulocyte-macrophage colony stimulating factor (GM-CSF) induced robust Ras-GTP, MEK, and Akt activation from baseline levels that was equivalent in both genotypes (data not shown). Because *Nf1-/-* and wild-type bone marrows showed marked differences with respect to the relative proportions of different cell types, the Shannon lab isolated Mac1+ cells and compared

MEK activation in this myeloid subpopulation. In these experiments, *Nf1-/-* cells showed sustained activation of MEK after exposure to GM-CSF (16). *Mx1-Cre, Nf1$^{flox/flox}$* mice and cells from these animals can be used to examine the biochemical consequences of *Nf1* inactivation in primary cells and to test molecularly targeted agents with pharmacodynamic monitoring of relevant biochemical endpoints. As summarized under Technical Objectives 2 and 3, the Shannon lab has launched major initiatives in these areas.

Plexiform Neurofibroma Formation in *Nf1$^{flox/flox}$* Conditional Mutant Mice. The Parada lab has continued to pursue the novel plexiform neurofibroma models developed in prior fund years. They have generated convincing genetic evidence that the etiology of plexiform neurofibromas requires homozygous inactivation of *Nf1* in Schwann cell (SC) precursors. Thus, *Nf1*-deficient SC in the context of wild type cells cannot give rise to frank tumors. The Parada lab is investigating the source of the heterozygous (haploinsufficient) contribution to these tumors. The first suspect is the mast cell due to their presence in peripheral nerves that contain null, but not heterozygous, SC (8). Thus, there appears to exist a unique affinity between these two cell types that could be the catalyst to tumor formation. Experiments are underway to determine whether the early appearance of mast cells in a heterozygous environment but not in a homozygous environment is critical for tumor formation.

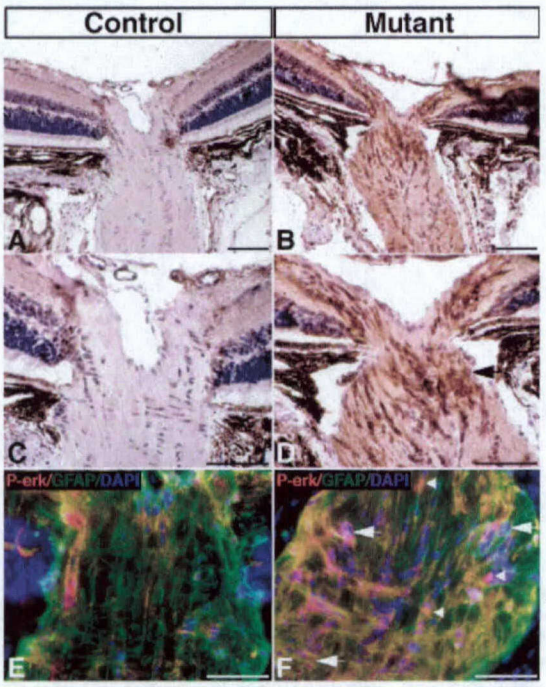


**Figure 1.** Glial cells in mutant optic nerves have elevated levels of activated ERK. Sections of the proximal optic nerves from control mice (A, C) and mutant mice (B, D) were stained with antibodies specific for phosphorylated form of ERK Sections from control (E) and mutant (F) optic nerves were subjected to triple labeling with anti-P-erk (red), anti-GFAP (green), and DAPI (blue). DAPI was used to label the nuclei. Scale bar, 100 u.

Two recent advances have been made. First microarray analysis of plexiform tumors, control Schwann cells, heterozygous mast cells, and control mast cells has provided a wealth of information that may assist us in identifying culprit genes that participate in this unique affinity between nullizygous Schwann cells and heterozygous mast cells. Second, the culturing of the purified Schwann and mast cell cultures permits studies on a variety of properties that demonstrate a unique interaction between the above mentioned phenotypes (not shown).

In humans with NF1, MPNSTs appear to invariably evolve from plexiform neurofibromas (i.e the latter require the appearance of the former). Moreover, a substantial proportion of human MPNSTs demonstrate mutations in both *NF1* and *P53*. To model this in the mouse, the Parada lab (8) added a *p53* mutation to the SC-specific ablation of *Nf1*. The resultant mice initially appeared normal but began exhibiting a phenotype reminiscent of the *Krox20-Cre;Nf1$^{flox}$* mice around 4 months of age. Necropsy and analysis of these *Nf1$^{flox}$; p53-/-* mice revealed neurofibromas (Fig. 1) that appeared earlier. Thus, the presence of *p53* mutation in SC in the context of an *Nf1* mutation, accelerated the

appearance of neurofibromas. In preliminary results, the Parada lab has observed progression of some neurofibromas into malignant tumors. In three cases, 6 month old mice lacking *Nf1* and one *p53* allele progressed to malignancy (Fig. 1). The Parada lab used laser capture microdissesction (LCM) to isolate both benign neurofibroma and malignant tumor samples from the same paraffin section and found that each neurofibroma retains heterozygosity at *p53* whereas the malignant tumor samples show *p53* inactivation. These exciting data promise to be a rich source for applying genomic approaches to dissect the changing molecular events in tumor progression of this model.

Modeling Astrocytoma in *Nf1* Mice. Approximately 15-20% of children with NF1 develop pilocytic astrocytomas, which predominantly occur within the optic pathway and hypothalamus (17, 18). Like their sporadic counterparts, most NF1-associated pilocytic astrocytomas are benign and can remain static for many years. However, despite histologically benign features, a significant portion of these tumors progress and cause vision impairment and other neurological symptoms (17). The Parada lab employed a human GFAP promoter to drive Cre recombinase expression in astrocytic precursors and found that *Nf1* inactivation promotes the proliferation of glial progenitor cells resulting in increased numbers of GFAP-expressing astrocytes in the adult brain. As shown in Figures 2 & 3, the optic nerves of these mice are enlarged and disorganized. Within the hyperplastic tissue, there appear foci of GFAP positive/Nestin negative pilocytic astrocytomas. The Parada lab is characterizing this model while pursuing new approaches to overcome limitations with the existing strains.

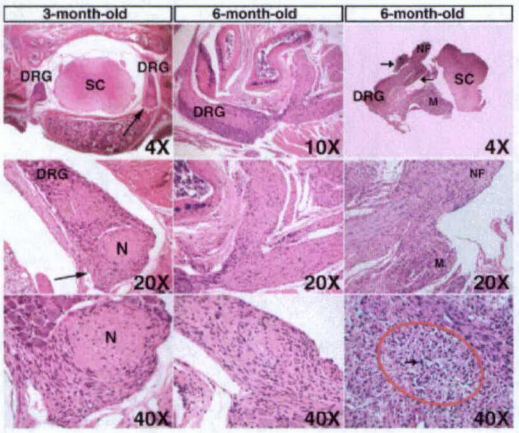


**Figure 2.** *Krox20-Cre;cisNf1flox/flox,p53-/+* mice develop neurofibromas and neuro-fibrosarcomas. Left Panel: transverse section through a 3 month old mouse spinal cord. Neurofibroma surrounds the nerve (see arrows). Middle Panel: plexiform neurofibroma from a 6 month old mouse. Note that both branches of the nerve are neoplastic. Right Panel: neurofibroma that has developing malignant (M) tissue. See encircled area in lower right panel. DRG, dorsal root ganglion. NF, neurofibroma, SC, spinal cord. N, nerve.

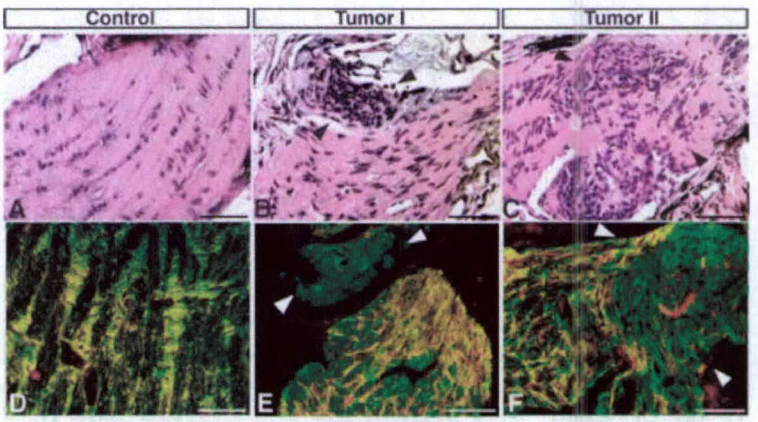


**Figure 3.** NF1hGFAPKO mice develop optic gliomas. Two independent optic gliomas (B, C) are shown with H&E staining as compared to the control (A). Adjacent sections from control (D) and mutant nerves with gliomas (E, F) were stained with anti-nestin (red) and anti-GFAP (green). Of note, unlike the more widely distributed hyperplastic cells that express both nestin and GFAP, optic gliomas only express GFAP (E, F, arrowheads). Scale bar,

*Nf2* and *p53* Mutations Cooperate in Neural Crest Tumor Formation. Schwannomas are frequent in NF2 patients and also occur as sporadic tumors. Both familial and sporadic schwannomas show mutations of the *NF2* gene. Specific biallelic *Nf2* gene mutation in the mouse neural crest

cell lineage results in Schwann cell hyperplasia at high frequency, but schwannomas are rare. This suggests that additional mutations are required for progression from hyperplasia to schwannoma. Dr. Giovannini's lab has evidence that the *Nf2* and *p53* tumor suppressor genes cooperate in neural crest tumorigenesis. The time window in which mutations are induced/occur determines whether malignant Schwann cell or osteogenic tumors arise, indicating its critical importance for accurate tumor modelling. In particular, they assessed the role of *p53* hemizygosity in conditional *Nf2* knockout mice and found strong synergy between *Nf2* and *p53* mutations in development of malignant tumors of neural crest origin. Nearly all P0$Cre^{B}$;$Nf2^{flox2/flox2}$;$p53^{+/-}$ mice rapidly died starting at a median age 4.5 months and developed malignant peripheral nerve sheath tumors (MPNSTs). Benign Schwann cell tumors were also seen, including schwannomas in 3 of 26 (11%) and neurofibromas in 2 of 26 (8%) animals (the distinction between the two entities in the mouse could not always be established with certainty following the criteria of human pathology).

Osteogenic Tumors Predominate in P0*Cre*;$Nf2^{flox2/+}$;$p53^{+/-}$ *cis* Mice. Dr. Giovannini found that the great majority of P0*Cre*;$Nf2^{flox2/+}$;$p53^{+/-}$ *cis* mice (81%) developed osteogenic tumors, both osteosarcomas (63%) and osteomas (25%) that all arose in the neural crest-derived bone at a mean age of 5.5 months. So, in contrast to the P0*Cre*;$Nf2^{flox2/+}$;$p53^{+/-}$ *cis* mice, P0*Cre*;$Nf2^{flox2/flox2}$;$p53^{+/-}$ mice did not develop osteogenic tumors suggesting that early loss of schwannomin may lead to compensatory signaling thereby preventing the generation of osteogenic tumors. Loss of merlin at a later developmental stage may disable this compensatory signaling leading to the generation of osteogenic tumors. Although the developmental stage of Schwann cells may determine their susceptibility to tumor-initiating alterations (19, 20), a concomittant modification of the tumor spectrum has not been described yet. Dr. Giovannini's observations may indicate that the proliferation rate and the probability of LOH are higher in homozygous than in heterozygous *Nf2* mutant cells or that functional loss of *Nf2* increases the risk of abnormal chromosomal segregation. Moreover, these data infer that the time window in which gene inactivation occurs is critical for accurate tumor modeling.

Construction of Drug-Inducible Cre Mice to Locally and Temporally Control Deletion of the *Nf2* Gene. In addition to using conventional transgenic Cre lines to inactivate the conditional $Nf2^{flox}$ allele generated by Dr. Giovannini, the Jacks lab has generated drug-inducible Cre mice that will permit local ablation and desired time points. They have inserted a modified Cre, $CreER^{T2}$ (Cre fused to an altered human estrogen receptor that is activated by the drug tamoxifen), downstream of the ubiquitous Rosa26 promoter. $CreER^{T2}$ is ten times more sensitive to tamoxifen than the first generation of CreER constructs; therefore, it will avoid confounding issues related to tamoxifen toxicity. The Jacks lab has demonstrated that the $CreER^{T2}$ construct is functional in ES cells, and has generated mice that have $CreER^{T2}$ in the germ line. By crossing the Rosa26-$CreER^{T2}$ mice to mice containing a Cre reporter (Rosa26-LSL-$LacZ^{2lox}$), they have determined the pattern of Cre expression. In the absence of tamoxifen no background Cre activity was detected. After intraperitoneal injection of 9 mg tamoxifen/40 g body weight for 5 consecutive days, Cre activity was detected throughout the liver and intestine and in a mosaic fashion within the brain and other organs (see Figure 4 on following page).

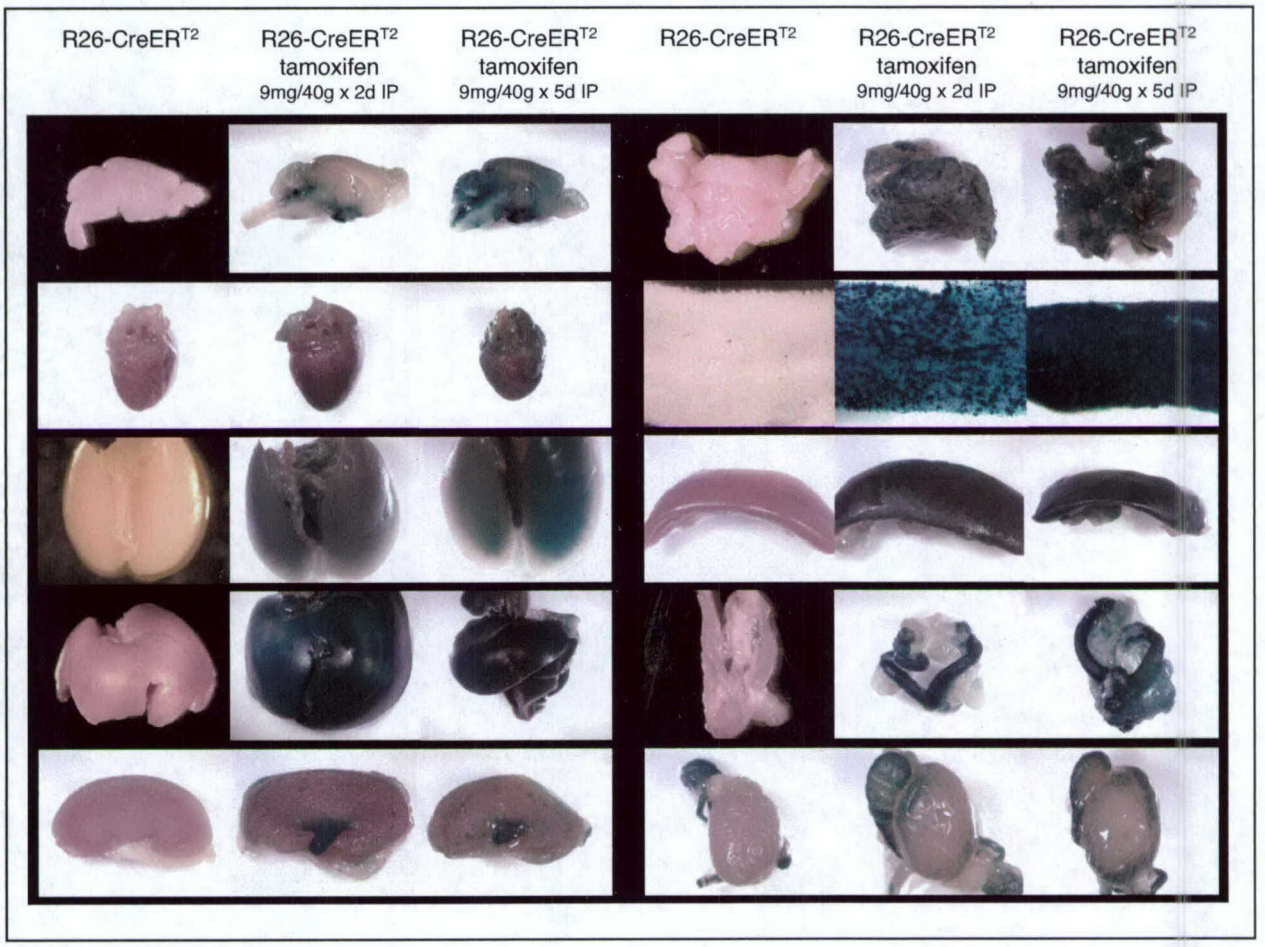


**Figure 4**. Cre expression (in blue) after intraperitoneal injection of tamoxifen for 2 or 5 days in (from top to bottom, left hand side) brain, heart, lung, liver, kidney, (right hand side) pancreas, gut, spleen, ovaries & uterus, testes. In the absence of tamoxifen, no background Cre activity was detected, indicating there is no leakiness.

Generation and Characterization of Mouse Models of Ependymoma. Pediatric primary brain tumors are the second most frequent malignancy of childhood and are now the leading cause of death from childhood cancer, accounting for approximately 24% of cancer-related deaths. Ependymoma, a type of primary brain tumor that arises from the specialized glial cells (ependymal cells) that line the ventricular system, may develop at any age. However, ependymomas are particularly common in young children, accounting for 6-12% of pediatric primary brain tumors, and this tumor type occurs at increased frequency in children with NF2. Although ependymomas are slow growing and histologically classified as WHO grade II/IV, the 5-year progression free survival is only 50%, with children under two years of age having a particularly dismal prognosis. Since mutation of the *NF2* gene is the only well documented genetic alteration in human ependymomas, the Jacks laboratory is generating mouse models of ependymoma in which the initiating event is loss of *Nf2*. Previous work from the Jacks lab has shown that $Nf2^{-/-}$ mice die in early embryogenesis secondary to defects in the extraembryonic tissues, and that $Nf2^{+/-}$ mice develop malignant tumors but not the tumor types characteristic of the human disease (schwannoma, meningioma, and ependymoma). Therefore, all of the mouse

models now under construction will make use of the conditional $Nf2^{flox}$ allele generated by Dr. Giovannini.

At this time, no ependymal cell-specific promoter has been characterized. Such a promoter would be the ideal way to drive Cre expression in ependymal cells. In the absence of such a promoter, the Jacks laboratory is using Cre transgenic mice in which Cre is expressed within ependymal cells but also within other cells of the body and/or brain. Like neurons and other glial cells that form the brain, ependymal cells develop from neuroepithelial cells, which express the intermediate filament nestin. Neuroepithelial cells are thought give rise to radial glial cells, which in turn give rise to immature ependymal cells (tanycytes). Tanycytes mature into ependymal cells that continue to express nestin and in the mouse but not in humans, express another intermediate filament glial fibrillary acidic protein (GFAP). A few tanycytes remain in adult animals. Both Nestin-Cre and *h*GFAP-Cre (Housman lab, unpublished data) transgenic mice are currently available.

By crossing Nestin-Cre and *h*GFAP-Cre mice to mice containing a Cre reporter (Rosa26-LSL-LacZ), Jacks laboratory has confirmed that both Nestin-Cre and *h*GFAP-Cre mice do express Cre within the ependymal cell layer. Nestin-Cre is highly expressed in neurons and other glial cells in the brain and throughout most tissues of the body. Nestin-Cre expression is detected as early as E8.5. *h*GFAP-Cre expression is restricted to neurons and glial cells, and is detected as early as E14.5. The *h*GFAP-Cre transgenic mouse was constructed with the human GFAP promoter; therefore, the pattern of Cre expression more closely resembles that of human GFAP.

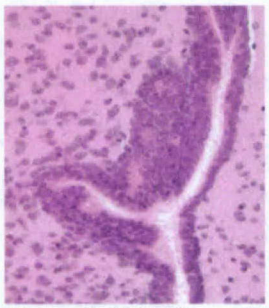

**Figure 5.** "Mini" ependymoma with true rosettes arising in the wall of the third ventricle in a postnatal day 11 Nestin-$Cre^{m}$;$Nf2^{flox/flox}$ mouse.

Nestin-$Cre^{p}$;$Nf2^{flox/flox}$ mice in which the neural tube has closed (70% of all mutants) showed diffuse hyperproliferation of ependymal cells around the ventricles and central canal of the spinal cord (Fig. 5). A single Nestin-$Cre^{m}$;$Nf2^{flox/flox}$ mouse that survived past birth had a focal lesion arising from the wall of the third ventricle in which the ependymal cells formed tubules resembling the true rosettes of human ependymomas. This lesion appears to represent the earliest stage of ependymoma. By contrast, the Jacks laboratory has generated 25 *h*GFAP-Cre;$Nf2^{flox/flox}$ mice, and to date none of the mice analyzed histologically has shown evidence of ependymal cell hyperproliferation. These studies suggest that Nestin-Cre-expressing neuroepithelial cells or ependymal cells, not *h*GFAP-Cre-expressing radial glia or tanycytes, are the most likely cells of origin of ependymomas.

Modeling the Interaction between *Nf1* Inactivation and Genotoxins in the Pathogenesis of Therapy-Induced Cancers. Therapy-induced malignant neoplasms are a severe late complication of mutagenic therapies. The pathogenesis of these cancers is obscure, and there is a lack of relevant animal models. The risk of therapy-induced cancers is of great importance to persons with NF1 and NF2 because they are predisposed to tumors that often require aggressive treatment and because they might be prone to therapy-induced cancers if chemotherapy and radiation induce mutations that cooperate with inactivation of *NF1* or *NF2*. Indeed, there is clinical evidence that patients with NF1 are susceptible to therapy-induced cancers. A systematic review of 64 children with NF1 who received chemotherapy and/or radiation (RAD) to treat a primary cancer revealed 11% with a second malignant neoplasm (SMN), all of which were either myeloid malignancies or sarcomas (21). Strikingly, six of eight patients (75%)

treated for an embryonal cancer developed one or more SMNs; this high risk likely results from aggressive multi-modal therapies. Two adults with NF1 have also been reported who developed therapy-related myelodysplastic syndrome (MDS) after treatment for *de novo* acute myeloid leukemia (AML) (22). These observations suggest that therapeutic exposure to genotoxic agents cooperates with germline *NF1* mutations in the genesis of common SMNs found in the general population, namely myeloid leukemia and sarcoma.

In studies that were initiated under US Army NF Research Project DAMD 17-02-1-0638, the Shannon and Jacks lab investigated tumor induction by RAD, the alklyating agent cyclophosphamide (CY), or both modalities in heterozygous *Nf1* mutant (*Nf1*+/-) mice. *Nf1*+/- mice that were exposed to these mutagens developed a spectrum of secondary cancers that are common in human patients, including myeloid malignancies, soft tissue sarcomas, and breast cancers. A total of 192 wild-type (WT) and *Nf1*+/- mice that were assigned to one of four groups: no treatment, CY alone, RAD alone, or CY followed by RAD were followed for tumor development for 18 months after exposure. Pathologic analysis was performed on 91% of the study cohort, including 95 of 104 WT mice and 77 of 86 *Nf1*-/- mice. Heterozygous inactivation of *Nf1* was strongly associated with an increased risk of premature death with a survival rate of 30% after 15 months in *Nf1*+/- mice compared with 78% in WT littermates (Fig. 6A). The risk of premature death was greater in *Nf1*+/- mice in each of the four treatment groups, and was due to cancer in 96% of the evaluable animals. Fifty-one malignancies occurred in 81 *Nf1*+/- mice that were available for pathologic examination compared with 17 cancers among 100 WT mice ($p < 0.0001$). Tumor types that occurred significantly more often in *Nf1*+/- mice included sarcomas with features of human MPNST (p=0.001), myeloid malignancies (p=0.0005), and pheochromocytomas (p=0.0007). Myeloid malignancies and sarcomas, which are the most common SMNs in human patients, accounted for 24 of the 52 cancers found in *Nf1*+/- mice. Four *Nf1*+/- mice unexpectedly developed breast cancer versus no cases in the WT animals (p=0.04, Fisher's exact test).

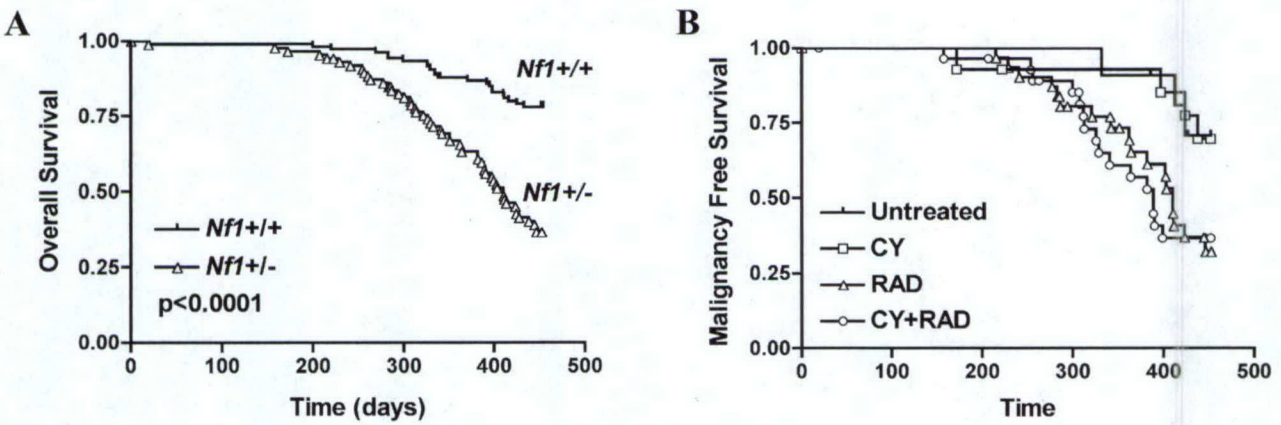


**Figure 6.** Reduced survival and increased incidence of cancer in *Nf1*+/- mice. Panel A. Kaplan-Meier analysis of overall survival demonstrates an increased risk of death in *Nf1*+/- versus wild-type mice with a hazard ratio of death of 3.83 (2.52-6.40). Panel B. *Nf1*+/- mice that were exposed to RAD alone or in combination with CY displayed a significantly higher incidence of cancer than *Nf1*+/- mice that were not irradiated. Control and CY-treated *Nf1*+/- mice had a similar incidence of malignancy.

RAD cooperated strongly with heterozygous *Nf1* inactivation in tumorigenesis whether administered alone or after CY (Figs. 6B). By contrast, the incidence of cancer was similar in untreated *Nf1*+/- mice and in animals that received CY only (Fig. 6B). Interestingly, the nature of the mutagen exposure influenced the tumor spectrum in *Nf1*+/- mice. In particular, RAD alone resulted in a greater frequency of myeloid malignancies, whereas exposure to RAD in combination with CY resulted in a high incidence of solid tumors, including breast cancer. Molecular analysis of tumors that develop spontaneously in persons with NF1 and in strains of *Nf1* mutant mice frequently reveals somatic loss of constitutional heterozygosity (LOH) (2, 23). Similarly, Southern blot analysis showed loss of the WT C57Bl/6 *Nf1* allele in 6 of 8 soft tissue sarcomas, confirming the important role of biallelic inactivation of *Nf1* in tumorigenesis (data not shown). LOH also occurred in 3 of 3 pheochromocytomas and in 4 of 4 breast cancers. By contrast, PCR analysis did not reveal LOH in any of the myeloid malignancies. Drs. Jacks and Parada found that inactivation of *Trp53* and *Nf1* cooperate in tumorigenesis, particularly sarcoma development (7, 24). The loci for these two genes are approximately 7 cM apart on mouse chromosome 11, while the human homologs are separated by approximately 22 Mb on chromosome 17. Surprisingly, while LOH at *Trp53* occurred in all of the breast tumors, most of the sarcomas from *Nf1*+/- mice retained both *Trp53* alleles (data not shown).

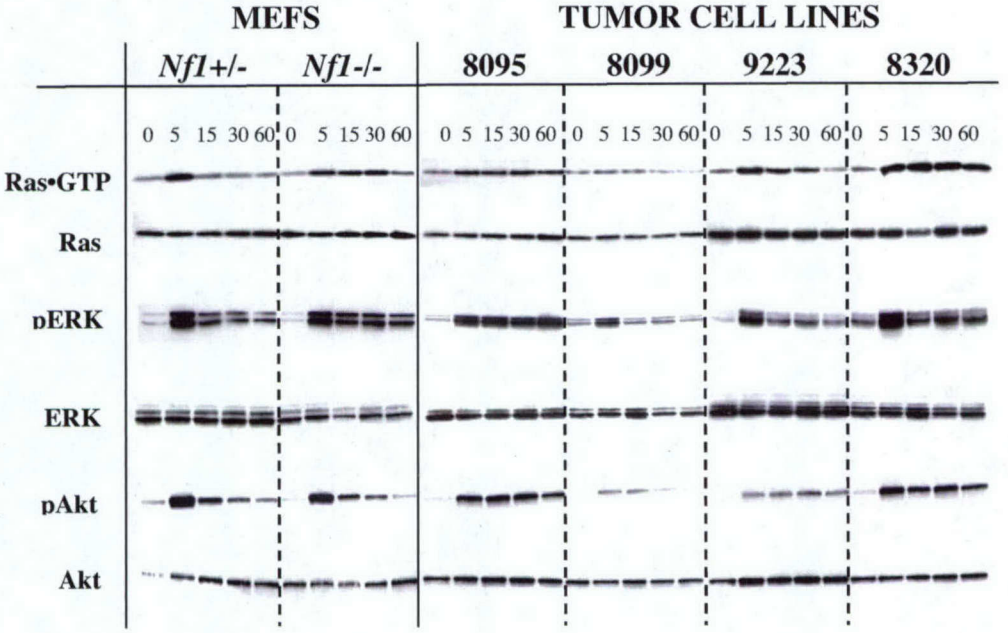


**Figure 7.** Biochemical analysis of MEFs and tumor cell lines developed from *Nf1*+/- mice. Panel A. EGF induces a transient spike in Ras-GTP levels in *Nf1*+/- MEFs, which is followed by a rapid return to baseline values. *Nf1*+/- MEFs show a sustained Ras-GTP response and prolonged ERK phosphorylation. Breast cancer cell lines 8095, 8320, and 9223 also show prolonged Ras-GTP levels as well as prolonged ERK and Akt phosphorylation. Panel B. Doxorubicin induces p21 expression in heterozygous and homozygous *Nf1* mutant MEFs. By contrast, p21 was not detected in any of the cell lines before or after doxorubicin exposure.

Based on previous data implicating aberrant epidermal growth factor receptor (EGFR) signaling in NF1-associated sarcomagenesis (25, 26), basal and EGF-induced activation of Ras and phosphorylation of downstream effectors were compared in these 4 tumor cell lines to *Nf1+/-* and *Nf1-/-* mouse embryonic fibroblasts (MEFs). *Nf1+/-* MEFs that were plated, serum starved, and stimulated with EGF displayed a marked increase in Ras-GTP levels with a rapid return to baseline levels (Fig 7). *Nf1-/-* MEFs showed slightly higher peak levels of Ras-GTP in response to EGF and demonstrated prolonged Ras activation, which is consistent with a recent report (27). Levels of phosphorylated ERK and Akt changed in parallel with Ras•GTP. Breast cancer cell lines 8095, 8320, and 9223 that were stimulated with EGF showed prolonged Ras activation with elevated levels of phosphorylated ERK and Akt. By contrast, basal and EGF-induced Ras activation showed no consistent differences between sarcoma cell line 8099 and control *Nf1+/-* MEFS (Fig. 7).

These data, which are being prepared for publication, establish a robust and tractable mouse model of common human SMNs. *Nf1+/-* mice can be harnessed to address the mutagenic potential of chemotherapeutic agents given alone and in combination and to test preventive strategies. This work has implications for treating tumors that arise in the patients with NF1. In particular, a single low dose of RAD cooperated strongly with heterozygous *Nf1* inactivation in tumorigenesis. Children with NF1 are strongly predisposed to optic tract gliomas and low-grade astrocytomas, which may be difficult to manage. Data in *Nf1+/-* mice suggest that the potential risk of SMN should be considered when deciding when to irradiate these and other NF1-associated tumors, and that patients who require RAD should be followed carefully for subsequent treatment-induced cancers.

*Technical Objective (Aim) 2: To perform in vitro and in vivo experiments that will elucidate molecular targets for therapeutic interventions.*

Functions of Neurofibromin and Merlin. The identification and validation of molecular targets remains a significant rate-limiting step in the discovery of effective therapies for the complications of NF1 and NF2 disease. Addressing this central question ultimately depends on having accurate cellular systems for interrogating how specific biochemical pathways are perturbed in *Nf1* and *Nf2* deficient cells. Cells from the strains of mice engineered by the members of this Consortium now provide robust systems for performing genetic, biochemical, and cell biologic experiments to uncover genes that cooperate in generating NF-associated tumors and to characterize proteins that might be targets for therapeutic intervention.

Considerable work from our laboratories and others has demonstrated that loss of *NF1/Nf1* function leads to hyperactivation of the Ras signaling pathway. Post-translational processing of Ras proteins has attracted interest as a potential target for drug discovery in various cancers and in NF1. Processing is initiated by farnesyltransferase (Ftase), which attaches a farnesyl lipid to the thiol group of the cysteine (the "C" of the CAAX motif). Prenylation targets Ras to membranes, and is required for biologic activity. However, K-Ras and N-Ras are substrates for geranylgeranyltransferase 1 (GGTase 1) and are processed by this alternative pathway when Ftase is inhibited and the initial clinical experience with Ftase inhibitors has been disappointing. Indeed, extensive data now support the view that non-Ras C*AAX* proteins are critical *in vivo* targets of the Ftase inhibitors (reviewed in (28)). After prenylation, the carboyxl terminal three amino acids are released by Rce1, an integral membrane endoprotease of the endoplasmic reticulum. The final step in Ras processing involves methylation of the prenylcysteine by

isoprenylcysteine carboxyl methyltransferase *(Icmt)*. Genetic experiments performed by Dr. Shannon's lab showed no detectable effects of ablating *Rce1* on normal hematopoiesis (29).

Agents that interfere with various signaling pathways downstream of Ras (such as the Raf1-MEK-MAPK and phosphoinositide-3-OH kinase (PI3K)-protein kinase B (PKB; also known as Akt) cascades) are of obvious interest in the treatment of NF1-associated tumors. Upstream receptor tyrosine kinases and their ligands may also be required for the growth of specific *NF1/Nf1* mutant tumors, including GM-CSF in the case of myeloid leukemia and epidermal growth factor receptor for MPNSTs (25). It is important to note that genetic experiments in *Drosophila* have also demonstrated link between loss of neurofibromin function and PKA signaling.

Until recently, much less was known about the biochemical consequences of *Nf2* inactivation. However, data from the McClatchey, Giovannini and Jacks laboratories are providing key insights into the molecular function of merlin and have identified several potential therapeutic targets. For example, accumulating evidence indicates a reciprocal relationship between merlin and the small GTPase Rac1. Drs. McClatchey and Jacks demonstrated that Rac1 activation leads to phosphorylation, reduced membrane:cytoskeleton association and impaired growth suppressing activity of merlin (30). Conversely, merlin overexpression blocks Rac activation and $Nf2^{-/-}$ cells exhibit features of excessive Rac signaling. A similar reciprocal relationship between the closely related ERM proteins and Rho has been demonstrated. Dr. Jacks and others went on to demonstrate that the Rac effector kinase Pak1 can phosphorylate merlin; indeed, recent work from the Jacks laboratory has now shown that merlin can bind to and inhibit PAK1 (31-33). Inhibitors of Rac/PAK1 signaling exist and represent attractive candidates for the treatment of *NF2*-deficient tumors.

Genetically engineered mice are a valuable source of primary cells for studying the consequences of gene deficiency. Drs. McClatchey and Giovannini found that a signature of *Nf2*-deficiency across several different types of cells is loss of contact-dependent inhibition of proliferation and abnormal cell:cell communication (34). Specifically, $Nf2^{-/-}$ cells cannot form stable cadherin-based cell:cell junctions known as adherens junctions (AJs) and merlin normally localizes to these structures in wild-type cells. Merlin may normally stabilize the interaction between nascent AJs and the actin cytoskeleton either by controlling Rac activity or stabilizing actin filaments, both of which are required for AJ assembly (30, 35). Accumulating evidence indicates that AJ assembly results in silencing of membrane tyrosine kinase receptors such as the epidermal growth factor receptor (EGFR) (36-38). Indeed, Dr. McClatchey's group has found that EGFR silencing is defective in several types of confluent $Nf2^{-/-}$ cells; their data indicate that merlin controls EGFR internalizing specifically in contacting cells. Importantly, Dr. McClatchey's group has also found that EGFR inhibitors such as gefitinib (Iressa, AstraZeneca) can restore contact inhibition to $Nf2^{-/-}$ cells (Figure 8). This work has been submitted for publication. This is consistent with several lines of evidence that link merlin function to growth factor receptor signaling in other systems. Several inhibitors of the EGFR (ErbB1) and its close family members (ErbB2, 3, and 4) have been developed and some are being evaluated in clinical trials for other types of cancer and therefore may be excellent candidates for therapeutic intervention in NF2 (39).

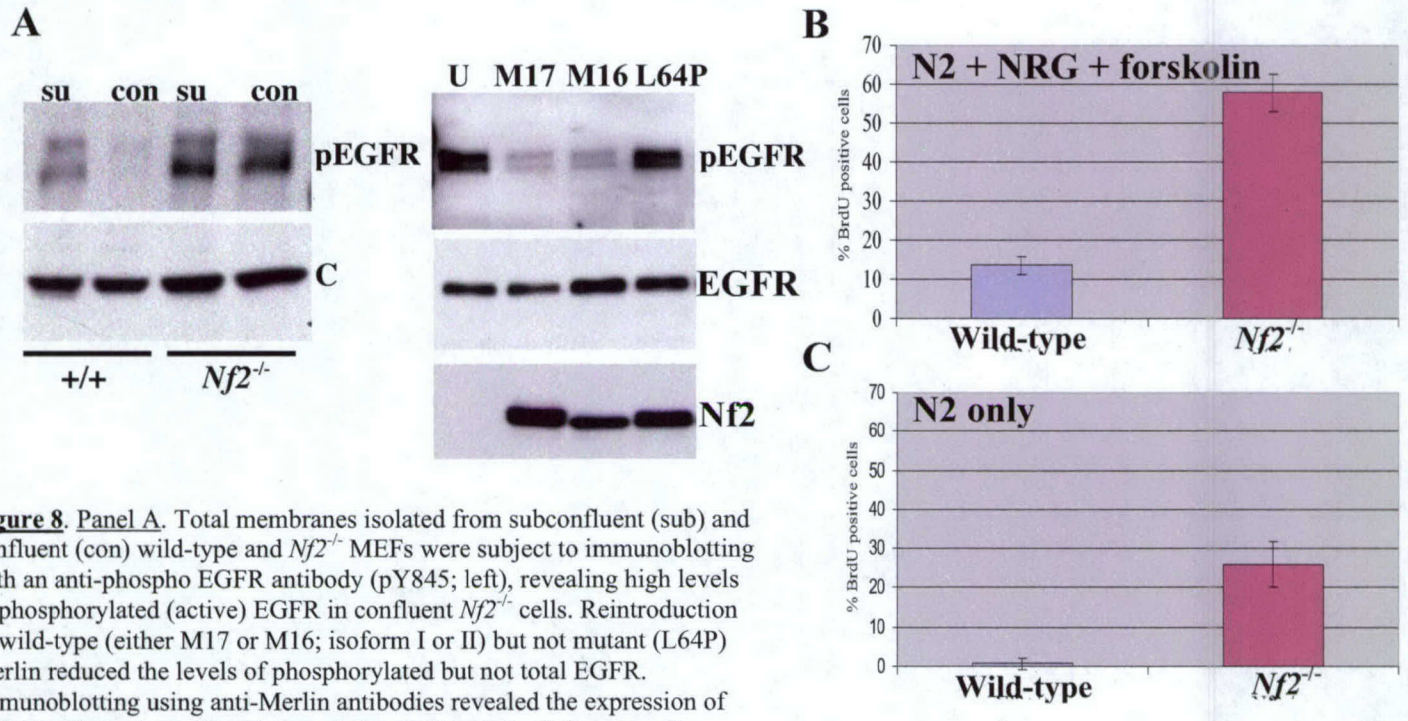


**Figure 8**. Panel A. Total membranes isolated from subconfluent (sub) and confluent (con) wild-type and *Nf2*$^{-/-}$ MEFs were subject to immunoblotting with an anti-phospho EGFR antibody (pY845; left), revealing high levels of phosphorylated (active) EGFR in confluent *Nf2*$^{-/-}$ cells. Reintroduction of wild-type (either M17 or M16; isoform I or II) but not mutant (L64P) Merlin reduced the levels of phosphorylated but not total EGFR. Immunoblotting using anti-Merlin antibodies revealed the expression of each Merlin isoform. U, uninfected. Panels B and C. Schwann cells isolated from E12.5 *Nf2*$^{lox/lox}$ DRG were infected with empty adenovirus (left, wild-type) or Ad-Cre (right, *Nf2*$^{-/-}$) and grown to confluence in either N2 plus NRG plus forskolin (B) or in N2 medium alone without NRG (C). Cells were exposed to Brd for 2 hours.

Signal Transduction in Primary *Nf1*-Deficient Hematopoietic Cells. A previous biochemical investigation of *Mx1-Cre, Nf1*$^{flox/flox}$ mice with MPD surprisingly revealed only modestly elevated levels of phopsho-MEK and phospho-ERK in the Mac1$^{+}$ fraction of bone marrow and spleen cells (16). By contrast, myeloid cell lines generated from *Nf1-/-* fetal liver cells show markedly elevated levels of Ras-GTP and hyperactivation of MEK and Akt, which infer that components of the Raf1-MEK-ERK and PI3 kinase/Akt/mTOR sigaling cascades are rational targets for drug development (40). The Shannon lab is exploiting bone marrow cells from *Mx1-Cre, Nf1*$^{flox/flox}$ mice in a concerted effort to extend their observations in *Nf1-/-* cell lines to primary cells. They considered a number of possible explanations for the subtle signaling differences that were detected in primary *Nf1-/-* bone marrow cells. First, the experimental conditions used to collect, starve, and stimulate primary cells might have obscured *in vivo* differences in the activation status of Ras and its downstream effectors between *Nf1*-deficient and normal bone marrow. Alternatively, because hematopoietic cells at various stages of differentiation are present in *Mx1-Cre, Nf1*$^{flox/flox}$ mice with MPD, aberrant activation of effector cascades within a minor subpopulation of immature myeloid cells would not be detected in lysates of whole bone marrow or spleen. Finally, primary *Nf1*-deficient cells might respond to hyperactive Ras by remodeling signaling networks over time. These potential explanations are not mutually exclusive, and all three may be operative at some level.

To address these issues, the Shannon lab first interrogated the activation status of a series of signaling molecules downstream of Ras in bone marrow cells *Mx1-Cre, Nf1*$^{flox/flox}$ mice under a variety of experimental conditions. They discovered that incubating cells with even a low concentration of serum (0.1%) increased basal signaling and blunted the response to GM-CSF stimulation (data not shown). They went on to define serum-free culture conditions under which wild-type and mutant cells down-regulated Ras-dependent pathways that could be robustly activated by adding serum and GM-CSF. These studies showed that optimal conditions for short-term culture include the use of serum-free medium supplemented with 1% BSA. Signaling experiments performed under these optimized conditions uncovered profound differences between wild-type and *Nf1-/-* bone marrow cells in the activation of effectors such as MEK and Akt that had been investigated previously (Fig. 9). Remarkably, they also observed pronounced differences in the activation status of components such as p70S6 kinase, a downstram target of Akt, under basal conditions and after stimulation with GM-CSF and/or serum (Fig. 9). These data also support testing agents that target components of the Raf1-MEK-ERK and PI3 kinase/Akt/mTOR signaling cascades in NF1-associated tumors. These potential therapeutics include a Raf kinase inhibitor developed by Bayer/Onyx, MEK kinase inhibitors, and the mTOR inhibitor rapamycin.

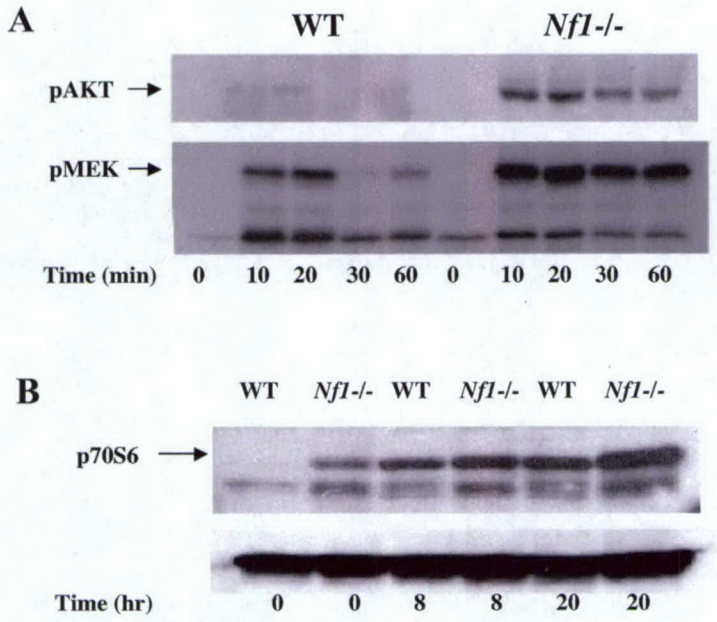


**Figure 9**. Signal transduction in bone marrow mononuclear cells from wild-type (WT) and *Mx1-Cre, Nf1* mutant mice with MPD. Panel A. show elevated basal levels of phosphorylated Akt and MEK with hyperactivation upon exposure to GM-CSF + serum. Panels B. *Nf1-/-* bone marrow cells have elevated levels of p70S6 kinase, which increase over time in culture after treatment with GM-CSF + serum. The levels of phosphorylated p70S6 kinase are also increased in *Nf1-/-* cells not shown).

The Shannon lab recently generated preliminary data indicating that bone marrow cells collected from *Mx1-Cre, Nf1*$^{flox/flox}$ mice with MPD show more profound signaling alterations that cells from mice that have not yet developed elevated white blood cell counts or enlarged spleens. It is uncertain if these differences are accounted for by the progressive increase in myeloid cells as the MPD develops, or if qualitative changes occur over time. Addressing this question will require methodologies for accurately assessing the phosphorylation status of signaling molecules in small subpopulations of primary cells. To achieve this goal, the Shannon lab is collaborating with Dr. Garry Nolan (Stanford) to utilize flow cytometry to measure the activation status of Ras effectors in subpopulations of blood, marrow, and spleen cells at defined

time points after *Nf1* inactivation. The Nolan lab pioneered this technology (41). In preliminary experiments, the Shannon lab found that levels of phopho-ERK increase in response to growth factors (Fig. 10). They are extending this analysis to primary hematopoeitic cells collected from *Mx1-Cre, Nf1*$^{flox/flox}$ mice with and without overt MPD at various times after treatment with pIpC. An important aspect of these studies is the ability to specifically examine signaling in subpopulations of hematopoietic cells such as the Gr1$^{lo}$/Mac1$^{+}$ subset, which is expanded in mice with MPD (14-16). These studies will define the signaling networks of each cell subpopulation in wild-type mice and *Nf1* mutant mice at different stages of the disease, which should uncover pathways that are deregulated directly by *Nf1* before the development of overt MPD. A major consideration for using mouse models of NF1 and NF2 disease as platforms for preclinical testing involves the need to correlate clinical and pharmacodynamic endpoints. Sensitive flow cytometric assays would allow investigators to measure inhibition of relevant biochemical targets by therapeutic agents in small numbers of blood cells without sacrificing the animal. Thus, developing assays of this type has general applicability for testing NF therapeutics with circulating blood cells serving as surrogate markers of tissue bioavailability.

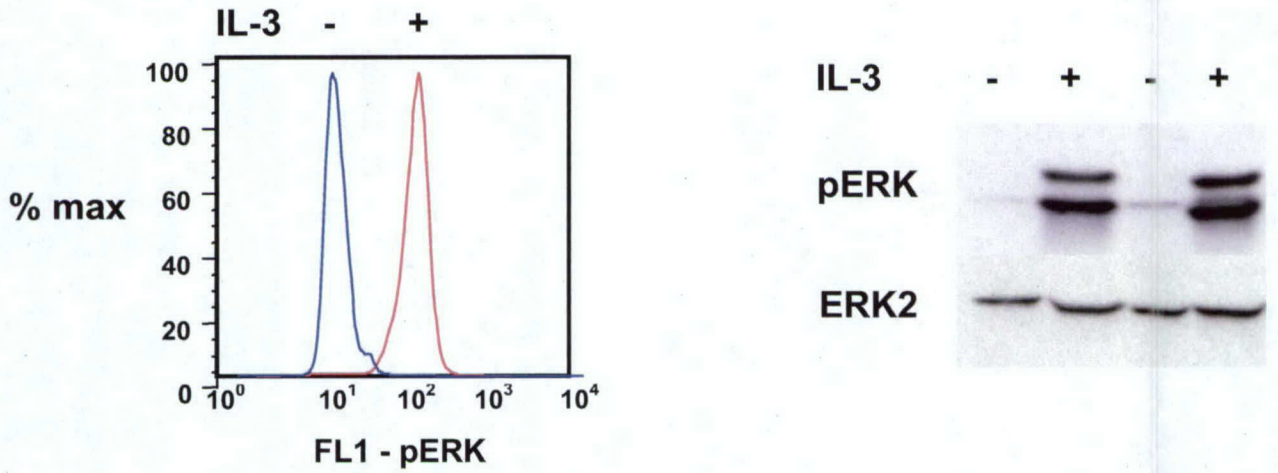


**Figure 10.** Panels A and B. The interluekin-3 dependent pro-B cell line Ba/F3 was starved for 4 hours, then exposed to a saturating dose of IL-3 ("+"). Staining with a conjugated phospho-ERK antibody reveals a marked increase in fluorescence intensity, which corresponds to ERK phosphorylation (panel B).

Ongoing Studies of Ras Processing and Upstream Adapter Molecules as Therapeutic Targets in NF1 Disease. Gab2 is an adapter molecule that links activated hematopoietic growth factor receptors to Ras. Although *Gab2* mutant mice are normal, the ability of the *BCR-ABL* oncogene to induce MPD was recently shown to be Gab2-dependent (42). Since signaling from the GM-CSF receptor plays a central role in the MPD that results from *Nf1* inactivation (15), we reasoned that Gab2 might similarly be required to induce leukemia in *Nf1* mice. The Shannon lab is pursuing a cross between *Mx1-Cre, Nf1*$^{flox/flox}$ and *Gab2* mutant mice to test this hypothesis. If these studies reveal a requirement for Gab2 in disease pathogenesis, this would identify a new class of potential therapeutic targets upstream of Ras and neurofibromin. Compound mutant mice have been generated and are being observed for evidence of MPD. In addition to analyzing the phenotypes of these mice, the Shannon lab will perform detailed cell biologic and biochemical studies.

Merlin Restricts Epithelial Detachment and Anoikis to the Leading Edge of Epithelial Sheets Undergoing Tissue Fusion. Because *Nf2*$^{-/-}$ mouse embryos die early in gestation due to an extraembryonic defect, the consequences of *Nf2* loss in the embryo proper were unknown. To examine merlin's role in development, the Jacks laboratory has again taken advantage of Cre/Lox technology. Through a series of crosses, they have generated mutant embryos that contain one copy of a conditional *Nf2*$^{flox}$ allele, which behaves like the wild-type allele until exposure to Cre recombinase, and one copy of the *Nf2*$^{1lox}$ allele in which the floxed exon 2 has already been deleted. The *Nf2*$^{1lox}$ allele behaves like the null. In addition, the mutant embryos contain a Nestin-Cre transgene. The Nestin-Cre transgene is unusual in that it inserted into an imprinted locus. Thus, mice that inherit paternally derived Nestin-Cre (Nestin-Cre$^{p}$) lose *Nf2* in virtually all cells within the brain and are mosaic for *Nf2* loss in the body, whereas mice that inherit maternally derived Nestin-Cre (Nestin-Cre$^{m}$) are mosaic for *Nf2* loss in the brain and body.

Nestin-Cre$^{p}$;*Nf2*$^{flox/1lox}$ mice exhibit a range of neural tube defects, including craniorachischisis, a condition in which the entire neural tube fails to close. Strikingly, tissue fusion fails at several other sites within the mutant embryos, suggesting that there may be a global requirement for merlin in tissue fusion. To understand on a molecular level the reason for the failure in tissue fusion, the Jacks laboratory studied two tissue fusion events, neural tube closure and eyelid fusion, in detail. Histologically, the mutant neuroepithelium exhibited foci of ectopic epithelial detachment. Loss of adherens junctions was noted in these foci by immunofluoresence for β-catenin and by electron microscopy. Similarly, in the eyelid ridge there was increased intercellular space between epidermal cells, and away from the ridge there was ectopic detachment of peridermal cells. These findings suggest that ectopic epithelial detachment resulting in a paucity of cells was the primary reason for failure of tissue fusion.

Merlin is an Inhibitor of the p21-Activated Kinase PAK1. Until recently, little was known about the biochemical consequences of *Nf2* inactivation. However, data from the McClatchey, Giovannini and Jacks laboratories are providing key insights into the molecular function of merlin and have identified several potential therapeutic targets. For example, accumulating evidence indicates a reciprocal relationship between merlin and the small GTPase Rac1. Drs. McClatchey and Jacks demonstrated that Rac1 activation leads to phosphorylation, reduced membrane:cytoskeleton association and impaired growth suppressing activity of merlin (30). Conversely, merlin overexpression blocks Rac activation and *Nf2*$^{-/-}$ cells exhibit features of excessive Rac signaling. A similar reciprocal relationship between the closely related ERM proteins and Rho has been demonstrated. The Jacks lab has recently shown that merlin expression inversely correlates with the activity of p21 activated kinases (PAKs), which are downstream regulators of Rac and other signaling pathways (see attached reprint by Kissel, *et al)*. Experiments utilizing conditional over-expression of *Nf2* in a human schwannoma cell line, and conditional deletion of *Nf2* in MEFs have led to this discovery of PAK activity regulation by merlin. In addition, merlin can form physical complexes with PAK, providing a possible mechanism of regulation. The Jacks lab has gone on to demonstrate that the interaction of merlin and PAK1 is dynamic and influenced by cellular adhesion and cell density (33). Complementary data have been published by the group of Maruta (31). These results provide a new therapeutic target for *Nf2* mutant tumors.

Growth and Survival of *Nf2*$^{-/-}$ Schwann cells (SC). SCs play a central role in the pathologic complications of NF2. It is therefore essential to rigorously interrogate the consequences of *Nf2*-deficiency in this cell type. Using their studies of primary *Nf2*$^{-/-}$ cells of other types as a guide, Drs. McClatchey and Giovannini have generated primary SC cultures from the conditional *Nf2*-mutant mice and begun to ask whether the 'signatures' of *Nf2*-deficiency found in other cell types are also apparent in SC.

Preliminary studies utilized primary SC isolated from the DRG of E12.5 *Nf2*$^{lox/lox}$ embryos or the sciatic nerves of 3-week-old mice. The cultures were infected with experimentally determined titers of empty vector or *Ad-Cre*. Recombination of the conditional allele was confirmed by PCR and loss of merlin was confirmed by Western blot. *Nf2*$^{-/-}$ SC isolated from the E12.5 DRG exhibited a marked growth advantage and, like other *Nf2*$^{-/-}$cell types, did not undergo contact-dependent inhibition of proliferation. Importantly, *Nf2*$^{-/-}$ SC also proliferated well without exogenous neuregulin (NRG or GGF); in contrast, wild-type SC are completely dependent upon NRG. Moreover, *Nf2*$^{-/-}$ SC readily formed subcutaneous tumors in nude mice, suggesting that few, if any additional genetic events are required for their transformation. Finally, preliminary studies indicate that the proliferation of wild-type and *Nf2*$^{-/-}$ SC isolated from the sciatic nerve of 3-week old mice is comparable, suggesting that either the timing or anatomical location may be a critical factor in determining the sensitivity of SC to *Nf2*-deficiency (not shown). The *P0-tva* and *P0-Cre*$^{ER}$ mice described above represent valuable tools for defining the temporal and spatial sensitivity of SC to *Nf2*-deficiency.

Dr. Giovannini devised a method to purify mitotically active SC from peripheral nerves of adult mice. Nerves are pre-degenerated *in vitro* for 7 days and after dissociation cells are plated on poly-L-lysine/laminin coated dishes in N2 serum-free culture medium supplemented with forskolin and heregulin-ß1. Primary cultures are purified from contaminating fibroblasts by magnetic cell sorting (MACS) based on SC membrane specific expression of p75$^{NGFR}$ and enriched to about 99% of SC after MACS from 34% to 91% before sorting. After sorting, purified wild-type adult mouse SC can be propagated for 3 passages until confluent to a total surface of 160 cm$^2$/mouse (2 sciatic and 2 trigeminal nerves). In addition, they have shown that this method can be used to purify tumoral SC from mouse NF2 and NF1-related schwannomas and neurofibromas.

Transcriptome Analysis of *Nf2* Mutant SC. To identify genes that are altered secondary to *Nf2* loss and that might be relevant to peripheral nerve tumorigenesis, Dr. Giovannini's lab has compared transcriptome of wild type and *Nf2* mutant SC samples (*Nf2*$^{flox/flox}$, *Nf2*$^{flox/flox}$ + adLacZ ; *Nf2*$^{flox/flox}$ + adCre, *Nf2*$^{+/+}$ +adCr ; *Nf2*$^{-/-}$ TXF) using microarray technology. *Nf2*$^{-/-}$ TXF cells had the greatest number of changes, and a more dramatic change in phenotype than the *Nf2*$^{-/-}$ mutant cells. Fifty five genes were expressed >2-fold above wild type levels in *Nf2*$^{-/-}$ versus wild-type SC, and 41 genes showed decreased expression ($p<0.05$, result of 3 independent experiments using MAS and d-Chip softwares). Differentially expressed genes were validated using QRT-PCR to obtain fold change in gene expression comparable to microarray analysis (43)with an ABI Prism 7700 Sequence Detection System. Dr. Giovannini is currently analyzing the transcriptome of human NF2-associated schwannomas. Cross-species comparison between these two transcriptomes will hopefully uncover new therapeutic targets in NF2-related tumorigenesis.

*Aim 3. Preclinical Studies of Experimental Therapeutics in Mouse Models*

Preclinical Evaluation of a MEK Inhibitor in the JMML Model. MEK is a dual specificity kinase that catalyzes the phosphorylation of $p44^{MAPK}$ (ERK1) and of $p42^{MAPK}$ (ERK2). In myeloid cells, MEK is directly activated by Raf and by cross-cascade signaling from the PI3K pathway (data not shown). PD184352 was identified in a screen for small molecule inhibitors of MEK (44). Biochemical studies infer an allosteric mechanism of action. PD184352 is a potent inhibitor of MAPK activation in cancer cell lines, and it induced regression of explanted tumors in nude mice that correlated with *in vivo* effects on MAPK phosphorylation (44). PD184352 is undergoing phase 1 testing in refractory malignancies. Dr. Shannon obtained PD184352 from Pfizer, Inc., and is currently studying this agent in the *Mx1-Cre, Nf1*$^{flox/flox}$ model of JMML. Dr. Shannon has shown that 0.01 μM to 10 μM of PD184352 abrogates CFU-GM colony formation in response to GM-CSF from normal murine bone marrow as well as from wild-type and *Nf1*$^{-/-}$ fetal livers (data not shown). A 4 week toxicity study in wild-type mice, in which treated animals received twice daily doses of 100 mg/kg of PD184352, showed that the drug was tolerated at this dose and blocked ERK activation by GM-CSF for ~4 hours. Thus, in contrast to FTI, PD184352 markedly inhibits a relevant biochemical target in primary *Nf1* mutant cells at tolerable doses. A controlled preclinical study was then performed in which this schedule was administered to *Mx1-Cre Nf1*$^{flox/flox}$ mice with MPD. Although PD184352 was well tolerated and we could demonstrate ERK kinase inhibition 2 and 4 hours after treatment, there was no beneficial effect on the MPD. In fact, control mice that were treated with this compound showed evidence of a reactive myeloproliferation, which is likely due to transient inhibition of hematopoiesis. We believe that better target inhibition will be required to assess the therapeutic efficacy and toxicity of this compound; however, PD184352 is difficult to administer more then twice daily and cannot be given through an implantable device. We are preparing these findings for publication and hope to obtain and screen better compounds in the tractable *Mx1-Cre Nf1*$^{flox/flox}$ model.

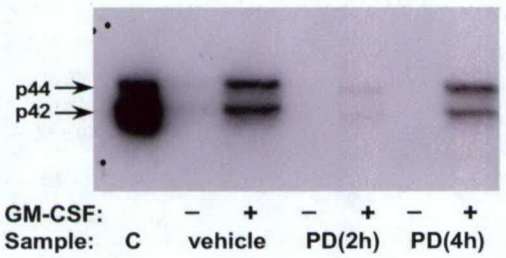


**Figure 11**. Phospho-ERK Western blot of *Nf1*$^{-/-}$ bone marow cells from mice treated with vehicle or the MEK inhibitor PD184352 (PD), analyzed 2h or 4h after treatment. Cells were starved, and indicated samples were stimulated with GM-CSF. Sample C, control 3T3 cells stimulated with platelet derived growth factor.

Preclinical Studies in the *Krox20 Nf1*$^{flox/flox}$ Model of Neurofibroma. The Parada lab is testing Gleevec to investigate if blocking c-kit receptor activity can hinder *Nf1* heterozygous mast cells from invading peripheral nerves and thus contributing to neurofibroma formation. In addition Brisotl Mayer Squibb has recently agreed to enter into a collaboration that will provide their new generations of c-kit inhibiting compounds. The outcome of these studies will help to define the functional role of mast cells in neurofibroma formation and could lead to therapies for NF1 patients in the near future.

*Aim 4. To sponsor specialized working group meetings and to support preclinical testing in mouse models of NF1 and NF2.*

Workshop on Pathologic Classification of Tumors in NF Mouse Models. Drs. Small and Giovannini organized a meeting of pathologists and basic scientists on February 8-10, 2003, in Boston, Massachusetts, to review all available genetically engineered murine (GEM) models of NF1 and NF2, and to draft a pathological classification of murine peripheral nerve sheath tumors to characterize these lesions in a uniform and consistent manner. The meeting and pathological classification followed a format successfully adopted by similar pathology workshops for murine models of other organ systems. Dr. Anat Stemmer-Rachamimov (Harvard University), who has extensive expertise in NF-associated tumors, led a panel of 10 pathologists that reviewed lesions from most published and unpublished NF mouse models and compared their histological features with the corresponding human tumors.

The panel members, who have different areas of expertise, reviewed 56 lesions from 8 laboratories. In formulating the GEM classification of peripheral nerve sheath tumors, the panel referred to criteria and terminology devised by the World Health Organization for classifying human nervous system tumors (45). However, although the WHO classification served as a useful point of reference, it was not adopted for the classification of the GEM lesions because of some important differences between the human and murine tumors. The WHO classification of human peripheral nerve sheath tumors (PNSTs) is based on both histological and clinical characteristics (and describes clinico-pathological entities), whereas the GEM classification must necessarily be based on histological features alone, as clinical features of murine PNSTs are not yet known. Furthermore, although many of the histological features displayed by GEM PNSTs were similar to those observed in human tumors, some GEM lesions presented unique and distinct morphology, and did not fit into the human classification by histological criteria.

In addition, because the human tumor nomenclature refers to histological features as well as predicted clinical behavior of tumors, some of these terms were deemed inappropriate for description of GEM tumors, in which biological behavior is still unknown. The panel therefore proposed a novel classification for GEM nerve sheath tumors based purely on morphological features. Although the term "grade" is used in the GEM classification, it is applied as a histological descriptor only and has no predictable bearing on the biological behavior of the tumor in the animals. In other words, as opposed to the WHO classification where grade is an indicator of biological behavior, grading in the GEM classification refers merely to the presence or absence of specific histological features such as high cellularity, necrosis, nuclear pleomorphism and brisk mitotic activity.

This classification represents a valuable tool for standardization and validation of tumors arising in NF mouse models, as it facilitates direct comparisons between models and enables effective design and interpretation of preclinical trials that are directly relevant to human NF disease. Finally, the panel also recommended general guidelines for the work-up and morphological evaluation of peripheral nerve sheath lesions in GEM models. A manuscript is in preparation, which describes the guidelines developed through this highly interactive and collaborative effort.

Workshop on Preclinical Therapeutics in NF Mouse Models. Dr. Shannon is organizing a second workshop that will be held in the summer-fall of 2005. This meeting will explore how mouse models of NF-associated tumors might be used to evaluate therapeutics. Dr. Shannon,

who is playing a leading role in this area within the MMHCC, will co-chair this meeting with an expert in human clinical trial design.

**KEY RESEARCH ACCOMPLISHMENTS**

(a) The investigators continue to extensively share expertise and reagents to pursue common research goals.

(b) The NF Modeling Group is participating in the activities of the MMHCC and is contributing to achieving the goals of this national cancer research inititative.

(c) We have developed accurate models of most NF1 and NF2-assocated tumors, have characterized these lesions, and are pursuing the goals of developing additional models and of enhancing existing mutant strains.

(d) The *Krox20 Nf1*$^{flox/flox}$ model of neurofibroma was enhanced by crossing onto a *p53* mutant strain background. These mice develop neurofibromas with reduced latency and our preliminary studies infer that this will be a robust *in vivo* model of MPNST.

(e) Pak-1 was shown to be is regulated by merlin, thus establishing this signaling kinase as an attractive therapeutic target.

(f) Signatures of *Nf2*-deficiency were shown to be loss of contact inhibition of proliferation, failure to form stable adherens junctions and failure to silence EGFR signaling upon cell:cell contact. EGFR inhibitors block the proliferation of primary *Nf2*-/- cells. Preliminary data indicate that the *Nf2*-/- Schwann cells also fail to undergo contact-dependent inhibition of proliferation and can proliferate in the absence of GGF.

(g) A new method was developed for isolating mitotically active Schwann cells.

(h) Progress was made toward engineering a mouse model of ependymona.

(i) A novel strain of drug-inducible Cre mice was constructed that will permit regulated deletions between loxP elements. These mice are being harnessed to inactivate of the *Nf2* gene in specific tissues at defined time points.

(j) *Mx1-Cre Nf1*$^{flox/flox}$ mice provide a tractable model of JMML that is being harnessed to fully characterize the biochemical consequences of *Nf1* inactivation in primary cells and to test an inhibitor of MEK *in vivo* with correlative biochemical (pharmacodynamic) monitoring.

(k) Radiation was shown to cooperate strongly with heterozygous *Nf1* inactivation in tumorigenesis.

(m) Strains of mutant mice have been shared widely with the NF research community (see list below in Reportable Outcomes). Through these collaborative experiments, the scientific

value of this Consortium has extended well beyond the studies being pursued in the participant's laboratories.

## REPORTABLE OUTCOMES

### (a) Previous Research Articles and Reviews (2000 – 2003)

Parada LF. Neurofibromatosis Type 1. *BBA,* 2000, 147, M13-M19.

Zhu Y, Romero M, Ghosh P, Charnay P, Rushing EJ, Marth J and Parada LF. Ablation of NF1 function in neurons induces abnormal development of cerebral cortex and reactive gliosis in the CNS and PNS. *Genes & Dev.,* 2000, 5:859-876.

McClatchey AI and Cichowski K. Mouse models of neurofibromatosis. *Biochim. Biophys. Acta* 2001;1471:M73-80.

Shannon KM, Le Beau MM, Largaespada DA and Killeen N. Modeling myeloid leukemia tumor suppressor gene inactivation in the mouse. *Semin. Cancer Biol.* 2001; 11: 191-199.

Shaw RJ, Paez JG, Curto M, Yaktine A, Pruitt WM, Saotome I, O'Bryan JP, Gupta V, Ratner N, Der CJ, Jacks T and McClatchey AI. The Nf2 tumor suppressor, merlin, functions in Rac-dependent signaling. *Dev. Cell,* 2001, 1:63-72.

Zhu Y and Parada LF. Neurofibromin, a tumor suppressor of the nervous system. *Exp. Cell Research,* 2001, 264, 19-28.

Bajenaru ML*, Zhu Y*, Hedrick NM, Donahoe J, Parada LF and Gutmann DH. Astrocyte-specific inactivation of the neurofibromatosis 1 (Nf1) gene is insufficient for astrocytoma formation. *Mol. Cell Biology,* 2002, 22:5100-5113 (*co-first authors).

Donovan S, Shannon KM and Bollag GE. GTPase activating proteins: critical regulators of intracellular signaling. *Biochem. Biophy.s Acta,* 2002, 1602:23-45.

Gautreau A, Manent J, Fievet B, Louvard D, Giovannini M and Arpin M. Mutant products of the NF2 tumor suppressor gene are degraded by the ubiquitin-proteasome pathway. *J Biol Chem*., 2002, 277:31279-82.

Gutmann D and Giovannini M. Mouse models of neurofibromatosis type 1 and 2. *Neoplasia,* 2002; 4: 279-290.

Gutmann D, Wu YL, Hedrick NM, Zhu Y, Guha A and Parada LF. Heterozygosity for the neurofibromatosis 1 *(Nf1)* tumor suppressor results in abnormalities in cell attachment, spreading and motility in astrocytes. *Human Molecular Genetics,* 2002, 10:3009-3016.

Johnson KC, Kissil JL Fry JL and Jacks T. Cellular transformation by a FERM domain mutant of the NF2 tumor suppressor gene. *Oncogene* 2002, 21:5990-97.

Kalamarides M, Niwa-Kawakita M, Leblois H, Abramowski V, Perricaudet M, Janin A, Thomas G, Gutmann D and Giovannini M. *Nf2* gene inactivation in arachnoidal cells is rate-limiting for meningioma development in the mouse. *Genes & Development,* 2002, 16:1060-1065.

Kissil JL, Johnson KC, Eckman MS and Jacks T. Merlin Phosphorylation by p21-activated Kinase 2 and Effects of Phosphorylation on Merlin Localization. *J Biol Chem*. 2002; 277:10394-99.

Le DT and Shannon KM. Ras processing as a therapeutic target in hematologic malignancies. *Curr. Opin. Hematol.,* 2002, 9:308-315.

Li H, Velasco-Miguel S, Vass WC, Parada LF and DeClue JE. Epidermal growth factor receptor (EGFR) signaling pathways are associated with tumorigenesis in *Nf1:p53* mouse tumor-derived cell lines. *Cancer Res.,* 2002, 8:616-26.

Messerli SM, Tang Y, Giovannini M, Bronson R, Weissleder R and Breakefield XO. Detection of spontaneous schwannomas by MRI in a transgenic murine model of neurofibromatosis type 2. *Neoplasia*, 2002, 4:501-509.

Sun CX, Haipek C, Scoles DR, Pulst SM, Giovannini M, Komada M and Gutmann DH. Functional analysis of the relationship between the neurofibromatosis 2 (NF2) tumor suppressor and its binding partner, hepatocyte growth factor-regulated tyrosine kinase substrate (HRS/HGS). *Hum. Mol. Gen.,* 2002, 11:3167-3178.

Weiss WA, Israel M, Cobbs C, Holland E, James CD, Louis DN, Marks C, McClatchey AI, Roberts T, Van Dyke T, Wetmore C, Chiu IM, Giovannini M, Guha A, Higgins RJ, Marino S, Radovanovic I, Reilly K, Aldape K. Neuropathology of genetically engineered mice: consensus report and recommendations from an international forum. *Oncogene*, 2002, 21(49):7453-63.

Zhu Y, Ghosh P, Charnay P, Burns DK, and Parada LF. Neurofibromas in NF1:Schwann cell origin and role of tumor environment. *Science,* 2002, 296:920-2.

Zhu Y and Parada LF. The molecular and genetic basis of neurologic tumours. *Nature Reviews on Cancer,* 2002, 8:616-26.

Aiyagari A, Taylor B, Aurora V, Young SG and Shannon KM. Hematologic effects of inactivating the Ras processing enzyme *Rce1*. *Blood* 2003; 101: 2250-2252.

Cichowski K, Santiago S, Jardim M, Johnson BW, Jacks T. Dynamic regulation of the Ras pathway via proteolysis of the NF1 tumor suppressor. *Genes Dev*. 2003. 17(4):449-54

Crone SA, Negro A, Trumpp A, Giovannini M, and Lee KF. Colonic Epithelial Expression of ErbB2 Is Required for Postnatal Maintenance of the Enteric Nervous System. *Neuron*, 2003, 37(1):29-40.

Denisenko-Nehrbass N, Goutebroze L, Galvez T, Bonnon C, Stankoff B, Ezan P, Giovannini M, Faivre-Sarrailh C, and Girault JA. Association of Caspr/paranodin with tumor suppressor schwannomin/merlin and b1 integrin in the CNS. *J. Neurochem.*, 2003, 84 :209-221.

Fleury-Feith J, Lecomte C, Renier A, Matrat M, Kheuang L, Abramowski A, Levy F, Janin A, Giovannini M and Jaurand M-C. Hemizygosity of Nf2 is associated with increased susceptibility to asbestos-induced peritoneal tumours. *Oncogene*, 2003, 22:3799-3805.

Gitler, A.D.*, Zhu, Y.*, Lu, M.M., Parada, L.F., and Epstein, J.A. Nf1 has an essential role in endothelial cells. *Nat. Genet.,* 2003, 33(1):75-9. (*co-first authors).

Gutmann DH, Baker SJ, Giovannini M, Garbow J and Weiss W. Mouse models of human cancer consortium symposium on nervous system tumors. *Cancer Res.*, 2003, 63(11):3001-4.

Ingram DJ, Wenning MJ, Shannon K and Clapp DW. Leukemic potential of doubly mutant *Nf1* and $W^v$ hematopoietic cells. *Blood* 2003; 101: 1984-1986.

Kissil JL, Wilker EW, Johnson KC, Eckman MS, Yaffe M, and Jacks T. Merlin, the product of the *Nf2* tumor suppressor gene, is an inhibitor of the p21-activated kinase Pak1. *Mol Cell* 2003; 12(4):841-849.

Lallemand D, Curto M, Saotome I, Giovannini M and McClatchey AI. *NF2* deficiency promotes tumorigenesis and metastasis by destabilizing adherens junctions. *Genes & Dev.*, 2003, 17(9):1090-100.

Leneuve P, Colnot S, Hamard G, Francis F, Niwa-Kawakita M, Giovannini M and Holzenberger M. Cre-mediated germline mosaicism: A new transgenic mouse for the selective removal of residual markers from tri-low conditional alleles. *Nucleic Acids Res.,* 2003, 31(5):1-8.

Manent J, Oguievetskaia X, Bayer J, Ratner N and Giovannini M. Magnetic cell sorting for enriching Schwann cells from adult mouse peripheral nerves. *J. Neuroscience Meth.*, 2003, 123:167-173.

McLaughlin, ME and Jacks, T. Progesterone receptor expression in neurofibromas. *Cancer Research,* 2003; 63 (4): 752-755.

McLaughlin, ME and Jacks, T. 2002. Thinking beyond the tumor cell: *Nf1* haploinsufficiency in the tumor environment. *Cancer Cell: June 2002*

McLaughlin, ME and Jacks, T. Neurofibromatosis type 1. *Methods Mol Biol.* 2003; 222:223-37.

McLaughlin, ME, Robson, CD, Kieran, MW, Jacks T, Pomeroy, SL, Cameron, S. Marked regression of metastatic pilocytic astrocytoma during treatment with imatinib mesylate (STI-571, Gleevec): a case report and laboratory investigation. *J Pediatr Hematol Oncol.* 2003; 25(8):644-8

McClatchey AI. Merlin and ERM proteins: unappreciated roles in cancer development? *Nat. Rev. Cancer,* 2003, 3:877-883.

Utermark T, Aleko A, Lerche H, Abramowski V, Giovannini M and Hanemann CO. Quinidine reduces proliferation in human malignant mesothelioma cell lines lacking Schwannomin/Merlin but not in those expressing the neurofibromatosis type 2 tumor suppressor gene. *Cancer*, 2003, 97:1955-1962.

Weiss BG and Shannon KM. Mouse cancer models as a platform for performing preclinical therapeutic trials. *Curr. Opin. Genet. Dev.,* 2003, 13(1): 84-9.

Yajnik V, Paulding C, Sordella R, McClatchey AI, Saito M, Wahrer DC, Reynolds P, Bell DW, Lake R, van den Heuvel S, Settleman J and Haber DA. DOCK4, a GTPase activator, is disrupted during tumorigenesis. *Cell*, 2003, 112(5):673-84.

**Publications in 2004-2005**

Curto, M, Liu, C, Lallemand, D and McClatchey, AI. The *Nf2* tumor suppressor, Merlin, controls contact-dependent EGFR silencing. (in revision).

Le DT, Kong N, Zhu Y, Aiyigari A, Braun BS, Wang E, Kogan SC, Le Beau MM, Parada L, Shannon KM. Somatic inactivation of *Nf1* in hematopoietic cells results in a progressive myeloproliferative disorder. *Blood* 2004; **103:** 4243-4250.

Weiss BG, Shannon KM. Preclinical trials in mouse cancer models *in* Holland EC (ed): Mouse Models of Human Cancer, Wiley-Liss, Hoboken NJ, 2004: pp. 437-446.

Romero M.I., Zhu Y., Lush, M.E., and Parada, L.F. Neuron-specific deletion of NF1 enhances functional recovery after spinal cord Sensory denervation. Submitted

Zhu, Y., Harada, T., Guignard, F., Harada, C., Burns, D. K., Bajenaru, M.L, Gutmann, D.H., Messing, A., and Parada, L.F. Ablation of NF1 in CNS causes transient neural progenitor hyperplasia and is sufficient to induce optic gliomas. Submitted.

**(b) Model Development and Distribution to the Research Community**

Studies conducted to date have established a number of novel models of NF1 and NF2-associated tumors and have generated several new strains of mice. *Nf1* and *Nf2* mutant mice have been deposited in the MMHCC Repository where they are readily available to the research community. In addition, the participants in this Consortium have provided strains directly to the investigators listed below.

Karlene Reilly (National Cancer Institute)
Jeffrey DeClue (National Cancer Institute)
Jonathan Epstein (University of Pennsylvania)
D. Wade Clapp (Indiana University)
David Guttmann (Washington University)

David Largaespada (University of Minnesota)
Jeffrey Lawrence (UCSF)
Alcino Silva (UCLA)
Gerard Karsenty (Baylor)
Shaojun Tang (UC Irvine)
Shalom Avraham (Beth Israel)
James Bieker (Mount Sinai, New York)
Abhijit Guha (Labatt Brain Tumor Research Center, Tornoto)
Andreas Kurtz, (Harvard)
Jim Gussella (Harvard)
Dan Haber (Harvard)
Antonio Chiocca (Harvard)
Isidro Sanchez-Garcia (IBMCC)
Victor Tybulewicz (National Institute for Medical Research, London)
Lindsay Hinck (UC Santa Cruz)
Keqiang Ye (Emory University School of Medicine)
Lynda Chin (Dana Farber Cancer Institute)
Joseph Testa (Fox Chase Cancer Center)
Nancy Ratner (U. of Cincinnati)
Stefan Mundlos (U. of Berlin)
Juha Peltonen (U. of Helsinki, Finland)
Warren Pear (University of Pennsylvania)

**(c) Employment and Research Opportunities**

This award has provided salary support for technical personnel in each of participating labs.

**CONCLUSIONS**

During the fourth year of its existence, this consortium made progress in accomplishing its primary goal of generating and characterizing mouse models of NF1 and NF2-associated tumors for biologic and preclinical therapeutic trials. A number of novel strains have been developed and reported, innovative strategies were deployed to make optimal use of these resources, and our recent research has provided a number of novel insights regarding mechnsism of tumor formation in Nf1 and NF2 patients, and have suggested potential therapeutic targets in NF disease. The investigators have collaborated closely and have shared expertise and reagents extensively. The proceedings of the meeting on Pathologic Classification of Mouse Models of NF-Associated Tumors, which Dr. Giovanini organized, were published in *Cancer Research* a highly successful meeting that focused. This NF Consortium is a full participant in the Mouse Models of Human Cancer Consortium of the NCI.

## REFERENCES

1. Brannan CI, Perkins AS, Vogel KS, Ratner N, Nordlund ML, Reid SW, et al. Targeted disruption of the neurofibromatosis type 1 gene leads to developmental abnormalities in heart and various neural crest-derived tissues. Genes and Development 1994;8:1019-1029.
2. Jacks T, Shih S, Schmitt EM, Bronson RT, Bernards A, Weinberg RA. Tumorigenic and developmental consequences of a targeted *Nf1* mutation in the mouse. Nat Genet 1994;7:353-361.
3. Zhu Y, Romero MI, Ghosh P, Ye Z, Charnay P, Rushing EJ, et al. Ablation of NF1 function in neurons induces abnormal development of cerebral cortex and reactive gliosis in the brain. Genes Dev 2001;15(7):859-76.
4. McClatchey AI, Saotome I, Ramesh V, Gusella JF, Jacks T. The Nf2 tumor suppressor gene product is essential for extraembryonic development immediately prior to gastrulation. Genes Dev 1997;11(10):1253-65.
5. Giovannini M, Robanus-Maandag E, Niwa-Kawakita M, van der Valk M, Woodruff JM, Goutebroze L, et al. Schwann cell hyperplasia and tumors in transgenic mice expressing a naturally occurring mutant NF2 protein. Genes Dev 1999;13(8):978-86.
6. Giovannini M, Robanus-Maandag E, van der Valk M, Niwa-Kawakita M, Abramowski V, Goutebroze L, et al. Conditional biallelic Nf2 mutation in the mouse promotes manifestations of human neurofibromatosis type 2. Genes Dev 2000;14(13):1617-30.
7. Cichowski K, Shih TS, Schmitt E, Santiago S, Reilly K, McLaughlin ME, et al. Mouse models of tumor development in neurofibromatosis type 1. Science 1999;286(5447):2172-6.
8. Zhu Y, Ghosh P, Charnay P, Burns DK, Parada LF. Neurofibromas in NF1: Schwann cell origin and role of tumor environment. Science 2002;296(5569):920-2.
9. Zhu Y, Parada LF. Neurofibromin, a tumor suppressor in the nervous system. Exp Cell Res 2001;264(1):19-28.
10. Mahgoub N, Taylor B, Le Beau M, Gratiot M, Carlson K, Jacks T, et al. Myeloid malignancies induced by alkylating agents in Nf1 mice. Blood 1999;93:3617-3623.
11. Mahgoub N, Taylor BR, Gratiot M, Kohl NE, Gibbs JB, Jacks T, et al. In vitro and In vivo effects of a farnesyltransferase inhibitor on Nf1- deficient hematopoietic cells. Blood 1999;94(7):2469-76.
12. Reilly KM, Loisel DA, Bronson RT, McLaughlin ME, Jacks T. Nf1;Trp53 mutant mice develop glioblastoma with evidence of strain- specific effects. Nat Genet 2000;26(1):109-13.
13. Arico M, Biondi A, Pui C-H. Juvenile myelomonocytic leukemia. Blood 1997;90:479-488.
14. Largaespada DA, Brannan CI, Jenkins NA, Copeland NG. *Nf1* deficiency causes Ras-mediated granulocyte-macrophage colony stimulating factor hypersensitivity and chronic myeloid leukemia. Nat Genet 1996;12:137-143.
15. Birnbaum RA, O'Marcaigh A, Wardak Z, Zhang YY, Dranoff G, Jacks T, et al. Nf1 and Gmcsf interact in myeloid leukemogenesis. Mol Cell 2000;5(1):189-95.
16. Le DT, Kong N, Zhu Y, Lauchle JO, Aiyigari A, Braun BS, et al. Somatic inactivation of Nf1 in hematopoietic cells results in a progressive myeloproliferative disorder. Blood 2004;103(11):4243-50.
17. Listernick R, Charrow J, Gutmann DH. Intracranial gliomas in neurofibromatosis type 1. Am J Med Genet 1999;89(1):38-44.

18. Listernick R, Louis DN, Packer RJ, Gutmann DH. Optic pathway gliomas in children with neurofibromatosis 1: consensus statement from the NF1 Optic Pathway Glioma Task Force. Ann Neurol 1997;41(2):143-9.
19. Sherman L, Sleeman JP, Hennigan RF, Herrlich P, Ratner N. Overexpression of activated neu/erbB2 initiates immortalization and malignant transformation of immature Schwann cells in vitro. Oncogene 1999;18(48):6692-9.
20. Jin JJ, Nikitin A, Rajewsky MF. Schwann cell lineage-specific neu (erbB-2) gene expression in the developing rat nervous system. Cell Growth Differ 1993;4(3):227-37.
21. Maris JM, Wiersma SR, Mahgoub N, Thompson P, Geyer RJ, Lange BJ, et al. Monosomy 7 myelodysplastic syndrome and other second malignant neoplasms in children with neurofibromatosis type 1. Cancer 1997;79:1438-46.
22. Papageorgio C, Seiter K, Feldman EJ. Therapy-related myelodysplastic syndrome in adults with neurofibromatosis. Leuk Lymphoma 1999;32(5-6):605-8.
23. Side LE, Shannon KM. The NF1 gene as a tumor suppressor. In: Upashyaya M, Cooper DN, editors. Neurofibromatosis type 1. Oxford, UK: Bios Scientific Publishers; 1998. p. 133-152.
24. Vogel KS, Klesse LJ, Velasco-Miguel S, Meyers K, Rushing EJ, Parada LF. Mouse tumor model for neurofibromatosis type 1. Science 1999;286(5447):2176-9.
25. DeClue JE, Heffelfinger S, Benvenuto G, Ling B, Li S, Rui W, et al. Epidermal growth factor receptor expression in neurofibromatosis type 1- related tumors and NF1 animal models. J Clin Invest 2000;105(9):1233-41.
26. Li H, Velasco-Miguel S, Vass WC, Parada LF, DeClue JE. Epidermal growth factor receptor signaling pathways are associated with tumorigenesis in the Nf1:p53 mouse tumor model. Cancer Res 2002;62(15):4507-13.
27. Cichowski K, Santiago S, Jardim M, Johnson BW, Jacks T. Dynamic regulation of the Ras pathway via proteolysis of the NF1 tumor suppressor. Genes Dev 2003;17(4):449-54.
28. Le DT, Shannon KM. Ras processing as a therapeutic target in hematologic malignancies. Curr Opin Hematol 2002;9(4):308-15.
29. Aiyagari AL, Taylor BR, Aurora V, Young SG, Shannon KM. Hematologic effects of inactivating the Ras processing enzyme Rce1. Blood 2003;101(6):2250-2.
30. Shaw R, Paez J, Curto M, Taktine A, Pruitt W, Sadtome I, et al. The neurofibromatosis type 2 tumor suppressor protein, merlin, functions in Rac-dependent signaling. Dev Cell 2001;1:63-72.
31. Hirokawa Y, Tikoo A, Huynh J, Utermark T, Hanemann CO, Giovannini M, et al. A clue to the therapy of neurofibromatosis type 2: NF2/merlin is a PAK1 inhibitor. Cancer J 2004;10(1):20-6.
32. Kissil JL, Johnson KC, Eckman MS, Jacks T. Merlin phosphorylation by p21-activated kinase 2 and effects of phosphorylation on merlin localization. J Biol Chem 2002;277(12):10394-9.
33. Kissil JL, Wilker EW, Johnson KC, Eckman MS, Yaffe MB, Jacks T. Merlin, the product of the Nf2 tumor suppressor gene, is an inhibitor of the p21-activated kinase, Pak1. Mol Cell 2003;12(4):841-9.
34. Lallemand D, Curto M, Saotome I, Giovannini M, McClatchey AI. NF2 deficiency promotes tumorigenesis and metastasis by destabilizing adherens junctions. Genes Dev 2003;17(9):1090-100.

35. James MF, Manchanda N, Gonzalez-Agosti C, Hartwig JH, Ramesh V. The neurofibromatosis 2 protein product merlin selectively binds F-actin but not G-actin, and stabilizes the filaments through a lateral association. Biochem J 2001;356(Pt 2):377-86.
36. Takahashi K, Suzuki K. Density-dependent inhibition of growth involves prevention of EGF receptor activation by E-cadherin-mediated cell-cell adhesion. Exp Cell Res 1996;226(1):214-22.
37. Lampugnani MG, Zanetti A, Breviario F, Balconi G, Orsenigo F, Corada M, et al. VE-cadherin regulates endothelial actin activating Rac and increasing membrane association of Tiam. Mol Biol Cell 2002;13(4):1175-89.
38. Qian X, Karpova T, Sheppard AM, McNally J, Lowy DR. E-cadherin-mediated adhesion inhibits ligand-dependent activation of diverse receptor tyrosine kinases. Embo J 2004;23(8):1739-84.
39. Noble ME, Endicott JA, Johnson LN. Protein kinase inhibitors: insights into drug design from structure. Science 2004;303(5665):1800-5.
40. Donovan S, See W, Bonifas J, Stokoe D, Shannon KM. Hyperactivation of protein kinase B and ERK have discrete effects on survival, proliferation, and cytokine expression in Nf1-deficient myeloid cells. Cancer Cell 2002;2(6):507-14.
41. Perez OD, Nolan GP. Simultaneous measurement of multiple active kinase states using polychromatic flow cytometry. Nat Biotechnol 2002;20(2):155-62.
42. Sattler M, Mohi MG, Pride YB, Quinnan LR, Malouf NA, Podar K, et al. Critical role for Gab2 in transformation by BCR/ABL. Cancer Cell 2002;1(5):479-92.
43. Schmittgen TD. Real-time quantitative PCR. Methods 2001;25(4):383-5.
44. Sebolt-Leopold JS, Dudley DT, Herrera R, Van Becelaere K, Wiland A, Gowan RC, et al. Blockade of the MAP kinase pathway suppresses growth of colon tumors in vivo [see comments]. Nat Med 1999;5(7):810-6.
45. Kleihues P, Sobin LH. World Health Organization classification of tumors. Cancer 2000;88(12):2887.

# Somatic inactivation of *Nf1* in hematopoietic cells results in a progressive myeloproliferative disorder

Doan T. Le, Namie Kong, Yuan Zhu, Jennifer O. Lauchle, Abigail Aiyigari, Benjamin S. Braun, Endi Wang, Scott C. Kogan, Michelle M. Le Beau, Luis Parada, and Kevin M. Shannon

**The *NF1* tumor suppressor gene encodes a guanosine triphosphotase (GTPase)–activating protein that negatively regulates Ras signaling and is inactivated in a subset of juvenile myelomonocytic leukemias (JMMLs). Adoptive transfer of fetal liver cells from *Nf1* mutant mice models JMML; however, this system has important limitations as a platform for performing biologic and preclinical studies. We have exploited the interferon-inducible *Mx1-Cre* transgene to ablate a conditional mutant *Nf1* allele in hematopoietic cells. Somatic inactivation of *Nf1* induces a myeloproliferative disorder with 100% penetrance that is associated with a subacute clinical course, tissue infiltration by myeloid cells, hypersensitivity to granulocyte-macrophage colony stimulating factor, hyperproliferation, and resistance to apoptosis. These *Mx1-Cre, Nf1*$^{flox/flox}$ mice establish a tractable experimental model for testing therapeutics and for identifying mutations that cooperate with hyperactive Ras in myeloid leukemogenesis. (Blood. 2004;103:4243-4250)**



## Introduction

Juvenile myelomonocytic leukemia (JMML) is an aggressive myeloproliferative disease (MPD) characterized by monocytosis, thrombocytopenia, splenomegaly, and malignant infiltration of the skin, lymph nodes, lungs, liver, and other organs (reviewed in Emanuel et al[1] and Arico et al[2]). The clinical course is relentless, and bone marrow transplantation is the only treatment that cures more than 10% of patients. Selective hypersensitivity of granulocyte-macrophage colony-forming unit (CFU-GM) progenitors to granulocyte-macrophage colony-stimulating factor (GM-CSF) is an in vitro hallmark of JMML.[3,4] The incidence of JMML is increased more than 200-fold in children with neurofibromatosis type 1 (NF1)[5,6]; this observation provided a starting point for elucidating the molecular basis of aberrant myeloid growth in this disorder. The *NF1* gene encodes neurofibromin, a guanosine triphosphotase (GTPase)–activating protein (GAP) that negatively regulates p21$^{ras}$ (Ras) output by accelerating GTP hydrolysis (reviewed in Boguski and McCormick,[7] Bernards,[8] and Donovan et al[9]). Analysis of JMML cells from children with NF1 revealed homozygous *NF1* inactivation because of somatic loss of the normal allele, which is associated with hyperactive Ras.[10-13]

Two groups used homologous recombination in embryonic stem cells to disrupt *Nf1*, the murine homolog of *NF1*.[14,15] Approximately 10% of heterozygous ($Nf1^{+/-}$) mutant mice spontaneously develop a MPD that resembles JMML during the second year of life.[14] Homozygous mutant ($Nf1^{-/-}$) embryos fail around embryonic day 13 (E13) with cardiovascular defects[14,15]; however, CFU-GM colonies derived from mutant fetal livers show hypersensitive growth in response to GM-CSF that is similar to human JMML cells.[11,16] Importantly, adoptive transfer of $Nf1^{-/-}$ fetal liver cells consistently induces a JMML-like MPD in irradiated recipient mice.[16] *Nf1* inactivation leads to deregulated growth in multiple hematopoietic compartments and confers a durable proliferative advantage in competitive repopulation assays.[17,18] In addition, a cross between *Nf1* and *Gmcsf* mutant mice demonstrated that aberrant GM-CSF signaling plays a central role in initiating and maintaining the JMML-like MPD in vivo.[19]

In a previous study, irradiated recipient mice that received transplants with $Nf1^{-/-}$ fetal liver cells were harnessed to evaluate the efficacy of an inhibitor of the Ras processing enzyme farnesyltransferase, which included pharmacodynamic monitoring in primary hematopoietic cells.[20] However, this model is both expensive and cumbersome because it requires maintaining a large breeding colony, performing multiple timed matings followed by embryo dissections around E13, and injecting fetal liver cells into irradiated hosts. A "second-generation" mutant strain was recently engineered by introducing loxP sites into the *Nf1* locus by homologous recombination.[21] Somatic inactivation of this $Nf1^{flox}$ allele, which is functionally wild type in the basal state, can be achieved by expressing Cre recombinase in specific cell types.[21,22] We have exploited the interferon-inducible *Mx1-Cre* strain[23] to ablate *Nf1* in hematopoietic cells, and we find that this consistently results in an MPD that is associated with leukocytosis, splenomegaly, hyperproliferation, impaired apoptosis, and in vitro hypersensitivity to GM-CSF. We further describe the consequences of *Nf1* inactivation on proliferation, survival, and Ras signaling in these mice.

From the Department of Pediatrics, University of California, San Francisco, California; the Department of Laboratory Medicine, University of California, San Francisco, California; University of Texas Southwestern, Dallas, Texas; Section of Hematology/Oncology, Department of Medicine, and The Cancer Research Center, University of Chicago, Chicago, Illinois.

Submitted August 7, 2003; accepted December 4, 2003. Prepublished online as *Blood* First Edition Paper, February 24, 2004; DOI 10.1182/blood-2003-08-2650.

Supported by the U.S. Army Neurofibromatosis Research Program (Project DAMD 17-02-1-0638), the National Institutes of Health (grants CA84221and CA72614), the Jeffrey and Karen Peterson Family Foundation, and the Frank A. Campini Foundation.

**Reprints:** Kevin M. Shannon, University of California, San Francisco, 513 Parnassus Ave, HSE 302, San Francisco, CA 94143; e-mail: kevins@itsa.ucsf.edu.

The publication costs of this article were defrayed in part by page charge payment. Therefore, and solely to indicate this fact, this article is hereby marked "advertisement" in accordance with 18 U.S.C. section 1734.

## Materials and methods

### Breeding and treatment with polyinosinic-polycytidylic acid (pI-pC)

*Nf1*$^{flox}$ and *Mx1-Cre* mice were produced and characterized as described elsewhere.[21,23] Compound mutant (*Mx1-Cre, Nf1*$^{flox/flox}$) animals were generated on a mixed 129/Sv × C57BL/6 background. Pups received a single intraperitoneal injection at 3 to 5 days of age with 50 μL pI-pC (Sigma, St Louis, MO) at a concentration of 10 μg/μL diluted in sterile phosphate-buffered saline (PBS). Mice were maintained in the sterile animal care facility at the University of California, San Francisco (UCSF) and were fed pelleted chow and acidified water ad libitum. The experimental procedures were approved by the UCSF Committee on Animal Research.

### Genotyping

We isolated DNA from blood samples using the GFX Genomic Blood DNA Purification Kit (Amersham, Arlington Heights, IL). Genotyping of the *Nf1*$^{flox}$ and recombined allele was carried out by using the primer sequence and polymerase chain reaction (PCR) conditions as described by Zhu et al.[21] Genotyping for the *Mx1-Cre* allele was performed by using primers Cre1 (5′-CTG CAT TAC CGG TCG ATG CAA C-3′) and Cre2 (5′-GCA TTG CTG TCA CTT GGT CGT G-3′). Thermal cycle conditions were 94°C for 5 minutes and then 32 cycles of 94°C for 30 seconds and 70°C for 1 minute. The presence of a 300-bp band is indicative of the *Mx1-Cre* transgene.

### Monitoring and isolation of hematopoietic cells

Mice were bled at 1.5, 3, and 5 months of age by nicking the dorsal tail veins with a surgical blade. Tail-vein blood samples (50-100 μL) were obtained for complete blood counts (CBCs). Samples were analyzed by using a Hemavet 850FS (DREW Scientific, Oxford, CT). Automated differential cell counts were used to monitor differentiated leukocyte populations over time. Criteria for killing mice by $CO_2$ inhalation included a disheveled appearance, hunching, abnormal gait, and pallor. Bone marrow cells were collected by removing tibias and femurs and flushing out the marrow cavity with Iscove modified Dulbecco medium (IMDM; GIBCO-BRL, Gaithersburg, MD) supplemented with 20% fetal calf serum (FCS; Hyclone Laboratories, Logan, UT). Single cell suspensions were prepared by gently drawing the cells through a 25-gauge needle. Cell viabilities were ascertained by trypan blue exclusion.

### Pathologic analysis and flow cytometry

Blood smears and cytospins were stained with Wright Giemsa (Sigma). Spleens and sternums were collected and sent for sectioning to the Mouse Pathology Shared Resource at the UCSF Comprehensive Cancer Center. CBCs were measured in peripheral blood, and manual differential counts (100-400 cells) were determined from Wright Giemsa–stained smears (blood) or cytospins (bone marrow or spleen) by using published recommendations.[24] Fluorescence activated cell sorting (FACS) analysis was performed on peripheral blood, bone marrow, and splenocytes. Peripheral blood cells were incubated in red blood cell lysis buffer (0.16 M $NH_4Cl$, 0.1 M $KHCO_3$, 0.1 mM EDTA [ethylenediaminetetraacetic acid]) for 10 minutes at room temperature. The cells were washed twice in PBS and resuspended in PBS/0.1% bovine serum albumin (BSA), divided into aliquots, and placed in tubes; antibodies were added on ice to prevent capping. Isotype control antibodies conjugated to the fluorochromes fluorescein isothiocyanate (FITC) or phycoerythrin (PE) were used to determine background fluorescence, and a panel of lineage-specific antibodies was used, including CD3, B220, Gr-1, Mac1, c-kit, and Sca-1 (all antibodies from Pharmingen). Analysis was performed using FlowJo (Tree Star, San Carlos, CA), and data were collected using CellQuest software (Becton Dickinson, San Jose, CA).

### Spectral karyotyping (SKY) analysis

Cytogenetic analysis was performed on spleen cells from mice with MPD. The initiation of short-term (24 hours) cultures, metaphase cell preparation, and spectral karyotyping were performed as described previously.[25] A minimum of 10 metaphase cells were analyzed per case.

### Adoptive transfer protocol

Recipient mice were lethally irradiated with a single fraction of 900 cGy by using a cesium source that delivered irradiation at 227 rad/min. Sublethal irradiation was administered at a dose of 450 cGy. Recipient mice (8 weeks old) were injected with donor cells immediately after irradiation. Mice were warmed for 5 minutes under a heat lamp to induce tail-vein dilation. Hematopoietic cells ($2 \times 10^6$ per recipient) were suspended in 500 μL IMDM with 20% FCS and injected through a 28-gauge needle into the dorsal tail vein. Recipients received prophylactic oral antibiotics, consisting of polymyxin sulfate and neomycin sulfate for 2 weeks after irradiation. CBCs were measured serially between 7 and 24 weeks after transplantation.

### Progenitor growth

CFU-GM colonies were grown from bone marrow cells and splenocytes. These assays were performed in methylcellulose medium (Stem Cell Technologies, Vancouver, BC, Canada) containing glutamine, penicillin/streptomycin, β-mercaptoethanol (BME), and varying doses of recombinant murine GM-CSF. Bone marrow and spleen cells were cultured at $5 \times 10^4$ and $1 \times 10^5$ cells/mL, respectively. Duplicate plates containing 1 mL medium were established and incubated at 37°C in 5% $CO_2$ for 8 days. The colonies were scored through a binocular light microscope under 4 × magnification. To assess the effects of 13 *cis* retinoic acid (13cRA) on CFU-GM growth, various concentrations of the drug ($10^{-4}$ M to $10^{-6}$ M) diluted in dimethyl sulfoxide (DMSO) were added to the medium immediately before plating.

### Proliferation assay

The incorporation of 5-bromo-2-deoxyuridine (BrdU; Sigma) was measured in vivo in mice that were injected intraperitoneally with 1 mg BrdU/6 g body weight. The mice were killed 6 hours later, and marrow cells and splenocytes were collected and resuspended in IMDM supplemented with 20% FCS. Red cell lysis was performed as described in "Monitoring and isolation of hematopoietic cells," and the cells were washed with PBS. Cells were incubated overnight with 1% paraformaldehyde and 0.01% Tween-20 at 4°C, washed twice with PBS, and resuspended in DNAse (Sigma) for 30 minutes at 37°C. After 2 additional washes with PBS, cells were stained with BrdU-FITC (Pharmingen) for 20 minutes. The cells were washed twice with PBS and then analyzed by flow cytometry.

### Apoptosis assay

Bone marrow cells were harvested in IMDM supplemented with 20% FCS, and the red cells were lysed as described in "Proliferation assay." The cells were resuspended in PBS with 2% FCS and 1.5 mM calcium chloride before staining with Annexin-GFP (a gift from Dr Joel Ernst, University of California, San Francisco) for 15 minutes at 4°C. The labeled cells were washed once in PBS and then analyzed by flow cytometry.

### Isolation of Mac1-positive bone marrow cells

Bone marrow cells were harvested from tibias and femurs in 0.1% serum without growth factors and were labeled with an antimouse CD11b (Mac1)–PE antibody (1:50; Pharmingen) after red cell lysis. The stained cells were incubated with paramagnetic anti-PE microbeads (Miltenyi Biotech, Bergisch Gladbach, Germany) for 15 minutes at 4°C. The cells were passed through a 40-μ filter and were separated on an AutoMACS instrument using program Possel (Miltenyi Biotech). This procedure consistently yields more than 98% Mac1-positive cells.

### Western blotting and Ras-GTP assay

Unfractionated bone marrow or Mac1-positive cells were incubated in 0.1% serum without growth factors for 4 hours, then stimulated with 0 or 10 ng/mL GM-CSF for 5 minutes. The cells were washed once with PBS containing 1 mM sodium orthovanadate and lysed in 25 mM HEPES (*N*-2-hydroxyethylpiperazine-*N*′-2-ethanesulfonic acid), pH 7.5, 150 mM

NaCl, 1% NP-40, 0.25% Na deoxycholate, 10% glycerol, 10 mM $MgCl_2$, 25 mM NaF, 1 mM Na orthovanadate, and COMPLETE protease inhibitors (Amersham). Protein concentrations were quantitated and equalized for loading by using the Bio-Rad protein assay (Bio-Rad, Hercules, CA). Samples were boiled for 5 minutes in 1 × Laemli buffer, run on a 10% Tris (tris(hydroxymethyl)aminomethane)–HCl Criterion Precast Gel (Bio-Rad), and transferred onto a nitrocellulose membrane. The membranes were blocked for 1 hour in TBS-Tween containing 5% milk prior to overnight incubation at 4°C with antiphospho-MEK 1/2 (mitogen-activated protein kinase kinase 1 and 2; 1:500; Cell Signaling Technologies, Beverly, MA), antiphospho-Akt (1:5000; a gift from Dr David Stokoe, University of California, San Francisco), anti-MEK 1/2 (1:5000; Cell Signaling Technologies), and anti-Akt (1:1000; Cell Signaling Technologies). The blots were developed with a horseradish peroxidase–conjugated secondary antirabbit antibody (Amersham). Proteins were visualized by enhanced chemiluminescence (Amersham). Ras-GTP levels were measured as described elsewhere by precipitating GTP-bound Ras with a fusion protein that includes the Ras binding domain of Raf.[26]

## Results

*Mx1-Cre*, $Nf1^{flox/flox}$, and $Nf1^{flox/flox}$ littermates received a single injection of pI-pC (500 μg in 50 μL) at 3 to 5 days of age and were genotyped at weaning by analyzing DNA prepared from tail clips. As an additional control, some litters that were not treated with pI-pC were observed for signs of systemic illness. PCR analysis of DNA extracted from peripheral blood leukocytes at 6 weeks of age demonstrated complete excision of exons 31 and 32 in *Mx1-Cre*, $Nf1^{flox/flox}$ mice that received pI-pC (Figure 1A). Somatic inactivation of *Nf1* was dependent on inheritance of the *Mx1-Cre* transgene (Figure 1A). Consistent with previous data, the *Mx1-Cre* transgene was active in other tissues, and we detected partial inactivation of *Nf1* in kidney, lung, and other tissues (data not shown).

Cohorts of mice were observed for evidence of disease and by performing serial blood counts. Leukocyte counts and the numbers of differentiated myeloid and lymphoid cells were significantly elevated in the *Mx1-Cre*, $Nf1^{flox/flox}$ animals by 3 months of age (Figure 1B). Blood smears revealed increased numbers of morphologically normal lymphocytes, monocytes, and neutrophils. Animals with marked leukocytosis showed occasional intermediate myeloid forms (Figure 1C). Hemoglobin concentrations as well as red blood cell and platelet counts remained within the normal range (data not shown). *Mx1-Cre*, $Nf1^{flox/flox}$ mice developed overt signs of disease beginning between 5 and 6 months of age, which was characterized by hunching, abnormal gait, and a disheveled appearance, and 50% of the animals succumbed by 7.5 months (Figure 1D). This clinical syndrome was generally not accompanied by dramatic changes in peripheral blood counts, and transformation to acute leukemia did not occur. The development of MPD in $Nf1^{flox/flox}$ mice was dependent on the presence of the *Mx1-Cre* transgene. Interestingly, *Mx1-Cre*, $Nf1^{flox/flox}$ mice that were not injected with pI-pC occasionally developed MPD. These animals showed somatic inactivation of *Nf1* in blood and bone marrow, which was likely because of endogenous interferon production in response to a subclinical infection or another stimulus (data not shown).

Pathologic analysis of sick *Mx1-Cre*, $Nf1^{flox/flox}$ mice revealed progressive splenomegaly with extensive infiltration of myeloid cells at various stages of maturation (Figure 2A-C). There was periportal invasion within the liver (Figure 2B) but not in other tissues. The bone marrow was highly cellular and comprised myeloid cells at various stages of differentiation (Figure 2C-D). FACS analysis confirmed the presence of a high percentage of myeloid cells ($Mac1^+$ and $Gr1^+$ cells) (Figure 2E). Increased numbers of Mac-$1^+$, Gr-$1^{lo}$ cells, which are likely to represent

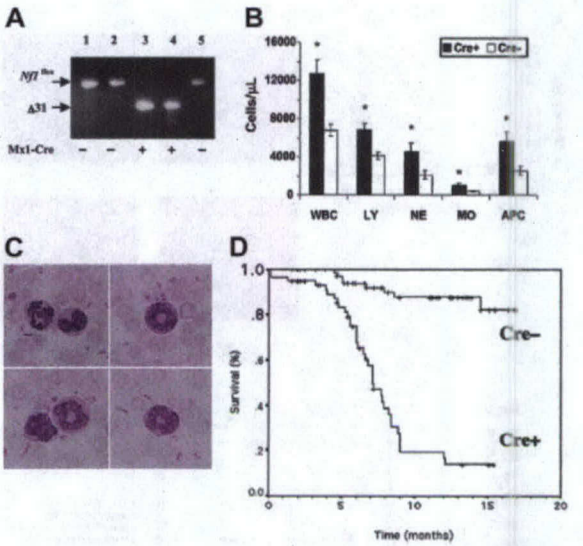


**Figure 1. Blood leukocyte values and survival in *Mx1-Cre*, $Nf1^{flox/flox}$ and $Nf1^{flox/flox}$ mice.** (A) PCR analysis of leukocyte DNA from 6-week-old pups that received a single injection of pI-pC shortly after birth. PCR amplification of the unrearranged $Nf1^{flox}$ allele yields a 350-bp product. A 280-bp fragment corresponding to a deletion of exon 31 (Δ31) is visible in 2 pups that inherited the *Mx1-Cre* transgene (+) but not in 3 pups that did not (−). Absence of the unrearranged allele in lanes 3 and 4 confirms a high efficiency of somatic recombination. (B) White blood cell counts (WBCs) in 3-month-old pI-pC–treated *Mx1-Cre*, $Nf1^{flox/flox}$ ($Cre^+$) (n = 21) and control $Nf1^{flox/flox}$ littermates that did not inherit the *Mx1-Cre* transgene ($Cre^-$) (n = 18). The abbreviations are LY, lymphocytes; NE, neutrophils; MO, monocytes; APC, absolute phagocyte count (neutrophils + monocytes). Leukocyte counts are expressed as ± SEM. Asterisks indicate significant differences ($P < .05$ by Student *t* test) between the $Cre^+$ and $Cre^-$ animals. (C) A composite photomicrograph (original magnification × 400) of peripheral blood from a $Cre^+$ mouse shows mature neutrophils (top left), intermediate forms (top right), a monocyte and a mature neutrophil (bottom left), and an intermediate form, which is likely in the monocytic lineage (bottom right). (D) Kaplan-Meier analysis demonstrates a significant reduction in survival in $Cre^+$ (n = 59) versus $Cre^-$ (n = 72) littermates ($P < .0001$).

immature monocytic cells, were identified consistently. Cytogenetic and spectral karyotype analysis of spleen samples from 6 diseased mice did not reveal clonal karyotypic abnormalities. According to guidelines published by the Hematopathology Subcommittee of the Mouse Models of Human Cancer Consortium (MMHCC),[24] this disorder is classified as a myeloproliferative disease. This MPD models many features of human JMML, including increased numbers of differentiated granulocytic and monocytic cells, hypersensitivity to GM-CSF (see later in this section), and a subacute course. It is similar to the MPD that arises in lethally irradiated mice that are repopulated with homozygous *Nf1*-deficient fetal liver cells[16,19]; however, the course is somewhat more indolent. A complete histologic and FACS panel on the model has been posted on the MMHCC website (http://emice.nci.nih.gov/emice/mouse_models/organ_models/hema_models/hema_mouse_class/myelopro_disease/mpd).

A recent study in which a *Krox20-Cre* transgene was used to ablate *Nf1* in Schwann cells found that the incidence and penetrance of benign neurofibromas was markedly increased in a heterozygous mutant background (ie, in *Krox20-Cre*, $Nf1^{flox/-}$ versus *Krox20-Cre*, $Nf1^{flox/flox}$ mice).[22] On the basis of these data, we generated *Mx1-Cre*, $Nf1^{flox/-}$ mice to determine whether heterozygous inactivation of *Nf1* in nonhematopoietic cells present in the bone marrow microenvironment might modulate the subacute course of the MPD. In this experiment, *Mx1-Cre*, $Nf1^{flox/-}$ pups that were injected with pI-pC at 3 to 5 days of age developed MPD with similar blood counts, disease latency, and survival as *Mx1-Cre*, $Nf1^{flox/flox}$ mice (data not shown).

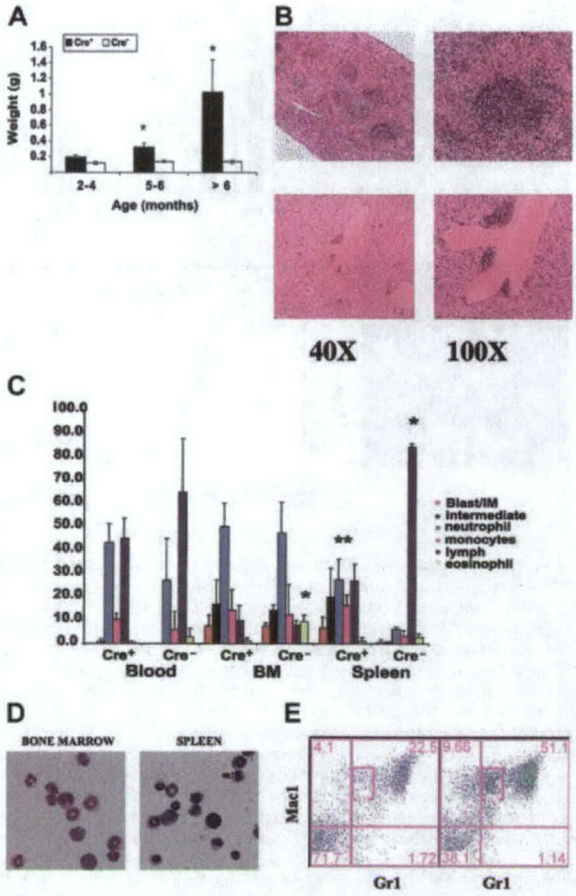


**Figure 2. Pathologic analysis of tissues from *Mx1-Cre, Nf1 flox/flox* mice.** (A) Cre$^+$ mice demonstrate progressive splenomegaly. Data are presented as the mean ± SEM. (A,C) Asterisks indicate significant differences ($P < .05$) between the Cre$^+$ and Cre$^-$ animals. (B) Spleen (top) sections from Cre$^+$ mice demonstrate expansion of the red pulp with myeloid infiltration. Liver sections (bottom) show periportal infiltration. (C) Manual differential counts of the percentage of nonerythroid cells in blood, bone marrow (BM), and spleen from Cre$^+$ and Cre$^-$ mice. Note that the bone marrow myeloid cells show a normal pattern of differentiation and that the spleen shows a massive increase in myelopoiesis. The data are shown as the mean ± SD. (D) Cytospins of bone marrow and spleen in a Cre$^+$ mouse with MPD show maturing neutrophilic and monocytic elements (original magnification × 200). (E) Representative FACS data from Cre$^-$ (left) and Cre$^+$ (right) bone marrows. Cre$^+$ mice with MPD demonstrate an increased percentage of Gr1$^+$/Mac1$^+$ cells (51% versus 22%). There is marked expansion in the Mac-1$^+$/Gr-1$^{lo}$ subset (11.5% in Cre$^+$ versus 2.13% in Cre$^-$ mice), which is consistent with an increase in monocytic cells. The numbers shown indicate the percentage of cells within each quadrant.

JMML bone marrows and *Nf1*$^{-/-}$ fetal liver cells form increased numbers of CFU-GM colonies in the presence of nonsaturating concentrations of recombinant murine GM-CSF.[3,11,16,17] We detected elevated numbers of CFU-GM in the bone marrows of *Mx1-Cre, Nf1*$^{flox/flox}$ mice that were hypersensitive to GM-CSF (Figure 3A-B). In addition, mutant CFU-GM colonies were larger than normal and showed an abnormal spreading morphology (Figure 3C-D). Increased proliferation of myeloid progenitors from *Mx1-Cre, Nf1*$^{flox/flox}$ mice was also reflected by a 2- to 3-fold expansion in the number of cells recovered from methylcellulose cultures stimulated with 10 ng/mL recombinant murine GM-CSF. Wright-Giemsa staining revealed a higher percentage of monocyte-macrophage cells in *Mx1-Cre, Nf1*$^{flox/flox}$ cultures than in the control cultures (Figure 3E-F). Consistent with the myeloid infiltration visible in pathologic sections, the spleens of *Mx1-Cre, Nf1*$^{flox/flox}$ mice contained large numbers of CFU-GM, which formed colonies that were similar in size and morphology to those found in the bone marrow. By contrast, no CFU-GM colonies were obtained from the spleens of control mice (data not shown).

Retinoids partially correct the abnormal pattern of CFU-GM colony growth that is a hallmark of JMML,[1,27] and 13*c*RA induces transient clinical and hematologic improvement in some patients.[28] We, therefore, compared the effects of 13*c*RA on CFU-GM growth from *Mx1-Cre, Nf1*$^{flox/flox}$ and control bone marrows. As shown in Figure 3, *Mx1-Cre, Nf1*$^{flox/flox}$ marrows contained elevated numbers of CFU-GM, which were larger than wild-type colonies. Addition of $10^{-6}$ to $10^{-4}$ M 13*c*RA to methylcellulose cultures stimulated with 10 ng/mL GM-CSF induced proliferation of background cells as well as a dose-dependent reduction in the size of CFU-GM colonies. These effects were not selective but were observed in both mutant and wild-type cultures. Furthermore, 13*c*RA treatment was not associated with a reduction in the abnormally high percentage of monocyte-macrophage cells in CFU-GM grown from *Mx1-Cre, Nf1*$^{flox/flox}$ mice (data not shown).

Bone marrow mononuclear cells from *Mx1-Cre, Nf1*$^{flox/flox}$ mice that had been treated with pI-pC were injected into lethally (n = 10) or sublethally (n = 10) irradiated recipients to ascertain whether the MPD could be transferred to secondary hosts. Each lethally irradiated recipient was repopulated with mutant cells and developed MPD (Figure 4A). By contrast, the leukocyte counts of mice that received a sublethal dose of irradiation remained normal over 6 months of observation (Figure 4A). Analysis of DNA extracted from blood leukocytes 2 to 4 months after transplantation revealed both host and donor-derived cells in all recipients (data not shown). *Nf1*-deficient cells made a sustained contribution to hematopoiesis in many animals, including some in which the wild-type band disappeared from the blood after 6 months (Figure 4B). Interestingly, pathologic evaluation of sublethally irradiated mice that were killed 8 months after injection of *Nf1*$^{-/-}$ cells revealed normal spleen size and architecture and no splenic CFU-GM despite a substantial contribution of mutant cells to the peripheral blood (data not shown).

We measured BrdU incorporation and performed annexin V staining to ascertain the effects of *Nf1* inactivation on the proliferation and survival of primary hematopoietic cells. *Mx1-Cre, Nf1*$^{flox/flox}$ mice with MPD and controls were killed 6 hours after a single injection of BrdU, and the percentages of bone marrow and spleen cells that had incorporated the label were determined by flow cytometry. Whereas the fraction of BrdU-positive cells was similar in the bone marrows of diseased and control animals, proliferation was substantially greater within the spleens of *Mx1-Cre, Nf1*$^{flox/flox}$ mice (Figure 5A). Because the percentages of erythroid and myeloid cells in bone marrow and spleen differ markedly between *Mx1-Cre, Nf1*$^{flox/flox}$ and control mice, we also assessed BrdU incorporation in Mac1$^+$ cells. Interestingly, proliferation was comparable in bone marrow–derived cells; however, a higher percentage of splenic Mac1$^+$ cells was labeled in the *Mx1-Cre, Nf1*$^{flox/flox}$ mice (Figure 5B). Apoptosis was assessed by performing flow cytometry on bone marrow cells that had been labeled with an annexin V–green fluorescent protein (GFP). The percentage of freshly isolated cells stained by annexin-V was similar in *Mx1-Cre, Nf1*$^{flox/flox}$ and normal mice (data not shown); however, the mutant cells displayed greatly enhanced survival after 24 hours in culture without exogenous growth factors (Figure 5C).

We compared the percentage of Ras in the active GTP-bound conformation and assayed activation of the Ras effectors Akt and MEK in bone marrow mononuclear cells isolated from *Mx1-Cre, Nf1*$^{flox/flox}$ and normal mice. Unstimulated mutant cells showed a modest increase in baseline Ras-GTP levels (Figure 6A,C), but phosphorylation of the downstream effectors MEK and Akt were similar in unfractionated mutant and control bone marrows (Figure 6B-C). Exposure to GM-CSF induced robust Ras-GTP, MEK, and

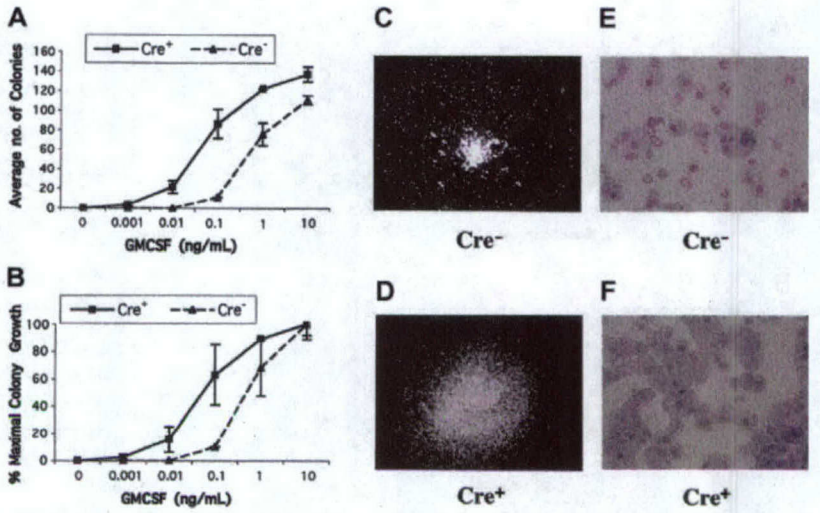


**Figure 3. CFU-GM colony growth from *Mx1-Cre, Nf1*$^{flox/flox}$ and Cre$^-$ mice.** (A-B) CFU-GM colony growth at various concentrations of GM-CSF. Bone marrow mononuclear cells were plated in duplicate in methylcellulose. Cre$^+$ bone marrow from mice with MPD show a left shift in the GM-CSF dose-response curve when expressed in terms of total numbers of colonies (A) or the calculated percentage of maximal colony growth (B). Colony numbers in duplicate 1-mL plates are shown with ranges from a representative experiment. (C-D) CFU-GM colonies grown from *Mx1-Cre, Nf1* $^{flox/flox}$ and control mice photographed at 40 × magnification. A typical CFU-GM morphology from a normal mouse is shown in panel C at 40 × magnification. The colonies grown from Cre$^+$ mice with MPD are larger and show abnormal spreading (D). (E-F) Cytospins of CFU-GM colonies stained with Wright-Giemsa from a wild-type mouse (E) contain approximately 70% neutrophils compared with 93% monocyte-macrophage cells in Cre$^+$ mice. Original magnification, × 500 for panels E and F.

Akt activation from baseline levels that was equivalent in both genotypes (Figure 6B-C). Because *Nf1*$^{-/-}$ and wild-type bone marrows showed marked differences with respect to the relative proportions of different cell types, we isolated Mac1-positive cells and compared MEK activation in this myeloid subpopulation. In these experiments, *Nf1*$^{-/-}$ cells showed sustained activation of MEK after exposure to GM-CSF (Figure 6D).

## Discussion

We have developed a robust and tractable model of MPD by harnessing the *Mx1-Cre* transgene to induce somatic inactivation of the *Nf1* tumor suppressor and have used these *Mx1-Cre, Nf1*$^{flox/flox}$ mice to investigate how loss of *Nf1* perturbs the in vivo growth of primary hematopoietic cells. This work extends previous studies of cultured *Nf1*-deficient fetal liver cells and of recipient mice repopulated with these cells.[11,16-19]

We selected the *Mx1-Cre* strain on the basis of data from other laboratories that imply that this Cre recombinase is active in both hematopoietic stem cells and in differentiated progeny.[29-31] By inducing biallelic excision of a targeted locus, we could readily monitor the relative levels of recombined and unrearranged *Nf1* in blood and bone marrow. We found that a single injection of pI-pC resulted in highly efficient *Nf1* inactivation in all lineages. These results and our data showing that bone marrow from *Mx1-Cre, Nf1*$^{flox/flox}$ mice mediate long-term reconstitution in lethally irradiated recipients provide strong evidence that *Nf1* is inactivated in the stem-cell compartment. Furthermore, although the ultimate contribution of cells that have undergone somatic recombination to hematopoiesis will be influenced by both the structure of the loxP-targeted allele and by how rearranging the locus modulates cell survival and proliferation, our data underscore the value of the *Mx1-Cre* strain for modifying conditional mutant alleles in hematopoietic cells. Importantly, although we detected significant levels of somatic *Nf1* inactivation in some nonhematopoietic tissues, this was not associated with any overt phenotypes in mice observed for 9 to 12 months. However, this lack of specificity could be problematic for analyzing other conditional mutations.

Somatic inactivation of *Nf1* results in progressive splenomegaly with a shift in hematopoiesis from the marrow to the spleen, and we identified proliferating myeloid cells within the spleens of *Mx1-Cre, Nf1*$^{flox/flox}$ mice. Splenomegaly is a prominent feature of JMML, and many centers perform splenectomies before transplantation. Although the benefits of this procedure are unclear, our data suggest that the spleen is an important site of disease that contributes to the evolution of the murine MPD. We also found that bone marrow cells from *Mx1-Cre, Nf1*$^{flox/flox}$ mice are resistant to apoptosis, which is consistent with data from *Myb*-transformed myeloid cell lines.[26]

Previous studies of mice repopulated with *Nf1*$^{-/-}$ cells have emphasized the effects of *Nf1* inactivation on stem cells and myeloid lineage progenitors.[16,17,19] However, limited attention has been paid to lymphopoiesis. In addition to uniformly developing MPD, *Mx1-Cre,*

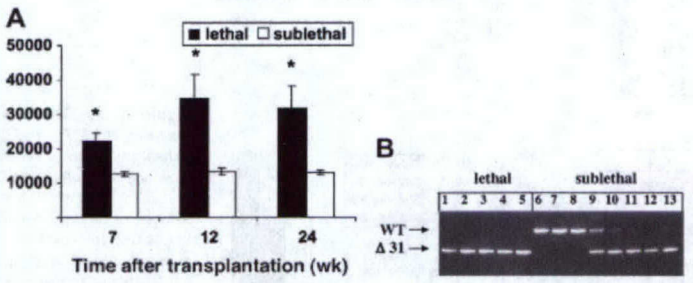


**Figure 4. Adoptive transfer of marrow cells from *Mx1-Cre, Nf1* $^{flox/flox}$ mice with MPD.** (A) WBCs in recipient mice that received a lethal or sublethal dose of radiation over time. Cells from 2 Cre$^+$ mice were injected into equal numbers of lethally and sublethally irradiated mice. Data represent the mean ± SEM. Asterisks indicate significant differences between recipients that received lethal versus sublethal radiation ($P < .05$). (B) PCR analysis of blood leukocytes from lethally irradiated recipients demonstrates reconstitution with mutant (Δ31) cells with absence of a signal from the wild-type host (lanes 1-5). By contrast, some sublethally irradiated recipients that were analyzed 6 months after adoptive transfer showed absence of mutant Δ31 cells (lanes 6-8), some showed repopulation with donor cells (lanes 11-13), and others demonstrated the presence of both wild-type and mutant cells (lanes 9,10). None of these sublethally irradiated recipients had developed evidence of MPD by 8 months after adoptive transfer.

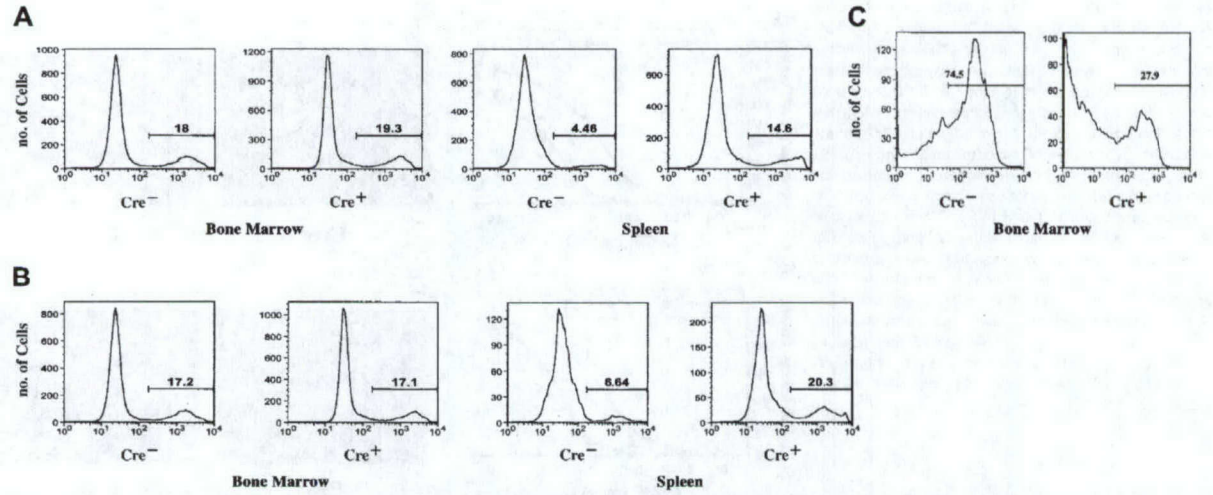


**Figure 5. Proliferation and apoptosis in *Mx1-Cre, Nf1 flox/flox* and Cre⁻ mice.** (A) BrdU incorporation in vivo by Cre⁺ and Cre⁻ bone marrow cells and splenocytes. Increased proliferation is seen in the spleens of Cre⁺ mice (14.6% versus 4.5% labeled cells). (B) BrdU labeling of Mac1⁺ cells from Cre⁺ and Cre⁻ mice. A higher percentage of splenic Mac1⁺ cells were labeled (20% versus 6.6%). (C) Annexin V staining of bone marrow mononuclear cells from Cre⁻ and Cre⁺ mice showing greatly reduced apoptosis of Cre⁺ cells after 24 hours in culture without exogenous growth factors (27.9% versus 74.5% in the controls). The histograms present representative data from an analysis of 3 mice of each genotype. The numbers shown in each panel indicate the percentage of positive cells.

*Nf1*$^{flox/flox}$ mice demonstrate lymphocytosis with increased numbers of differentiated T and B cells. These data are consistent with competitive repopulation studies, which revealed that loss of *Nf1* is associated with a proliferative advantage in both myeloid and lymphoid compartments.[18] The risk of lymphoid malignancies has been examined in large population-based studies of pediatric cancer registries in Japan and the United Kingdom. Whereas one group identified no significant increase,[32] the other report found a 5- to 10-fold higher incidence of acute lymphoblastic leukemia and non-Hodgkin lymphoma in children with NF1.[6] A child with NF1 has been described who presented with JMML and subsequently developed a T-cell lymphoma, both of which showed loss of the normal *NF1* allele.[33] Ingram et al[34] recently reported greater thymic cellularity and a modest increase in Ras-GTP levels in RAG2-deficient mice that received transplants with *Nf1*$^{-/-}$ fetal liver cells. Paradoxically, *Nf1*$^{-/-}$ T cells showed impaired proliferation in response to T-cell mitogens. *Mx1-Cre, Nf1*$^{flox/flox}$ mice provide a model that can be used to dissect the functional consequences of ablating *Nf1* in lymphoid cells.

Consistent with previous studies of primary fetal livers and of irradiated recipients reconstituted with these cells,[11,16,17] we found that

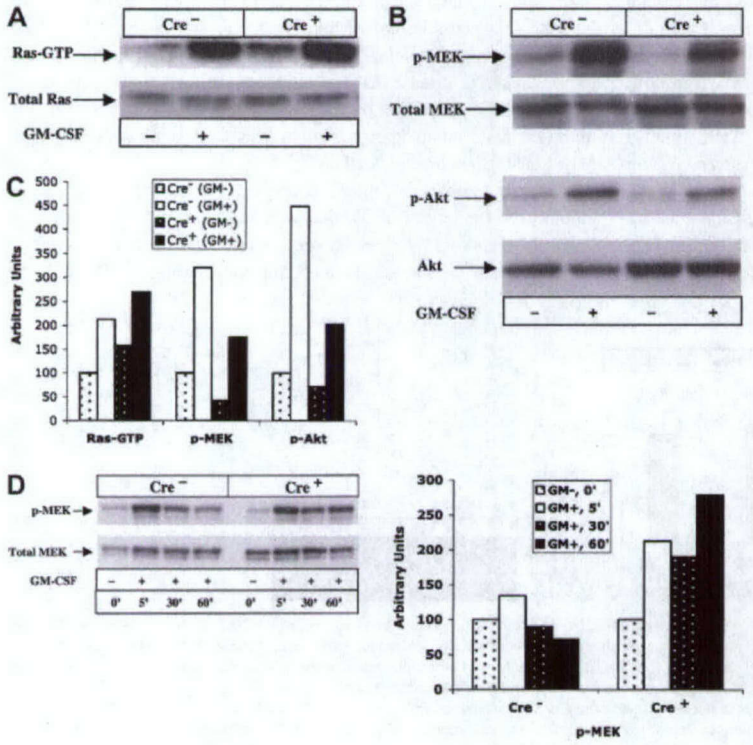


**Figure 6. Signal transduction in bone marrow cells from *Mx1-Cre, Nf1 flox/flox* and Cre⁻ mice.** (A) Bone marrow cells from mutant and control mice showing Ras-GTP levels in unstimulated cells and 5 minutes after GM-CSF. (B) Bone marrow cells from mutant and control mice showing basal and growth factor–induced levels of phosphorylated (p)–Akt and p-MEK in response to GM-CSF (at 5 minutes). (C) Ras-GTP, p-MEK, and p-Akt from panels A and B were quantified by densitometry. (D) Mac1-positive bone marrow cells from mutant and control mice showing basal and growth factor–induced activation of p-MEK in response to GM-CSF. The time course is shown from 5 to 60 minutes. Relative p-MEK activity is shown in the right panel. Levels in mutant and control cells were normalized for background and loading, with the unstimulated sample assigned arbitrary units of 100.

*Mx1-Cre, Nf1*$^{flox/flox}$ bone marrow cells model the hypersensitive pattern of CFU-GM colony growth that is a hallmark of JMML. These data establish a link between *Nf1* inactivation and this distinctive cellular phenotype. On the basis of this precedent, we exposed *Mx1-Cre, Nf1*$^{flox/flox}$ bone marrow cells to retinoids, but we did not observe selective effects on the growth of mutant CFU-GM colonies. These data imply that the therapeutic effects of 13*c*RA in JMML are not mediated though the GM-CSF/Ras/neurofibromin pathway.

Our adoptive transfer data are consistent with a previous report in which bone marrow from recipient mice repopulated with *Nf1*$^{-/-}$ fetal liver cells induced MPD in secondary hosts that received a myeloablative dose of radiation.[19] In addition, serial studies of sublethally irradiated mice demonstrated engraftment of mutant cells in most of the recipients without overt evidence of MPD after 8 months of observation. Furthermore, we did not detect splenomegaly or myeloid infiltration even in mice in which 100% of the peripheral blood leukocytes were derived from mutant cells. These data are remarkably consistent with the results of competitive repopulation experiments in which *Nf1*$^{-/-}$ fetal liver cells out-competed wild-type cells in the stem-cell compartment and in the lymphoid and myeloid lineages but failed to induce MPD in the absence of a high degree of chimerism.[18] In another study in which heterozygous *Nf1* inactivation cooperated with exposure to cyclophosphamide in leukemogenesis, some *Nf1*$^{+/-}$ mice showed loss of the wild-type allele without evidence of MPD when the experiment was terminated.[20] Together with these data, our results in sublethally irradiated recipients suggest that the presence of wild-type bone marrow cells can retard the development of MPD in vivo. These observations also support a model in which loss of *Nf1* in a susceptible bone marrow precursor confers a subtle growth advantage that progresses to *Nf1*-deficient hematopoiesis, followed by splenic invasion by myeloid precursors and, finally, by overt MPD. An unsettled question involves whether the MPD induced by *Nf1* inactivation is caused by progressive overgrowth of a stable population of mutant cells or involves clonal selection of a subpopulation that has acquired one or more cooperating mutations. Although the absence of acquired cytogenetic aberrations in the spleens of diseased mice is consistent with the former model, additional studies are required to resolve this issue.

We and others have detected hyperactive Ras signaling in JMML bone marrows,[11] in cell lines from *Nf1* mutant mice,[16,26] in c-kit–positive bone marrow cells isolated from the recipients of *Nf1*$^{-/-}$ fetal liver cells,[17] and in heterozygous *Nf1* mutant mast cells.[35] We were, therefore, surprised that bone marrow mononuclear cells from *Mx1-Cre, Nf1*$^{flox/flox}$ mice demonstrated a small increase in the percentage of Ras-GTP in unstimulated cells but similar levels of phosphorylated Akt and MEK compared with control cells. However, bone marrow–derived Mac1-positive cells from *Mx1-Cre, Nf1*$^{flox/flox}$ mice that were stimulated with GM-CSF showed sustained phosphorylation of MEK. Similarly, prolonged activation of extracellular-regulated kinase (ERK) was recently reported in *Nf1*-deficient mouse embryonic fibroblasts in response to 1% serum.[36] Our data support a mechanism whereby *Nf1* inactivation deregulates Ras signaling in a subset of hematopoietic cells, which may be difficult to detect in whole bone marrow. The CFU-GM fraction comprises approximately 0.1% of the nucleated cells in *Mx1-Cre, Nf1*$^{flox/flox}$ marrow, and we speculate that these cells are especially sensitive to loss of *Nf1*. Measuring the activation status of signaling cascades in rare subsets of primary cells is a challenging problem that will likely require adapting new methodologies such as the flow cytometry–based approach recently described by Perez and Nolan.[37] Our data also raise the possibility that some types of hematopoietic cells compensate for loss of *Nf1* by attenuating signaling networks, which may further complicate ascertaining the biochemical consequences of leukemia-associated mutations in vivo.

In addition to facilitating studies that directly address the role of *Nf1* in signal transduction and myeloid growth control, *Mx1-Cre, Nf1*$^{flox/flox}$ mice are a tractable experimental system for identifying molecular events that contribute to acute myeloid leukemia (AML). The classic studies of Land et al[38] demonstrated the principle of oncogene cooperativity in cellular transformation. Kelly et al[39] have applied this concept to AML and proposed that transcription factor fusion proteins cooperate with mutations that constitutively activate growth-promoting signal transduction pathways in leukemogenesis. Indeed, data from mice generally support the idea that neither type of leukemia-associated genetic lesion is sufficient to induce AML. For example, transgenic or knock-in models of transcription factor fusions such as *AML1-ETO, PML-RARA,* and *MLL-AF9* either do not spontaneously develop AML or show incomplete penetrance and prolonged latency.[29,40,41] By contrast, although inactivating *Nf1* or expressing either *BCR-ABL* or a mutant *FLT3* allele induces MPD,[16,39,42,43] additional events are required for AML. We envision 2 general strategies for harnessing *Mx1-Cre, Nf1*$^{flox/flox}$ mice to discover genes that cooperate with *Nf1* inactivation in leukemogenesis. The first strategy involves either performing genetic crosses with transgenic or knock-in strains that express fusion oncoproteins such as *PML-RARA, AML1-ETO,* or *MLL-AF9,* or transducing *Nf1*-deficient bone marrow with retroviruses that encode these or other leukemia-associated fusions followed by adoptive transfer into irradiated recipients. The second approach is to harness retroviral insertional mutagenesis to identify novel genes that cooperate with loss of *Nf1* in leukemogenesis.[44,45] In an important "proof of principle" experiment, Largaespada et al[16] found that *Nf1*$^{+/-}$ mice that were infected with the BXH-2 retrovirus developed AML with increased penetrance and reduced latency compared with wild-type littermates. These investigators identified inactivation of the normal *Nf1* allele in approximately 85% of BXH-2/*Nf1*$^{+/-}$ AMLs. Because both *Nf1* alleles are already mutated in *Mx1-Cre, Nf1*$^{flox/flox}$ animals that have been treated with pI-pC, this strain is theoretically superior to *Nf1*$^{+/-}$ mice for performing forward genetic screens. The predictable onset of MPD and the prolonged survival of *Mx1-Cre, Nf1*$^{flox/flox}$ mice may prove advantageous for uncovering genes that cooperate in the development of AML.

Finally, *Mx1-Cre, Nf1*$^{flox/flox}$ mice and cells from these animals can be used to test molecularly targeted agents with pharmacodynamic monitoring of relevant biochemical end points in primary target cells. Potential therapeutic strategies for treating JMML include developing GM-CSF receptor antagonists (reviewed in Iversen et al[46,47] and Frankel et al[48]), inhibitors of Ras processing enzymes (reviewed in Le and Shannon[49]), and agents that interfere with the activation of downstream effectors such as MEK.[50] Given the important role of hyperactive Ras in myeloid malignancies (reviewed in Lee and Shannon[49] and Sawyers and Denny[51]) and other cancers (reviewed in Bos[52] and Hingorani and Tuveson[53]), studies in this tractable disease model might identify agents that have therapeutic potential that extend beyond hematopoietic malignancies.

## Acknowledgments

We thank Bhumi Patel and Elizabeth Davis for assistance in spectral karyotyping analysis, Sara Jew-Lim for assistance in genotyping, Jacob Rozmus for assistance with the Ras-GTP assay, Andrew Kim for assisting with adoptive transfer experiments, and Philip Chan for preparing pathologic specimens and downloading images to the MMHCC website.

## References


1. Emanuel PD, Shannon KM, Castleberry RP. Juvenile myelomonocytic leukemia: molecular understanding and prospects for therapy. Mol Med Today. 1996;2:468-475.
2. Arico M, Biondi A, Pui C-H. Juvenile myelomonocytic leukemia. Blood. 1997;90:479-488.
3. Emanuel PD, Bates LJ, Castleberry RP, Gualtieri RJ, Zuckerman KS. Selective hypersensitivity to granulocyte-macrophage colony-stimulating factor by juvenile chronic myeloid leukemia hematopoietic progenitors. Blood. 1991;77:925-929.
4. Schiro R, Longoni D, Rossi V, et al. Suppression of juvenile chronic myelogenous leukemia colony growth by interleukin-1 receptor antagonist. Blood. 1994;83:460-465.
5. Bader JL, Miller RW. Neurofibromatosis and childhood leukemia. J Pediatr. 1978;92:925-929.
6. Stiller CA, Chessells JM, Fitchett M. Neurofibromatosis and childhood leukemia/lymphoma: a population-based UKCCSG study. Br J Cancer. 1994;70:969-972.
7. Boguski M, McCormick F. Proteins regulating Ras and its relatives. Nature. 1993;366:643-653.
8. Bernards A. Neurofibromatosis type 1 and Ras-mediated signaling: filling in the GAPs. Biochim Biophys Acta. 1995;1242:43-59.
9. Donovan S, Shannon KM, Bollag G. GTPase activating proteins: critical regulators of intracellular signaling. Biochim Biophys Acta. 2002;1602: 23-45.
10. Shannon KM, O'Connell P, Martin GA, et al. Loss of the normal NF1 allele from the bone marrow of children with type 1 neurofibromatosis and malignant myeloid disorders. N Engl J Med. 1994;330: 597-601.
11. Bollag G, Clapp DW, Shih S, et al. Loss of NF1 results in activation of the Ras signaling pathway and leads to aberrant growth in murine and human hematopoietic cells. Nat Genet. 1996;12: 144-148.
12. Miles DK, Freedman MH, Stephens K, et al. Patterns of hematopoietic lineage involvement in children with neurofibromatosis, type 1, and malignant myeloid disorders. Blood. 1996;88:4314-4320.
13. Side L, Taylor B, Cayouette M, et al. Homozygous inactivation of the NF1 gene in bone marrow cells from children with neurofibromatosis type 1 and malignant myeloid disorders. N Engl J Med. 1997;336:1713-1720.
14. Jacks T, Shih S, Schmitt EM, Bronson RT, Bernards A, Weinberg RA. Tumorigenic and developmental consequences of a targeted Nf1 mutation in the mouse. Nat Genet. 1994;7:353-361.
15. Brannan CI, Perkins AS, Vogel KS, et al. Targeted disruption of the neurofibromatosis type 1 gene leads to developmental abnormalities in heart and various neural crest-derived tissues. Genes Dev. 1994;8:1019-1029.
16. Largaespada DA, Brannan CI, Jenkins NA, Copeland NG. Nf1 deficiency causes Ras-mediated granulocyte-macrophage colony stimulating factor hypersensitivity and chronic myeloid leukemia. Nat Genet. 1996;12:137-143.
17. Zhang Y, Vik TA, Ryder JW, et al. Nf1 regulates hematopoietic progenitor cell growth and Ras signaling in response to multiple cytokines. J Exp Med. 1998;187:1893-1902.
18. Zhang Y, Taylor BR, Shannon K, Clapp DW. Quantitative effects of Nf1 inactivation on in vivo hematopoiesis. J Clin Invest. 2001;108:709-715.
19. Birnbaum RA, O'Marcaigh A, Wardak Z, et al. Nf1 and Gmcsf interact in myeloid leukemogenesis. Mol Cell. 2000;5:189-195.
20. Mahgoub N, Taylor BR, Gratiot M, et al. In vitro and in vivo effects of a farnesyltransferase inhibitor on Nf1-deficient hematopoietic cells. Blood. 1999;94:2469-2476.
21. Zhu Y, Romero MI, Ghosh P, et al. Ablation of NF1 function in neurons induces abnormal development of cerebral cortex and reactive gliosis in the brain. Genes Dev. 2001;15:859-876.
22. Zhu Y, Ghosh P, Charnay P, Burns DK, Parada LF. Neurofibromas in NF1: Schwann cell origin and role of tumor environment. Science. 2002; 296:920-922.
23. Kuhn R, Schwenk F, Aguet M, Rajewsky K. Inducible gene targeting in mice. Science. 1995;269: 1427-1429.
24. Kogan SC, Ward JM, Anver MR, et al. Bethesda proposals for classification of nonlymphoid hematopoietic neoplasms in mice. Blood. 2002;100: 238-245.
25. Le Beau MM, Bitts S, Davis EM, Kogan SC. Recurring chromosomal abnormalities in leukemia in PML-RARA transgenic mice parallel human acute promyelocytic leukemia. Blood. 2002;99:2985-2991.
26. Donovan S, See W, Bonifas J, Stokoe D, Shannon KM. Hyperactivation of protein kinase B and ERK have discrete effects on survival, proliferation, and cytokine expression in Nf1-deficient myeloid cells. Cancer Cell. 2002;2:507-514.
27. Emanuel PD, Zuckerman KS, Wimmer R, Cohn S, Chaffee S, Castleberry RP. In vivo 13-cis retinoic acid therapy decreased the in vitro GM-CSF hypersensitivity in JCML [abstract]. Blood. 1991; 78(suppl 1):170a.
28. Castleberry RP, Emanuel PD, Zuckerman KS, et al. A pilot study of isotretinoin in the treatment of juvenile chronic myelogenous leukemia. N Engl J Med. 1994;331:1680-1685.
29. Higuchi M, O'Brien D, Kumaravelu P, Lenney N, Yeoh E, Downing JR. Expression of a conditional AML1-ETO oncogene bypasses embryonic lethality and establishes a murine model of human t(8;21) acute myeloid leukemia. Cancer Cell. 2002;1:63-74.
30. Roberts CW, Leroux MM, Fleming MD, Orkin SH. Highly penetrant, rapid tumorigenesis through conditional inversion of the tumor suppressor gene Snf5. Cancer Cell. 2002;2:415-425.
31. Gerber HP, Malik AK, Solar GP, et al. VEGF regulates haematopoietic stem cell survival by an internal autocrine loop mechanism. Nature. 2002; 417:954-958.
32. Matsui I, Tanimura M, Kobayashi N, Sawada T, Nagahara N, Akatsuka J. Neurofibromatosis type 1 and childhood cancer. Cancer. 1993;72:2746-2754.
33. Cooper LJ, Shannon KM, Loken MR, Weaver M, Stephens K, Sievers EL. Evidence that juvenile myelomonocytic leukemia can arise from a pluripotential stem cell. Blood. 2000;96:2310-2313.
34. Ingram DA, Zhang L, McCarthy J, et al. Lymphoproliferative defects in mice lacking the expression of neurofibromin: functional and biochemical consequences of Nf1 deficiency in T-cell development and function. Blood. 2002; 100:3656-3662.
35. Ingram DA, Yang FC, Travers JB, et al. Genetic and biochemical evidence that haploinsufficiency of the Nf1 tumor suppressor gene modulates melanocyte and mast cell fates in vivo. J Exp Med. 2000;191:181-188.
36. Cichowski K, Santiago S, Jardim M, Johnson BW, Jacks T. Dynamic regulation of the Ras pathway via proteolysis of the NF1 tumor suppressor. Genes Dev. 2003;17:449-454.
37. Perez OD, Nolan GP. Simultaneous measurement of multiple active kinase states using polychromatic flow cytometry. Nat Biotechnol. 2002; 20:155-162.
38. Land H, Parada LF, Weinberg RA. Tumorigenic conversion of primary embryo fibroblasts requires at least two cooperating oncogenes. Nature. 1983;304:596-602.
39. Kelly L, Clark J, Gilliland DG. Comprehensive genotypic analysis of leukemia: clinical and therapeutic implications. Curr Opin Oncol. 2002;14: 10-18.
40. Corral J, Lavenir I, Impey H, et al. An Mll-AF9 fusion gene made by homologous recombination causes acute leukemia in chimeric mice: a method to create fusion oncogenes. Cell. 1996; 85:853-861.
41. Brown D, Kogan S, Lagasse E, et al. A PML-RARalpha transgene initiates murine acute promyelocytic leukemia. Proc Natl Acad Sci U S A. 1997;94:2551-2556.
42. Daley GQ, Van Etten RA, Baltimore D. Induction of chronic myelogenous leukemia in mice by the P210bcr/abl gene of the Philadelphia chromosome. Science. 1990;247:824-830.
43. Kelly LM, Liu Q, Kutok JL, Williams IR, Boulton CL, Gilliland DG. FLT3 internal tandem duplication mutations associated with human acute myeloid leukemias induce myeloproliferative disease in a murine bone marrow transplant model. Blood. 2002;99:310-318.
44. Li J, Shen H, Himmel KL, et al. Leukaemia disease genes: large-scale cloning and pathway predictions. Nat Genet. 1999;23:348-353.
45. Wolff L, Koller R, Hu X, Anver MR. A Moloney murine leukemia virus-based retrovirus with 4070A long terminal repeat sequences induces a high incidence of myeloid as well as lymphoid neoplasms. J Virol. 2003;77:4965-4971.
46. Iversen P, Rodwell RL, Pitcher L, Taylor KM, Lopez AF. Inhibition of proliferation and induction of apoptosis in JMML cells by the granulocyte-macrophage colony-stimulating factor analogue E21R. Blood. 1996;88:2634-2639.
47. Iversen PO, Lewis ID, Turczynowicz S, et al. Inhibition of granulocyte-macrophage colony-stimulating factor prevents dissemination and induces remission of juvenile myelomonocytic leukemia in engrafted immunodeficient mice. Blood. 1997;90: 4910-4917.
48. Frankel AE, Lilly M, Kreitman R, et al. Diphtheria toxin fused to granulocyte-macrophage colony-stimulating factor is toxic to blasts from patients with juvenile myelomonocytic leukemia and chronic myelomonocytic leukemia. Blood. 1998; 92:4279-4286.
49. Le DT, Shannon KM. Ras processing as a therapeutic target in hematologic malignancies. Curr Opin Hematol. 2002;9:308-315.
50. Sebolt-Leopold JS, Dudley DT, Herrera R, et al. Blockade of the MAP kinase pathway suppresses growth of colon tumors in vivo. Nat Med. 1999;5: 810-816.
51. Sawyers CL, Denny CT. Chronic myelomonocytic leukemia: tel-a-kinase what ets all about. Cell. 1994;77:171-173.
52. Bos JL. ras oncogenes in human cancer: a review. Cancer Res. 1989;49:4682-4689.
53. Hingorani SR, Tuveson DA. Ras redux: rethinking how and where Ras acts. Curr Opin Genet Dev. 2003;13:6-13.

Molecular Cell, Vol. 12, 841–849, October, 2003, Copyright ©2003 by Cell Press

# Merlin, the Product of the Nf2 Tumor Suppressor Gene, Is an Inhibitor of the p21-Activated Kinase, Pak1

Joseph L. Kissil,[1] Erik W. Wilker,[1] Kristen C. Johnson,[1] Matthew S. Eckman,[1,2] Michael B. Yaffe,[1] and Tyler Jacks[1,2,*]
[1]Department of Biology and
Center for Cancer Research
[2]Howard Hughes Medical Institute
Massachusetts Institute of Technology
Cambridge, Massachusetts 02139

## Summary

**The Nf2 tumor suppressor gene codes for merlin, a protein whose function has been elusive. We describe a novel interaction between merlin and p21-activated kinase 1 (Pak1), which is dynamic and facilitated upon increased cellular confluence. Merlin inhibits the activation of Pak1, as the loss of merlin expression results in the inappropriate activation of Pak1 under conditions associated with low basal activity. Conversely, the overexpression of merlin in cells that display a high basal activity of Pak1 resulted in the inhibition of Pak1 activation. This inhibitory function of merlin is mediated through its binding to the Pak1 PBD and by inhibiting Pak1 recruitment to focal adhesions. This link provides a possible mechanism for the effect of loss of merlin expression in tumorigenesis.**

## Introduction

Neurofibromatosis type 2 is an inherited disorder, characterized by development of Schwann cell tumors of the eighth cranial nerve. Mutations and loss of heterozygosity of the *NF2* locus have been detected at high frequency in various tumors of the nervous system, including schwannomas, meningiomas, and ependymomas (Gusella et al., 1999). Mice heterozygous for an *Nf2* mutation are predisposed to a wide variety of malignant tumors (McClatchey et al., 1998). Inactivation of *Nf2* specifically in Schwann cells leads to development of schwannomas and Schwann cell hyperplasia in mice (Giovannini et al., 2000). The *NF2* gene codes for a 595 amino acid protein, termed merlin, which is highly related to the ERM proteins ezrin, radixin, and moesin.

Recent work has shown that merlin protein levels and phosphorylation are affected by growth conditions such as cell confluence, loss of adhesion, or serum deprivation. One site of phosphorylation of merlin is serine 518, and phosphorylation at this site can be induced by active forms of Rac and cdc42 but not Rho (Shaw et al., 2001). Rac/cdc42-induced phosphorylation at merlin serine 518 is mediated by p21-activated kinase (Pak) (Kissil et al., 2002; Xiao et al., 2002). Such phosphorylation can disrupt merlin intramolecular interactions and its association with the actin cytoskeleton and induces a shift in the subcellular localization of merlin in LLC-PK1 cells (Kissil et al., 2002; Shaw et al., 2001).

*Correspondence: tjacks@mit.edu

The p21-activated kinases (Pak1 through 3) are immediate downstream effectors of Rac/cdc42. They comprise a subgroup of serine/theronine kinases, termed the "group I" Paks, belonging to a larger protein family, which also contains the "group II" kinases (Pak4, 5, and 6). The group I Paks, which have been studied in more detail, have been shown to mediate signals to cytoskeletal reorganization and transcriptional activation (reviewed by Bagrodia and Cerione, 1999; Jaffer and Chernoff, 2002). The Paks are regulated by diverse mechanisms. Based on three-dimensional structure analysis, it has been suggested that inactive Pak is in a conformation in which the autoinhibitory domain interacts with the kinase domain. The binding of active Rac/cdc42 to Pak alleviates this inhibition and enables Pak activation. Once the inhibition is relieved, Pak undergoes autophosphorylation, and this prevents a conformational switch back into an inactive state (Li et al., 2001). Several additional mechanisms and molecules have been shown to regulate Pak activation, including phospholipids and proteolysis. In addition, membrane localization via NCK, localization to focal adhesions via p95/PKL-Cool/Pix, and signals converging from both growth factor receptors and integrins can all effect Pak activation (Brown et al., 2002; del Pozo et al., 2000; Turner et al., 1999).

Recently, merlin has been implicated as a negative regulator of Rac signaling. The overexpression of merlin inhibited Rac-induced activation of c-Jun N-terminal kinase (JNK) and activation of the AP-1 transcriptional activator. Conversely, in Nf2-deficient fibroblasts, basal JNK activity was found to be elevated, as was the activity of AP-1 (Shaw et al., 2001). Thus, it would seem that merlin both is regulated by the Rac/cdc42 signaling pathway and can serve as an inhibitor of this pathway. Here we describe the interaction of merlin with Pak1, a critical mediator of Rac/cdc42 signaling, and the effect of this interaction on the activity of the kinase.

## Results and Discussion

### Direct Interaction between Merlin and Pak1

Based on the observations that merlin inhibits Rac signaling at some level, we assessed the possibility of a stable interaction between merlin and Pak. NIH3T3 cells were cotransfected with expression vectors for merlin and Pak1, and association of the proteins was assessed by coimmunoprecipitations. As shown in Figure 1A, immunoprecipitation of merlin led to coimmunoprecipitation of Pak1. Likewise, immunoprecipitates of Pak1 contained merlin (Figure 1A). To assess the interaction in an additional cell type, a rat schwannoma cell line (RT4-DP6) was examined. These cells express relatively low levels of endogenous merlin and detectable endogenous levels of Pak1. Neither Pak2 nor Pak3 was detected in these cells by Western blot analysis (data not shown). As in the case of NIH3T3 cells, association of the proteins was assessed by coimmunoprecipitations. As shown in Figure 1A, the immunoprecipitation of merlin also precipitated endogenous Pak1. In the reciprocal experi-

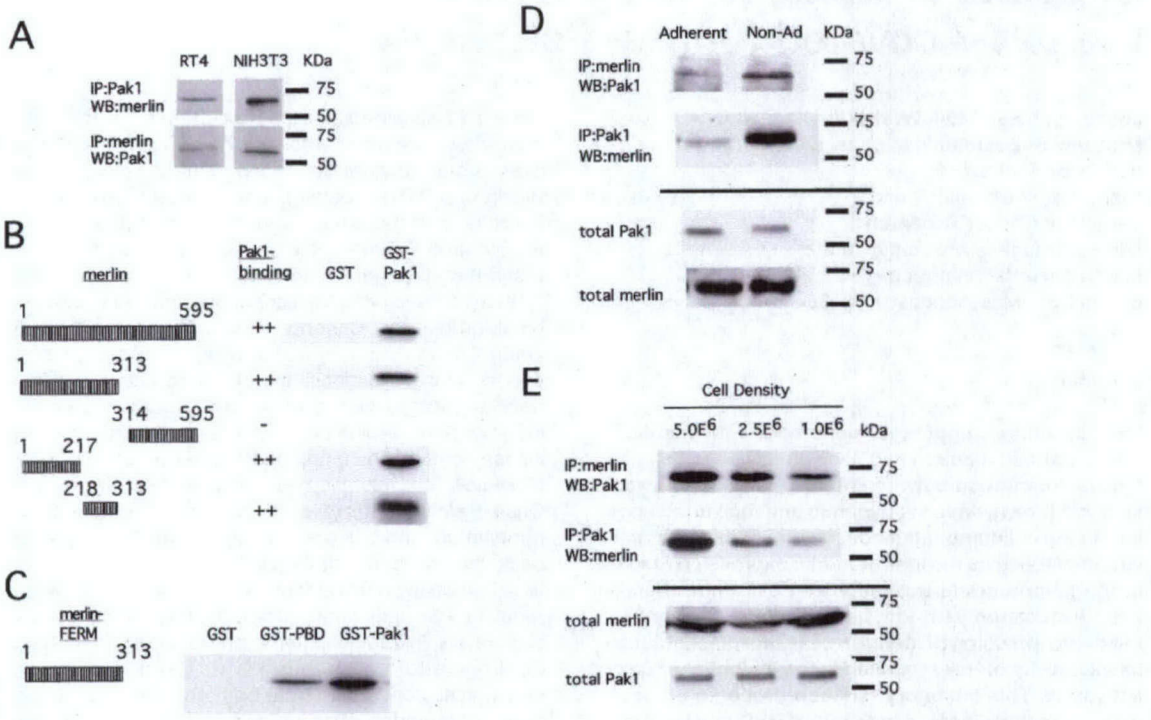


Figure 1. Merlin and Pak1 Interact In Vitro and In Vivo

Western blot analysis of merlin and Pak1 immunoprecipitates from NIH3T3 cells transfected with expression vectors for merlin and Pak1, and from RT4 Schwann cells expressing endogenous levels of merlin and Pak1 (A). In vitro interactions of GST only or GST-Pak1 proteins with $S^{35}$-labeled full-length merlin (1–595), FERM domain (1–313), C-terminal half (314–595), FERM lobes F1-F2 (1–217), and lobe F3 (218–313) (B). In vitro interactions of the merlin FERM domain with GST, GST-Pak1 (1–545), and GST-PBD (70–143) (C). Western blot analysis of merlin and Pak1 immunoprecipitates and total expression levels of protein from RT4-67 grown under adherent or nonadherent growth conditions for 4 hr prior to harvesting (D) or grown at increasing cellular densities as indicated (E).

ment, the immunoprecipitation of endogenous Pak1 also resulted in the coimmunoprecipitation of endogenous or exogenous merlin (Figure 1A).

To determine if merlin and Pak can interact directly, the association of the two proteins was assessed in vitro. Full-length Pak1 was produced in bacteria as a GST-fusion protein and purified on glutathione- agarose beads. Merlin was produced by in vitro transcription/translation. The $S^{35}$-labeled merlin protein was incubated with either GST-Pak1 or GST bound to the agarose beads. The interaction of the proteins was assessed by separation of the proteins by SDS-PAGE and autoradiography. As shown in Figure 1B, GST-Pak1 bound to merlin, whereas GST alone did not. Thus, the interaction between Pak and merlin is likely to be direct.

To further delineate the regions of Pak1 that mediate interaction with merlin, we assessed the binding of different merlin domains to full length Pak1 in vitro. The N-terminal FERM domain (1–313) and the C-terminal tail of merlin (314–595) were transcribed and translated in vitro and tested for their ability to interact with GST-Pak1. While the N-terminal FERM domain interacted efficiently with GST-Pak1, the C-terminal fragment failed to interact (Figure 1B). This was not due to different levels of expression, as all merlin fragments were produced at similar levels (data not shown). Trying to further narrow down the interacting domains in the merlin FERM, we tested the ability of either the F1-F2 domain (1–217) or the F3 domain (218–313) (Pearson et al., 2000) to bind to Pak1. Both domains interacted well with the kinase, indicating there are multiple binding sites in the FERM domain involved in the interaction of merlin with Pak1 (Figure 1B). The interaction of both the F1-F2 and F3 fragments with GST-Pak1 appeared to be stronger than that of the entire FERM domain (F1-F3). This could be due to intramolecular associations within the intact FERM domain (Gutmann et al., 1999) that partially mask the Pak1 interaction sites. We next tested the possibility that the FERM domain could bind to the N-terminal regulatory domain of Pak1 (70–143), which contains the cdc42/Rac binding domain (PBD). The FERM domain interacted with the PBD, although the interaction was weaker than the interaction with full-length Pak1.

We attempted to identify additional merlin binding sites on Pak1 by generating additional truncation mutants; however, we were unable to obtain these mutants due to the high toxicity of the Pak1 kinase domain in bacteria (J. Chernoff and E. Manser, personal communication). Thus, it remains possible that additional interaction domains exist between merlin and Pak1. However, the identification of an interaction between the FERM domain with the PBD is of functional significance, as it implicates merlin in a regulatory role for Pak1 (see below).

### The Interaction of Merlin and Pak Is Dynamic

To assess whether the interaction between Pak and merlin is dynamic, we examined the effect of cell adhesion and confluence on the interaction. Exogenous expression of merlin was employed in these experiments to circumvent the fact that merlin expression is regulated by different cellular growth conditions (Shaw et al., 1998). Toward this aim, the RT4-67 cell line was employed. The RT4-67 cells were constructed from the RT4-DP6 rat schwannoma cells and harbor a tetracycline-inducible allele of NF2 (Morrison et al., 2001). RT4-67 cells were grown in the presence of doxycycline and placed into suspension by plating them on poly-HEME coated dishes, which prevents the cells from adhering to the plastic (Folkman and Moscona, 1978). Four hours after being placed into suspension, the cells were harvested, and either merlin or Pak1 was immunoprecipitated. The precipitates were resolved by SDS-PAGE and Western blotting and compared to precipitates from adherent RT4-67 cells. While merlin and Pak1 could be coimmunoprecipitated under adherent growth conditions, the interaction between the two proteins was greatly enhanced when adhesion was lost (Figure 1D).

To test the effect of cell confluence on the merlin-Pak1 interaction, protein extracts were prepared from RT4-67 cells grown at high or low confluence. The cells were plated at increasing densities in the presence of doxycycline and were harvested 24 hr after plating. Merlin or Pak1 was immunoprecipitated from the cellular extracts and resolved by SDS-PAGE. Both merlin and Pak1 can reciprocally coimmunoprecipitate under conditions of either low or high confluence. However, the interaction between merlin and Pak1 was enhanced when cells were grown to a higher density (Figure 1E). Importantly, the observed differences in the precipitated levels of merlin or Pak1 are not due to differences in the expression levels of these proteins. The levels merlin and Pak1 were not altered in the RT4-67 Schwann cells, whether the cells were adherent or nonadherent or grown at high or low cellular densities.

These experiments indicate that the interaction of merlin and Pak1 is dynamic and influenced by cellular adhesion and cell density. The interaction of merlin and Pak was enhanced under conditions demonstrated to be inhibitory to Pak activation in NIH3T3 cells (del Pozo et al., 2000) and in the RT4-67 Rat schwannoma cells (J.L.K. and T.J., unpublished data). The regulation of the Paks is complex and involves many different factors (discussed below). However, the localization of Pak to specific regions at the plasma membrane might be an important determinant of its activation. Earlier work has shown that the SH2/SH3 domain protein NCK is required for the recruitment of Pak to the cell membrane (Lu et al., 1997; Sells et al., 1997). Interestingly, NCK interaction with Pak is enhanced upon adhesion and lost when cells are suspended (Howe, 2001), which is opposite to the pattern of interaction of merlin and Pak shown here.

### Merlin Inhibits the Pak1-Rac and Pak1-Paxillin Interactions

As merlin bound the Pak1 PBD domain, we tested the possibility that merlin can inhibit the interaction between Rac and Pak1. RT4-67 cells were grown in the presence or absence of doxycycline, and Pak1-Rac interaction was examined by immnuoprecipitations. Overexpression of merlin inhibited the interaction between Pak1 and Rac, as demonstrated by the reduced levels of Rac coimmunoprecipitated with Pak1 and vice versa. The overall reduction in this interaction was approximately 4-fold in the presence of merlin (Figure 2A). While the levels of Rac1 were not altered in the presence or absence of merlin (Figure 2A), the levels of the GTP-bound form of Rac1 were decreased by approximately 2-fold in cells expressing merlin (Figure 2A). These reduced levels of Rac-GTP could explain in part the lower levels of Rac-Pak1 complexes in the presence of merlin.

We also examined the effect of merlin expression on the interactions of Pak1 with other adaptor proteins. This was done by immunoprecipitation and Western blot analysis of the relevant interactions. Merlin expression did not affect the interaction between Pak1 and NCK, Pak1 and β-pix, or Pak1 and p95PKL, as similar amounts of Pak1 and the various binding proteins were coimmunoprecipitated in the presence or absence of increased merlin expression (Figures 3B–3D). Merlin expression also did not alter the overall expression levels of these proteins (data not shown). In contrast, the interaction of Pak1 and paxillin was greatly reduced upon increased merlin expression (Figure 3A). When merlin was overexpressed in the RT4-67 cell lines, an average of 10-fold reduction in the Pak1-paxillin interaction was evident from the reduced levels of paxillin coimmunoprecipitated with Pak1 and vice versa. Again, expression of merlin did not affect the overall levels of paxillin or Pak1 expression in the cells (Figure 3A).

Based on these observations, we propose that merlin can inhibit Pak1 activation by binding directly to the Pak1 PBD and interfere with the binding of active Rac to the Pak1 PBD. Merlin might also function by directly reducing the level of active Rac1 that is available to bind and activate Pak1. Similarly, merlin could interfere directly with the interaction of Pak1 to paxillin, or this effect could be a consequence in the reduction of active Rac, which is required for the recruitment of Pak1 to focal adhesion complexes (Brown et al., 2002).

### Loss of Merlin Results in Increased Pak Activity

We next tested the possibility that merlin expression might affect Pak1 activation. The phosphorylation status of Pak1 serves as a direct indication of the activation status of the kinase (Buchwald et al., 2001; Chong et al., 2001). To examine differences in the phosphorylation state of Pak1, we used 2-dimensional gel analysis to separate the different forms of activated Pak1 (Garcia Arguinzonis et al., 2002). MEFs were serum starved for 24 hr and then treated for 5 min with PDGF. Extracts were prepared from cells directly into sample buffer and quantified. Equal amounts of protein were separated by isoelectric focusing on an immobilized 4–7 pH gradient. Subsequently, the extracts were separated by SDS-PAGE in the second dimension, transferred to membranes, and analyzed by Western blotting using an anti-Pak1 antibody. As shown in Figure 4B, under conditions of serum starvation only two forms of Pak1 were detected in the extracts, most likely corresponding to non- or hypophosphorylated forms of Pak1. When extracts

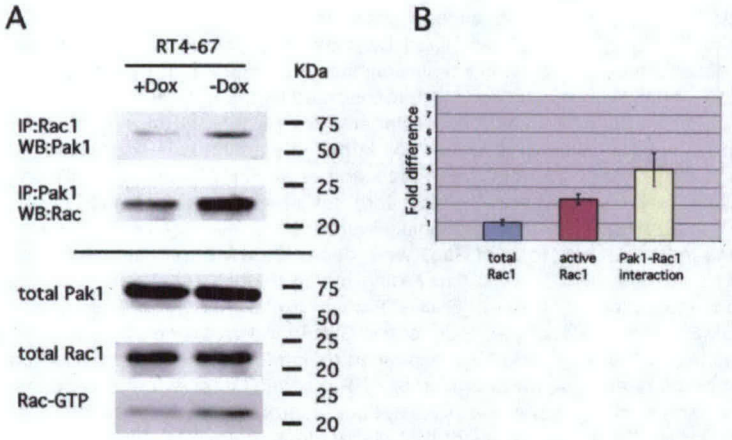


Figure 2. Merlin Reduces Levels of Rac-GTP and Interferes with Pak1-Rac Interactions

Western blot analysis of total protein levels and immunopreciptates from RT4-67 Schwann cells grown in the presence or absence of doxycycline. Pak1 and Rac1 (A). Quantification of the fold-differences in the levels of Rac1 and Rac1-GTP and in the interaction between Rac1 and Pak1 (B). The data represent the average of five independent experiments.

prepared from PDGF-treated MEFs were examined, however, several additional spots were detected. These spots correspond to hyperphosphorylated forms of Pak1, as they appear to be more acidic than the forms of Pak1 found in the serum-starved cells and separate in a signature pattern of a phospho-protein with multiple phosphorylation sites (Garcia Arguinzonis et al., 2002). This also correlated with the increased kinase activity of Pak1, as assessed directly by an in vitro kinase assay employing MBP (myelin basic protein) as a substrate (Figure 4A). To confirm that the additional Pak1 forms are due to phosphorylation, extracts of PDGF-treated cells were incubated with protein phosphatase 1 (PP1) in the presence or absence of protein phosphatase inhibitors. The protein phosphatase treatment resulted in the disappearance of the additional acidic forms of the protein that appear after the PDGF treatment (see Figure 4B), indicating that the additional spots appearing after PDGF stimulation are phosphorylated forms of Pak1. As expected, the inclusion of phosphatase inhibitors in the reaction prevented the loss of the phosphorylated species (data not shown).

To address the effect of merlin on Pak1 activation in vivo, the consequence of loss of merlin expression in MEFs was examined. Mouse embryo fibroblasts (MEFs) were prepared from animals carrying a conditional knockout (floxed) allele of *Nf2* ($Nf2^{flox2}$) (Giovannini et al., 2000). In addition to the $Nf2^{flox2}$ allele, the cells carried either a wild-type *Nf2* allele ($Nf2^{flox2/+}$) or a *Nf2* deletion allele ($Nf2^{flox2/-}$) (McClatchey et al., 1998). The MEFs were then infected with adenovirus expressing Cre-recombinase (ad-Cre), which led to the inactivation of the floxed *Nf2* allele. To test for loss of merlin expression in the ad-Cre treated $Nf2^{flox2/-}$ MEFs, extracts were prepared 96 hr after infection. One milligram of extract was used to immunoprecipitate merlin, and merlin levels were examined by Western blotting. The ad-Cre-treated $Nf2^{flox2/-}$ MEFs lacked detectable merlin protein 96 hr after infection, while merlin levels were not altered in ad-Cre $Nf2^{flox2/+}$ MEFs (Figure 5B). As a control, infection of the

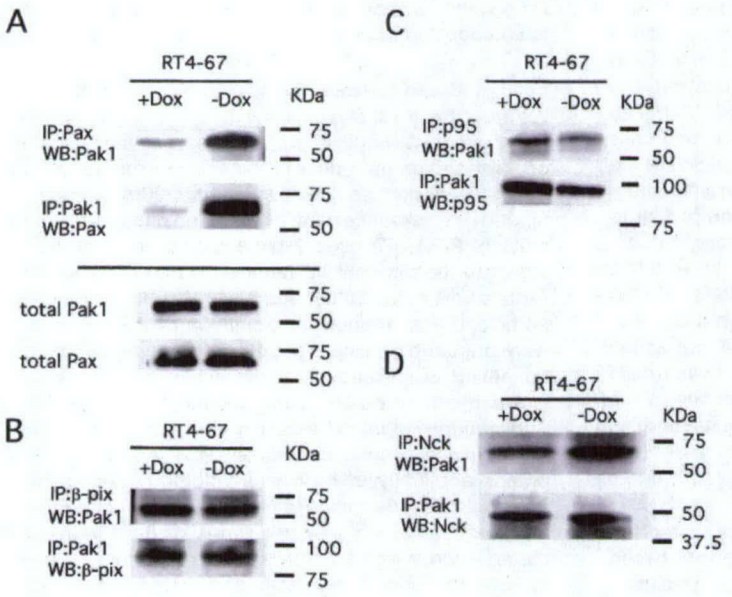


Figure 3. Merlin Interferes with Pak1-Paxillin Interactions

Western blot analysis of total protein levels and immunopreciptates from RT4-67 Schwann cells grown in the presence or absence of doxycycline: Pak1 and paxillin (A), Pak1 and β-pix (B), Pak1 and p95PKL (C), and Pak1 and Nck (D).

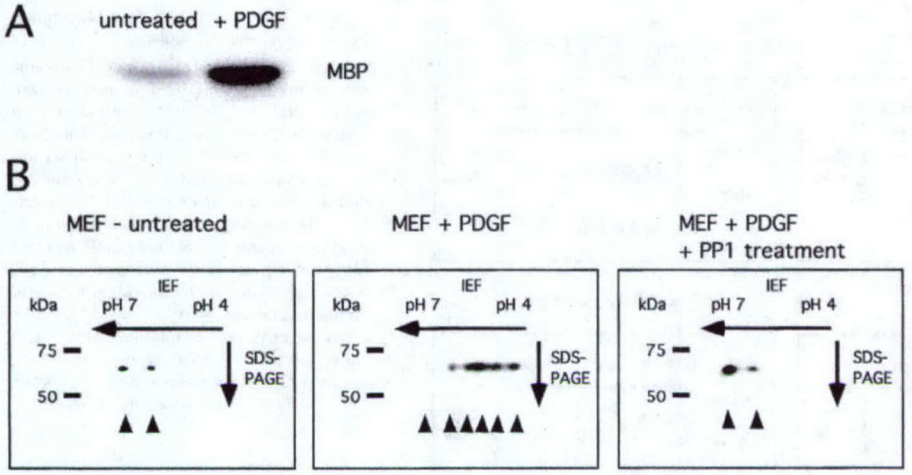


Figure 4. Analysis of Pak1 Phosphorylation by 2-Dimensional Gel Analysis

In vitro kinase assay of Pak1 immunoprecipitated from serum-starved or PDGF-treated (5 ng/ml) NIH3T3 cells, employing MBP as a substrate (A). Western blot analysis of Pak1 in MEFs that were serum starved (left), treated with PDGF (5 ng/ml) (center), and treated with protein phosphatase 1 (2.5 U/ml) (right).

cells with an adenovirus expressing the LacZ gene did not alter merlin levels (data not shown). The status of Pak1 was then analyzed in the MEFs. The ad-Cre-treated and adenovirus control-treated $Nf2^{flox2/-}$ and ad-Cre-treated $Nf2^{flox2/+}$ MEFs were plated at the same cellular densities and allowed to adhere to the tissue culture dish. The MEFs were then serum starved for 24 hr and extracted into sample buffer, and the status of Pak1 phosphorylation was analyzed by 2D gel analysis. Under conditions of serum starvation, Pak1 was not activated in control-treated MEFs, as demonstrated by detection of only hypophosphorylated forms of Pak1 (Figure 5A). However, in the ad-Cre treated $Nf2^{flox2/-}$ MEFs, which had lost the expression of merlin, a marked activation of Pak1 was observed, as indicated by the appearance of several phosphorylated forms of the kinase (Figure 5A). Thus, loss of merlin expression in MEFs promoted Pak1 activation under conditions normally associated with inactivity. These data are consistent with merlin functioning as an inhibitor of Pak1.

### Merlin Expression Inhibits Pak Activation

As loss of merlin expression resulted in the appearance of activated forms of Pak1, we examined the possibility that the overexpression of merlin would inhibit Pak1 activation. In the RT4-67 Schwann cells basal levels of merlin are extremely low (Morrison et al., 2001). To assess Pak1 activity in these cells, RT4-67 cells were serum starved for 24 hr, protein was extracted, and the activation status of Pak1 was examined by 2D gel analysis. As shown in Figure 5C, the basal activity of Pak1 was relatively high in the RT4 cells. To assess whether the expression of merlin would affect the activity of Pak1 in these cells, the expression of merlin was induced by the addition of doxycycline into the growth media 48 hr prior to the harvesting of the cells, in the same manner as described above. Indeed, increased expression of merlin significantly reduced the levels of activated forms of Pak1 (Figure 5C). Thus, the reintroduction of merlin into the RT4 schwannoma cells, which display a high level of basal Pak1 activity, results in inhibition of Pak1 activation.

The data reported here are in agreement with previous work from us and others implicating merlin as a negative regulator of Rac-signaling. Specifically, overexpression of merlin has been shown to inhibit Rac-induced activation of c-Jun N-terminal kinase (JNK) and AP-1 transcription, while loss of merlin further resulted in elevated JNK basal activity and activation of AP-1. Loss of merlin also induced cytoskeleton changes that are phenotypically consistent with Rac activation, including membrane ruffling and increased cellular motility (Shaw et al., 2001). This is similar to the higher motility of cells expressing activated Rac alleles. While these data support a functional connection between merlin and Rac, they do not establish where in the Rac pathway merlin might act. Our data indicate that merlin can act both at the level of Rac activation and downstream of Rac, at the level of Pak activation.

The overexpression of Rac can induce transformation and anchorage-independent growth of cells (Khosravi-Far et al., 1995; Qiu et al., 1995). As Rac effectors, PAKs have been shown to mediate some of these signals. Using activated or dominant-negative forms of the proteins, the Paks have been shown to be involved in focal complex formation and membrane ruffling in various cell types (Daniels et al., 1998; Manser et al., 1997; Sells et al., 1997). Paks also have a role in signal transduction from Rac to JNK. Some reports have concluded that activated Pak1 or Pak3 can lead to upregulation of JNK activity; however, further studies are required to fully establish this connection (Brown et al., 1996; Zhang et al., 1995). In addition, recent data point to involvement of Pak in the regulation of the MAPK pathway. Pak can phosphorylate Raf-1 on serine 338 and induce phosphorylation of Mek1 on serine 298 (Diaz et al., 1997; Frost et al., 1997; King et al., 1998). Moreover, Rac or

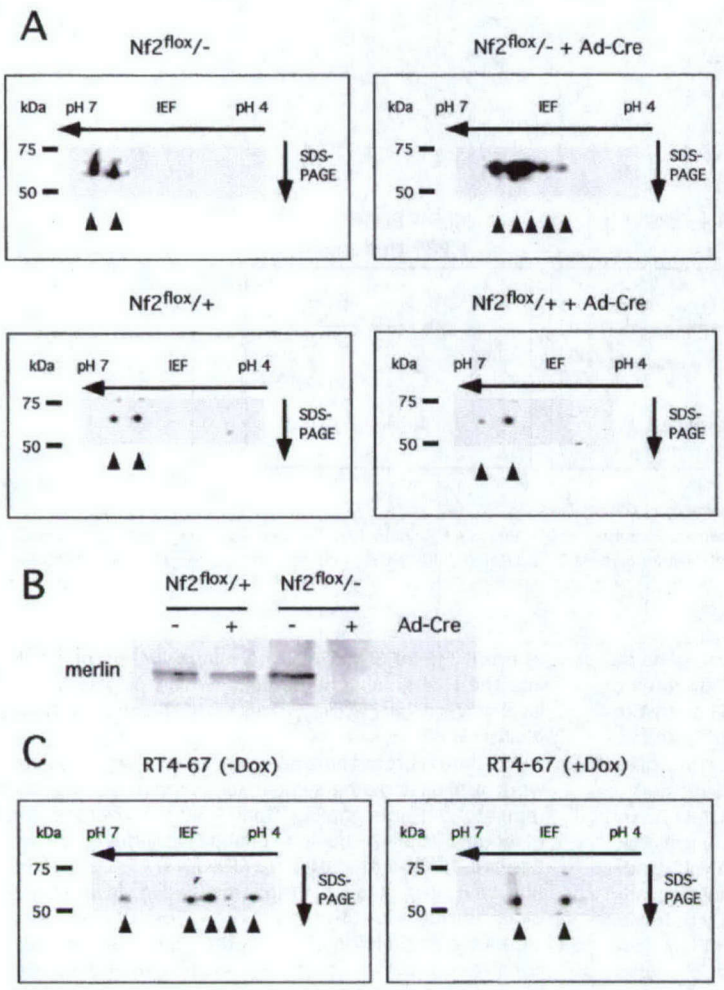


Figure 5. Analysis of Pak1 Phosphorylation by 2-Dimensional Gel Analysis

Western blot analysis of Pak1 in serum-starved untreated MEF clones that express merlin ($Nf2^{flox2/-}$, $Nf2^{flox2/+}$), serum-starved clones infected with adenovirus-Cre that express merlin ($Nf2^{flox2/+}$ + ad-Cre), and serum-starved clones infected with adenovirus-Cre that does not express merlin ($Nf2^{flox2/-}$ + ad-Cre). The various phosphorylated forms of Pak1 are indicated by arrows (A). IP-Western blot analysis of merlin expression in non-treated and ad-Cre-treated MEF lines (B). Western blot analysis of Pak1 in RT4 Schwann cells that are serum starved and either untreated (−Dox) or overexpressing merlin (+Dox). The various phosphorylated forms of Pak1 are indicated by arrows (C).

cdc42 has been reported to be required for the full activation of Ras by Raf. Pak may mediate the effect of Rac/cdc42 through phosphorylation of Raf (Li et al., 2001; Macara et al., 1996).

Merlin might exert its inhibitory function by several different mechanisms, which could be overlapping. As we have shown, expression of merlin in the RT-4 inducible cell line resulted in reduced levels of Rac-GTP, without affecting the levels of total Rac1. Merlin, interestingly, binds RhoGDI (Maeda et al., 1999) and therefore may link between RhoGDI and Rac1, thus stabilizing the inactive state of Rac1. Alternatively, merlin might act by affecting the activity of β-pix, which is a Rac GEF (Manser et al., 1998). We have also demonstrated here that merlin binds to the PBD domain of Pak1, and this interaction could well disrupt association with Rac and the subsequent activation of Pak1.

The localization of Pak is important in the regulation of its activity. Pak1 activation requires signals converging from both growth factor receptors and integrins. One possible site of physical integration of these pathways is the scaffold protein paxillin (Turner, 2000). Pak has been shown to bind to paxillin via the p95PKL-Cool/Pix protein complex (Turner et al., 1999). The recruitment of Pak1-PIX-p95PKL to paxillin is triggered by binding of Rac-GTP to Pak1 and activation of the adaptor function of Pak1 (Brown et al., 2002). We have demonstrated that merlin interferes with the Pak1-paxillin interaction, but does not affect the interaction between Pak1 and β-pix, p95PKL, or NCK. It is probable that NCK and p95/PKL-Cool/Pix target Pak to different subcellualr locations, where Pak is activated by different stimuli. Thus, it is possible that merlin can specifically inhibit the cellular fraction of Pak1 that is to be recruited to focal adhesion complexes. Interestingly, merlin has been demonstrated to bind to paxillin and to β-integrin (Fernandez-Valle et al., 2002; Obremski et al., 1998). Therefore, merlin may bind Pak while it is bound to paxillin and act to both release it from paxillin and inhibit its full activation by Rac. Alternatively, there could exist separate pools of merlin with distinct functions. One pool of merlin may function by binding to Pak1 prior to its association with paxillin and prevent the association. Another fraction of merlin, which is associated with paxillin, might have other, additional functions. The existence of pools of merlin with different functions can be demonstrated with the identification of merlin mutants impaired in their ability to bind Pak1 and the functional comparison of these

mutants with the mutants of merlin unable to bind paxillin (Fernandez-Valle et al., 2002). It is important to note that the localization and function of merlin is also likely to be affected by phosphorylation at serine 518 (Kissil et al., 2002; Shaw et al., 2001). The effects of different merlin mutants, including those affecting serine 518, on the interaction with and inhibition of Pak are currently being investigated.

The data described here, combined with the fact that Pak phosphorylates and, perhaps, inactivates merlin supports a "feedforward" signaling model (Kissil et al., 2002; Xiao et al., 2002). In such a model, merlin would function normally to downregulate Rac/cdc42-induced signaling. Once activated, Rac/cdc42 can stimulate Pak activity, which in turn would lead to merlin phosphorylation and relief from its inhibitory effect. Given the fact that Rac signaling is necessary, and in some cases sufficient, for transformation, it is possible that merlin's inhibition of Rac/cdc42-signaling represents its tumor suppressor function. Studies employing dominant-negative mutants have shown that Rac is required for cellular transformation by Ras (Khosravi-Far et al., 1995; Qiu et al., 1995; Ridley et al., 1992; Roux et al., 1997). Rac has also been shown to regulate cell motility and invasiveness (del Peso et al., 1997; Evers et al., 2000; Habets et al., 1994; Sahai et al., 2001). The fact that $Nf2^{+/-}$ mice develop highly metastatic tumors, which display loss of the wild-type Nf2 allele, is also consistent with a merlin-Rac functional connection (McClatchey et al., 1998).

The data presented here demonstrate a direct connection between merlin and the Rac-signaling pathways, via the inhibition of Pak. The work ascribes a biochemical function to a tumor suppressor with previously unknown function. In addition, it identifies an established tumor suppressor in the process of Pak1 regulation, possibly linking Pak deregulation to tumorigenesis. Understanding the regulation of merlin by Rac/cdc42 and merlin's impact on these signaling pathways could lead to a more complete understanding for the role of merlin in tumor formation. Once these interactions are fully elucidated, the use of specific inhibitors can be assessed as therapeutic modalities for tumors bearing mutations in NF2.

## Experimental Procedures

### Cell Culture Conditions and Transfections

The RT4 Schwann cells and MEFs were grown in DME, 10% fetal calf serum, and antibiotics. In cases where merlin expression was involved, expression was induced by addition of 1 μg/ml Doxycycline for 48 hr prior to the experiment. All transfections were done with Lipofectamine (Invitrogen). For the experiments where Pak1 activation was examined, cells were serum starved by growing them for 24 hr in serum-free DME and antibiotics. Pak1 activation was stimulated by adding PDGF-BB (Sigma) at 5 ng/ml for 5 min. In experiments where cells were in suspension, tissue culture plates were coated with poly-HEME (Sigma) as previously described (Folkman and Moscona, 1978). Cells were trypsinized, treated with soybean Trypsin inhibitor (Sigma), and placed back onto regular tissue culture dishes or the poly-HEME coated plates for 4 hr before harvesting.

### Plasmids and Antibodies

Expression plasmids used for transfection are pCDNA3-Nf2 (Kissil et al., 2002), pCMV-Pak1 (Sells et al., 1997), and pCDNA3-β-pix (Hashimoto et al., 2001). Plasmids for the in vitro translation were constructed by PCR of the FERM domain (1–313), C-terminal half (342–595), F1-F2 (1–217), and F3 (218–313) (sequences available upon request) and subcloning of the fragments into pCDNA3. Antibodies used were: for merlin, SC-331; Pak1, sc-881 and sc-882; β-pix, sc-10932; Nck, sc-290; Rac1, sc-217 (Santa Cruz Biotechnology); anti-paxillin mAb, anti-Rac1 mAb and anti-p95PKL mAb (BD Transduction Laboratories), and anti-paxillin pAb (Chemicon International).

### Immunoprecipitations, Kinase Assays, and Rac Activation Assays

Cells were plated at $7.5 \times 10^5$/10 cm dish and transfected the next day. 48 hr after transfection the cells were serum starved for 24 hr and extracted into extraction buffer (10 mM Tris-HCl [pH 7.6], 150 mM NaCl, 0.5% NP40, 0.1% deoxycholate, 1 mM $NaVO_4$, and protease inhibitors). Lysates were precleared for 1 hr, then incubated with the primary antibody for 3 hr at 4°C, and protein-A or protein-G beads were added for an additional 2 hr. Complexes were washed extensively with extraction buffer and separated by SDS-PAGE. Pak1 kinase assays were preformed as described (Kissil et al., 2002), except that Pak1 was immunoprecipitated from the extracts and MBP was added as substrate at 0.5 μg/ml. Quantification of active Rac was done employing the Rac activation assay kit, according to manufacturer's instructions (Upstate). Quantification of all Western blot experiments was done by densitometry analysis using NIH image v.1.63 of scanned data from at least three independent experiments.

### In Vitro Binding Assays

Full-length and truncation mutants of merlin were produced using the TnT kit (Promega) with Methionine $S^{35}$. GST-Pak1 and GST-Pak1(70-143) were produced in bacteria as described (Thiel et al., 2002). The in vitro binding assays were preformed by incubation of 30 μl of GST, GST-Pak1, or GST-Pak1(70-143) bound to gluthathione beads (0.5 mg/ml) with equal amounts of in vitro translated merlin-$S^{35}$ (determined beforehand by running 5% of each reaction on SDS-PAGE and autoradiography) in reaction buffer (50 mM Tris-HCl [pH 7.5], 120 mM NaCl, 10 mM $MgCl_2$, 5% Glycerol, 1% Triton X-100) at 4°C for 3 hr and washed several times with the reaction buffer. The beads were then boiled, separated by SDS-PAGE, treated with Amplify (Amersham Pharmacia), dried, and exposed to film.

### 2-Dimensional Analysis of Pak1 Activity

Cells were harvested directly into sample buffer (9.8 M Urea, 2% CHAPS, 5 ml IPG buffer 4-7, DTT 15 mg/ml). Extracts were incubated on ice for 10 min and centrifuged 10 min, 14,000 × g, 4°C. Extracts (100 μg) were cup loaded onto 7 cm, pH 4–7 IPG strips (Amersham Pharmacia) and resolved at 50 mA/strip for 100V for 30 min, 200V for 30 min, 400V for 30 min, 1000V for 60 min, 3500V for 5 hr, and 500V to a total of 20,000V-hours using a IPGphor unit (Pharmacia biotech). Strips were then washed in wash solution (50 mM Tris-HCl [pH 8.8], 6 M Urea, 30% Glycerol, 2% SDS) supplemented with 20 mg/ml DTT for 10 min at RT and followed by a wash in wash buffer supplemented with 25 mg/ml iodoacetamide for 10 min. The strips were then loaded onto a standard SDS-PAGE, separated, and transferred to Immobilon (Millipore). The blots were then used in Western blot analysis. Equal loading of protein was determined by blotting with an actin antibody (Santa Cruz Biotechnology).

## Acknowledgments

We Thank Dr. Chernoff for the Pak1 and GST-Pak expression plasmids, Dr. Sabe for the pCDNA3-β-pix plasmid, Drs. Herrlich and Morrison for the merlin-inducible RT4-67 Schwann cell line, and Dr. Giovannini for the $Nf2^{flox}$ mice. This work is supported by a grant from the Department of Defense. T.J. is an investigator of the Howard Hughes Medical Institute. J.K. was supported by a young investigator award from the National Neurofibromatosis Foundation.

Received: January 6, 2003
Revised: August 5, 2003
Accepted: August 13, 2003
Published: October 23, 2003

## References


Bagrodia, S., and Cerione, R.A. (1999). Pak to the future. Trends Cell Biol. *9*, 350–355.

Brown, J.L., Stowers, L., Baer, M., Trejo, J., Coughlin, S., and Chant, J. (1996). Human Ste20 homologue hPAK1 links GTPases to the JNK MAP kinase pathway. Curr. Biol. *6*, 598–605.

Brown, M.C., West, K.A., and Turner, C.E. (2002). Paxillin-dependent paxillin kinase linker and p21-activated kinase localization to focal adhesions involves a multistep activation pathway. Mol. Biol. Cell *13*, 1550–1565.

Buchwald, G., Hostinova, E., Rudolph, M.G., Kraemer, A., Sickmann, A., Meyer, H.E., Scheffzek, K., and Wittinghofer, A. (2001). Conformational switch and role of phosphorylation in PAK activation. Mol. Cell. Biol. *21*, 5179–5189.

Chong, C., Tan, L., Lim, L., and Manser, E. (2001). The mechanism of PAK activation: auto-phosphorylation events in both regulatory and kinase domains control activity. J. Biol. Chem. *276*, 17347–17353.

Daniels, R.H., Hall, P.S., and Bokoch, G.M. (1998). Membrane targeting of p21-activated kinase 1 (PAK1) induces neurite outgrowth from PC12 cells. EMBO J. *17*, 754–764.

del Peso, L., Hernandez-Alcoceba, R., Embade, N., Carnero, A., Esteve, P., Paje, C., and Lacal, J.C. (1997). Rho proteins induce metastatic properties in vivo. Oncogene *15*, 3047–3057.

del Pozo, M.A., Price, L.S., Alderson, N.B., Ren, X.D., and Schwartz, M.A. (2000). Adhesion to the extracellular matrix regulates the coupling of the small GTPase Rac to its effector PAK. EMBO J. *19*, 2008–2014.

Diaz, B., Barnard, D., Filson, A., MacDonald, S., King, A., and Marshall, M. (1997). Phosphorylation of Raf-1 serine 338-serine 339 is an essential regulatory event for Ras-dependent activation and biological signaling. Mol. Cell. Biol. *17*, 4509–4516.

Evers, E.E., Zondag, G.C., Malliri, A., Price, L.S., ten Klooster, J.P., van der Kammen, R.A., and Collard, J.G. (2000). Rho family proteins in cell adhesion and cell migration. Eur. J. Cancer *36*, 1269–1274.

Fernandez-Valle, C., Tang, Y., Ricard, J., Rodenas-Ruano, A., Taylor, A., Hackler, E., Biggerstaff, J., and Iacovelli, J. (2002). Paxillin binds schwannomin and regulates its density-dependent localization and effect on cell morphology. Nat. Genet. *31*, 354–362.

Folkman, J., and Moscona, A. (1978). Role of cell shape in growth control. Nature *273*, 345–349.

Frost, J.A., Steen, H., Shapiro, P., Lewis, T., Ahn, N., Shaw, P.E., and Cobb, M.H. (1997). Cross-cascade activation of ERKs and ternary complex factors by Rho family proteins. EMBO J. *16*, 6426–6438.

Garcia Arguinzonis, M.I., Galler, A.B., Walter, U., Reinhard, M., and Simm, A. (2002). Increased spreading, Rac/p21-activated kinase (PAK) activity, and compromised cell motility in cells deficient in vasodilator-stimulated phosphoprotein (VASP). J. Biol. Chem. *277*, 45604–45610.

Giovannini, M., Robanus-Maandag, E., van der Valk, M., Niwa-Kawakita, M., Abramowski, V., Goutebroze, L., Woodruff, J.M., Berns, A., and Thomas, G. (2000). Conditional biallelic Nf2 mutation in the mouse promotes manifestations of human neurofibromatosis type 2. Genes Dev. *14*, 1617–1630.

Gusella, J.F., Ramesh, V., MacCollin, M., and Jacoby, L.B. (1999). Merlin: the neurofibromatosis 2 tumor suppressor. Biochim. Biophys. Acta *1423*, M29–M36.

Gutmann, D.H., Haipek, C.A., and Hoang Lu, K. (1999). Neurofibromatosis 2 tumor suppressor protein, merlin, forms two functionally important intramolecular associations. J. Neurosci. Res. *58*, 706–716.

Habets, G.G., Scholtes, E.H., Zuydgeest, D., van der Kammen, R.A., Stam, J.C., Berns, A., and Collard, J.G. (1994). Identification of an invasion-inducing gene, Tiam-1, that encodes a protein with homology to GDP-GTP exchangers for Rho-like proteins. Cell *77*, 537–549.

Hashimoto, S., Tsubouchi, A., Mazaki, Y., and Sabe, H. (2001). Interaction of paxillin with p21-activated Kinase (PAK). Association of paxillin alpha with the kinase-inactive and the Cdc42-activated forms of PAK3. J. Biol. Chem. *276*, 6037–6045.

Howe, A.K. (2001). Cell adhesion regulates the interaction between Nck and p21-activated kinase. J. Biol. Chem. *276*, 14541–14544.

Jaffer, Z.M., and Chernoff, J. (2002). p21-activated kinases: three more join the Pak. Int. J. Biochem. Cell Biol. *34*, 713–717.

Khosravi-Far, R., Solski, P.A., Clark, G.J., Kinch, M.S., and Der, C.J. (1995). Activation of Rac1, RhoA, and mitogen-activated protein kinases is required for Ras transformation. Mol. Cell. Biol. *15*, 6443–6453.

King, A.J., Sun, H., Diaz, B., Barnard, D., Miao, W., Bagrodia, S., and Marshall, M.S. (1998). The protein kinase Pak3 positively regulates Raf-1 activity through phosphorylation of serine 338. Nature *396*, 180–183.

Kissil, J.L., Johnson, K.C., Eckman, M.S., and Jacks, T. (2002). Merlin phosphorylation by p21-activated kinase 2 and effects of phosphorylation on merlin localization. J. Biol. Chem. *277*, 10394–10399.

Li, W., Chong, H., and Guan, K.L. (2001). Function of the Rho family GTPases in Ras-stimulated Raf activation. J. Biol. Chem. *276*, 34728–34737.

Lu, W., Katz, S., Gupta, R., and Mayer, B.J. (1997). Activation of Pak by membrane localization mediated by an SH3 domain from the adaptor protein Nck. Curr. Biol. *7*, 85–94.

Macara, I.G., Lounsbury, K.M., Richards, S.A., McKiernan, C., and Bar-Sagi, D. (1996). The Ras superfamily of GTPases. FASEB J. *10*, 625–630.

Maeda, M., Matsui, T., Imamura, M., and Tsukita, S. (1999). Expression level, subcellular distribution and rho-GDI binding affinity of merlin in comparison with Ezrin/Radixin/Moesin proteins. Oncogene *18*, 4788–4797.

Manser, E., Huang, H.Y., Loo, T.H., Chen, X.Q., Dong, J.M., Leung, T., and Lim, L. (1997). Expression of constitutively active alpha-PAK reveals effects of the kinase on actin and focal complexes. Mol. Cell. Biol. *17*, 1129–1143.

Manser, E., Loo, T.H., Koh, C.G., Zhao, Z.S., Chen, X.Q., Tan, L., Tan, I., Leung, T., and Lim, L. (1998). PAK kinases are directly coupled to the PIX family of nucleotide exchange factors. Mol. Cell *1*, 183–192.

McClatchey, A.I., Saotome, I., Mercer, K., Crowley, D., Gusella, J.F., Bronson, R.T., and Jacks, T. (1998). Mice heterozygous for a mutation at the Nf2 tumor suppressor locus develop a range of highly metastatic tumors. Genes Dev. *12*, 1121–1133.

Morrison, H., Sherman, L.S., Legg, J., Banine, F., Isacke, C., Haipek, C.A., Gutmann, D.H., Ponta, H., and Herrlich, P. (2001). The NF2 tumor suppressor gene product, merlin, mediates contact inhibition of growth through interactions with CD44. Genes Dev. *15*, 968–980.

Obremski, V.J., Hall, A.M., and Fernandez-Valle, C. (1998). Merlin, the neurofibromatosis type 2 gene product, and beta1 integrin associate in isolated and differentiating Schwann cells. J. Neurobiol. *37*, 487–501.

Pearson, M.A., Reczek, D., Bretscher, A., and Karplus, P.A. (2000). Structure of the ERM protein moesin reveals the FERM domain fold masked by an extended actin binding tail domain. Cell *101*, 259–270.

Qiu, R.G., Chen, J., Kirn, D., McCormick, F., and Symons, M. (1995). An essential role for Rac in Ras transformation. Nature *374*, 457–459.

Ridley, A.J., Paterson, H.F., Johnston, C.L., Diekmann, D., and Hall, A. (1992). The small GTP-binding protein rac regulates growth factor-induced membrane ruffling. Cell *70*, 401–410.

Roux, P., Gauthier-Rouviere, C., Doucet-Brutin, S., and Fort, P. (1997). The small GTPases Cdc42Hs, Rac1 and RhoG delineate Raf-independent pathways that cooperate to transform NIH3T3 cells. Curr. Biol. *7*, 629–637.

Sahai, E., Olson, M.F., and Marshall, C.J. (2001). Cross-talk between Ras and Rho signalling pathways in transformation favours proliferation and increased motility. EMBO J. *20*, 755–766.

Sells, M.A., Knaus, U.G., Bagrodia, S., Ambrose, D.M., Bokoch, G.M., and Chernoff, J. (1997). Human p21-activated kinase (Pak1) regulates actin organization in mammalian cells. Curr. Biol. *7*, 202–210.

Shaw, R.J., McClatchey, A.I., and Jacks, T. (1998). Regulation of

the neurofibromatosis type 2 tumor suppressor protein, merlin, by adhesion and growth arrest stimuli. J. Biol. Chem. *273*, 7757–7764.

Shaw, R.J., Guillermo, J.P., Curto, M., Yaktine, A., Pruitt, W.M., Saotome, I., O'Bryan, J.P., Gupta, V., Ratner, N., Der, C.J., et al. (2001). The Nf2 Tumor Suppressor, Merlin, Functions in Rac-Dependent Signaling. Dev. Cell *1*, 63–72.

Thiel, D., Reeder, M., Pfaff, A., Coleman, T., Sells, M., and Chernoff, J. (2002). Cell cycle-regulated phosphorylation of p21-activated kinase 1. Curr. Biol. *12*, 1227–1232.

Turner, C.E. (2000). Paxillin interactions. J. Cell Sci. *113*, 4139–4140.

Turner, C.E., Brown, M.C., Perrotta, J.A., Riedy, M.C., Nikolopoulos, S.N., McDonald, A.R., Bagrodia, S., Thomas, S., and Leventhal, P.S. (1999). Paxillin LD4 motif binds PAK and PIX through a novel 95-kD ankyrin repeat, ARF-GAP protein: a role in cytoskeletal remodeling. J. Cell Biol. *145*, 851–863.

Xiao, G.H., Beeser, A., Chernoff, J., and Testa, J.R. (2002). p21-activated kinase links Rac/Cdc42 signaling to merlin. J. Biol. Chem. *277*, 883–886.

Zhang, S., Han, J., Sells, M.A., Chernoff, J., Knaus, U.G., Ulevitch, R.J., and Bokoch, G.M. (1995). Rho family GTPases regulate p38 mitogen-activated protein kinase through the downstream mediator Pak1. J. Biol. Chem. *270*, 23934–23936.